4. Results

L. pneumophila possesses secreted and cell-associated phospholipase A (PLA), lysophospholipase A (LPLA) as well as secreted glycerophospholipid:cholesterol acyltransferase (GCAT) activities (73, 75). At the onset of this work, only one *L. pneumophila* PLA had been described, PlaA, responsible for the major secreted lysophospholipase A activity of *L. pneumophila* (75). Since an *L. pneumophila plaA* mutant still possesses secreted PLA activities and residual LPLA activities, the bacterium obviously owns further phospholipases A (75). Phospholipases are considered as potential bacterial virulence factors which might promote the establishment of the severe pneumonia due to their capability of destroying lung surfactant, a phospholipid monolayer in the alveoli, essential for the stability of the lung (74). Furthermore, PLAs could be involved in the remodeling and lysis of the phagosomal membrane and might generate reaction products capable of interfering with the signal transduction of the host (136, 206). Thus, it was of interest to investigate these enzymes. There are a number of different *L. pneumophila* strains used in investigations. Most of the earlier studies concerning lipolytic enzymes have been conducted in strain 130b and therefore this strain was chosen for most of the following experiments. However, the whole genome of the 130b strain has not been sequenced yet. Only the sequences of three *L. pneumophila* strains have been completed, namely strain Philadelphia-1, Paris, and Lens (35, 38). All gene and protein information were obtained from the *L. pneumophila* Philadelphia-1 database (38). In some cases, the experiments were performed with the *L. pneumophila* strains Corby or Philadelphia-1. Towards identifying novel *Legionella* phospholipases A, four different approaches were conducted:

1. Screening the *L. pneumophila* genome for paralogs of PlaA
2. Screening an *L. pneumophila* genomic library in *E. coli* for hemolytic activities
3. Screening the *L. pneumophila* genome for patatin-like protein genes
4. Purification of proteins with PLA activity followed by N-terminal protein sequencing

4.1 Screening the *L. pneumophila* genome for paralogs of PlaA

4.1.1 Identification of two new *Legionella* genes that code for putative lipolytic enzymes

Since *L. pneumophila* secretes PLA and acyltransferase activities encoded by yet unidentified genes, it was of interest to find potential candidates coding for these activities. The genome of *L. pneumophila* encodes two paralogs of PlaA, the major secreted lysophospholipase A (75). These two proteins were viewed as likely candidates for possessing lipolytic properties as well. These two putative lipolytic enzymes were designated PlaC and PlaD for PLA protein C and D, respectively. As shown in figure 4.1, an alignment of PlaC and PlaD with PlaA showed that all three enzymes possessed the five blocks of conserved amino acid sequences which are characteristic for the GDSL group of putative lipolytic enzymes defined by Upton and Buckley (209). GDSL enzymes are found in prokaryotes and eukaryotes and show PLA, LPLA, acyltransferase, and/or hemolytic activities. Figure 4.1 also features the GDSL proteins SatA of *Aeromonas salmonicida* which is a glycerophospholipid:cholesterol acyltransferase (GCAT) and the type III translocated effector SseJ of *Salmonella typhimurium* which was recently shown to possess lipolytic properties as well (146).

	Organism	Gi No.	Name	Function	Δ	Block I	Δ
A)	*Legionella pneumophila*	52843033	PlaC	GCAT, PLA, LPLA	30	I**V**VF**GDSLSD**NG	113
B)	*Legionella pneumophila*	52842793	PlaD	PLA, LPLA	10	L**V**VL**GDSLSD**RG	103
C)	*Legionella pneumophila*	52842553	PlaA	LPLA	23	I**V**VF**GDSLSD**NG	46
D)	*Aeromonas salmonicida*	39028	SatA	GCAT, PLA, LPLA	27	I**V**MF**GDSLSD**TG	42
E)	*Salmonella typhimurium*	9931614	SseJ	deacylase	144	L**V**FF**GDSLSD**SL	44

	Block II	Δ	Block III	Δ	Block IV	Δ	Block V	Δ
A)	KAF**GG**SWSATYD	43	SDET**L**YFIYS**G**S**N**DYI	34	A**G**ARRFVIMGI**P**HVGDT**P**	118	**F**W**D**EI**HPT**TRA**H**	30
B)	YCE**GG**LTSHDYS	39	KSET**L**VVEWS**G**A**N**DLI	78	N**G**YRNFVLFNL**P**NLSLT**P**	49	**F**W**D**DV**HPT**ATM**H**	170
C)	YAF**GG**AGVSVDE	24	SPDS**L**FVIWI**G**A**N**NYL	26	K**G**AKHILVLNL**P**DLGRT**P**	99	**FF**D**L**V**HPT**ALA**H**	25
D)	EAE**GG**ATAVAYN	27	KPDD**L**VILWV**G**A**N**DYL	26	N**G**AKQILLFNL**P**DLGQN**P**	123	**F**W**D**QV**HPT**TVV**H**	24
E)	FAE**GG**STSASYS	21	SHQD**L**AIFLL**G**A**N**DYM	23	G**G**VNNVLVMGI**P**DLSLT**P**	88	**F**N**D**LV**HPT**QEV**H**	18

FIG.4.1. Alignment of homologous amino acid blocks of the three members of the *L. pneumophila* Philadelphia-1 GDSL family hydrolases and homologous proteins. PlaC, PlaD, and PlaA as well as *Aeromonas salmonicida* SatA and *Salmonella typhimurium* SseJ were aligned and the conserved blocks of amino acids are shown. Members of the putative catalytic triad are underlined. Alignments were performed with the web-based program MaliP (www.softberry.com).

4.1.2 Expression kinetics of *L. pneumophila* 130b *plaC* and *plaD*

Since *plaC* and *plaD* were identified by genome analysis, nothing was known about the conditions of their expression. Therefore, it was necessary to determine whether *plaC* and *plaD* were expressed during extracellular growth of *L. pneumophila* in the standard laboratory medium BYE. The *L. pneumophila* strain 130b was chosen for the following investigations, because most of the studies concerning lipolytic enzymes of *L. pneumophila* have been conducted with this strain, which is one of the most virulent laboratory strains (9, 10, 72, 73, 75). Thus, *L. pneumophila* 130b was grown in BYE broth and samples were taken at six different optical densities, corresponding to different growth phases (OD_{660}=0.5 lag phase, OD_{660}=0.8, OD_{660}=1.1 early logarithmic growth phase, OD_{660}=1.7, OD_{660}=2.0 mid to late logarithmic growth phase, OD_{660}=2.3 early stationary growth phase) and mRNA was isolated. The isolated mRNA samples were used in a RT-PCR with primers specific for *plaC* (gdsl2_s2_f and gdsl2_s2_r) and *plaD* (gdsl3_s4_f and gdsl3_s3_r) with expected product lengths of 461 bp and 435 bp, respectively (see chapter 3.2.2.1). Figure 4.2 shows the result of such a qualitative RT-PCR experiment. The expression of the gyrase gene served as a control for the presence of mRNA, because the gyrase gene is expressed during all phases of *L. pneumophila* extracellular growth (29). Samples were also checked for contamination with DNA which was found to be absent (lanes D). The *plaC* gene was expressed during all growth phases of extracellular growth. In contrast, the *plaD* gene was not expressed during any of the examined growth phases of *L. pneumophila* 130b. Since only *L. pneumophila* 130b *plaC* was found to be expressed during extracellular growth of the bacterium, the characterization of PlaC was chosen as the next step.

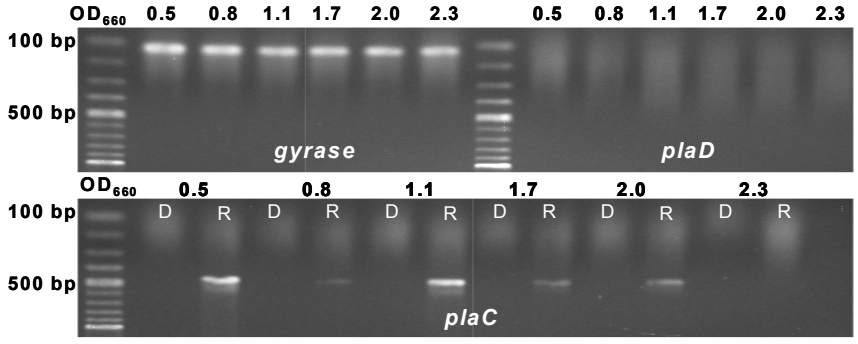

FIG.4.2. Expression kinetics of *L. pneumophila* 130b *plaC* and *plaD*. RT-PCR of *L. pneumophila* 130b *plaC* and *plaD* with specific primers from RNA templates isolated from bacterial liquid cultures at six different optical densities at 660 nm as indicated. The detection of the constitutively expressed gyrase gene served as a control for the presence of RNA. Samples were also checked for DNA contamination (lanes D). Lanes R represent the amplification of the *plaC* gene from RNA. Number of experiments: 2.

4.1.3 Characterization of the *L. pneumophila* GDSL enzyme PlaC

4.1.3.1 Genetic locus of *plaC* in *L. pneumophila* Philadelphia-1

One of the PlaA paralogs, designated PlaC (gi52843033), is coded by an ORF of 1302 bp length and was predicted to represent a protein of 433 amino acids with a molecular mass of about 49.8 kDa and an isoelectric point of 5.27. Moreover, the PlaC protein was predicted to have a signal sequence of 22 amino acids at its N-terminus and might therefore be secreted by the sec-system and additionally be a further candidate for a type II secreted protein. The PlaC sequence showed 26% identity and 46% similarity to the sequence of its paralog PlaA and 22% similarity and 40% identity to the sequence of *A. salmonicida* SatA, an orthologous GDSL protein with acyltransferase, PLA and LPLA activities (33). In addition, PlaC contained all five conserved blocks characteristic for members of the GDSL family (Fig. 4.1). Next, the genetic *plaC* locus was examined in the completely sequenced *L. pneumophila* strain Philadelphia-1 (38). Two uncharacterized genes flank *plaC* (Fig. 4.3).

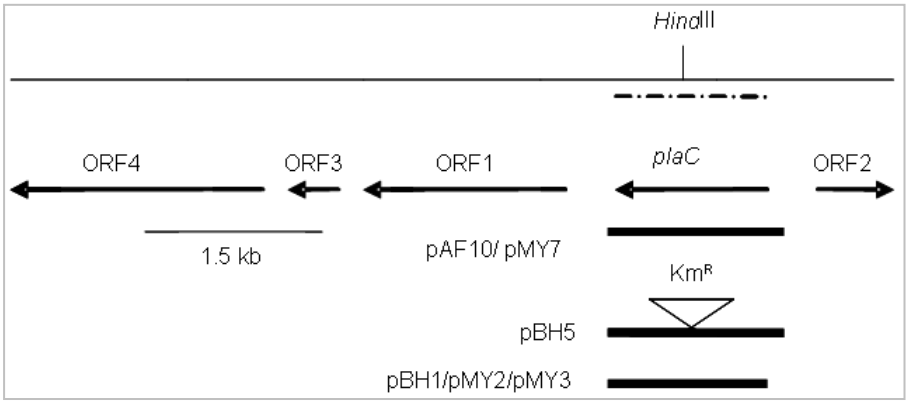

FIG.4.3. The *plaC* locus in *L. pneumophila* and recombinant *E. coli*. The upper line represents the *L. pneumophila* Philadelphia-1 chromosome region that contains the *plaC* gene, along with the location of the relevant *Hind*III restriction site which was utilized for introduction of a Km^R cassette. The dotted line below illustrates the region which was sequenced from 130b. The arrows below this line depict the relative location, size, and orientation of *plaC* and neighboring ORFs. The lines at the bottom of the figure represent the segments of *Legionella* DNA that were cloned into plasmid vectors. Plasmid pBH5 contained a Km^R gene cassette in the *plaC* gene.

Interestingly, the ORFs 1 to 3 surrounding *plaC*, encoded proteins which showed homology to different transferases. The downstream ORF1 which is oriented in the same direction as *plaC* possesses homology to a putative glucosamine-fructose-6-phosphate aminotransferase of *Pseudomonas aeruginosa* (gi15600742) (195). The oppositely oriented upstream ORF2 displays homology to a putative sulfurtransferase of *Microbulbifer degradans* (gi 48862923). ORF3 is homologous to a putative thiopurine methyltransferase of *Photobacterium profundum* (CAG20091). A gene encoding a predicted transcriptional accessory protein is located farther downstream (ORF4) which shows homology to the Tex protein of *Bordetella*

pertussis involved in toxin expression (78) (Fig. 4.3). It is unlikely that *plaC* and ORF1 form an operon as they are separated by 367 bp and because -10 and -35 promotor sequences exist within the intergenomic region. Thus, *plaC* most probably is transcribed monocistronically.

4.1.3.2 Isolation of *L. pneumophila* 130b *plaC* mutants

To investigate the enzymatic activities of PlaC in *L. pneumophila* and its importance for bacterial infection, knockout mutants of the *plaC* gene were generated. First, an approximately 1.6 kb fragment was amplified using 130b DNA by means of the primers gdsl2_a1_f and gdsl2_b1_r and cloned into pGEMTeasy, yielding pAF10 (Fig. 4.3). Then a Km^R cassette was inserted into the *Hind*III restriction site of pAF10, resulting in pBH5 (Table 3.19). pBH5 was subsequently used to introduce a Km^R cassette into the chromosomal *plaC* gene of strain 130b by allelic exchange taking advantage of the natural competence of *L. pneumophila* when grown at 30°C (75, 194). Four independent *plaC* mutants (plaC2, plaC4, plaC5, plaC8) were obtained. The mutation in the *plaC* gene was confirmed by PCR and Southern blot analysis (data not shown and see Appendix). In the following experiments, results are shown mostly for plaC5, but plaC2 and plaC4 behaved similarly. plaC8 differed from the other clones regarding colony morphology and intracellular multiplication in host cells which might be due to a second-site mutation in a gene or genes other than *plaC* (data not shown).

4.1.3.3 Lipolytic activities of *L. pneumophila plaC* mutants

As PlaA, the major secreted LPLA of *L. pneumophila* is a paralog of PlaC, the *L. pneumophila* 130b *plaC* mutants were tested for loss of lipolytic activities. Lipolytic activities were determined by measuring the amount of free fatty acids (FFA) released from respective substrates. Accordingly, culture supernatants and cell lysates of the *plaC* mutants obtained at late logarithmic growth phase (OD_{660}=2.0) were incubated with diacylphospholipids (DPPC, DPPG), substrates for PLA activity; lysophospholipids (MPLPC, MPLPG), substrates for LPLA activity; and a non-phospholipid (1-MPG), a substrate for lipase activity, and monitored for the release of FFA. Compared to the 130b wild type, the culture supernatant of the *plaC* mutants liberated less FFA from all the lipids tested (Fig. 4.4), implying that PlaC contributes to the exported PLA, LPLA, and lipase activities of *L. pneumophila*. That a LPLA can also cleave non-phospholipids and thereby show lipase activity has been already shown for PlaA, because the *L. pneumophila plaA* mutant exhibits a 50 % reduced capacity to cleave 1-MPG (73, 75). Interestingly, the *plaC* mutants also showed a decrease in the release of FFA from

the diacylphospholipids DPPC and DPPG (Fig. 4.4). On the other hand, the cell lysates of wild type and *plaC* mutants released comparable amounts of FFA from the substrates (data not shown). In conclusion, it was found that PlaC is a PLA and LPLA which is transported into the *Legionella* culture supernatant.

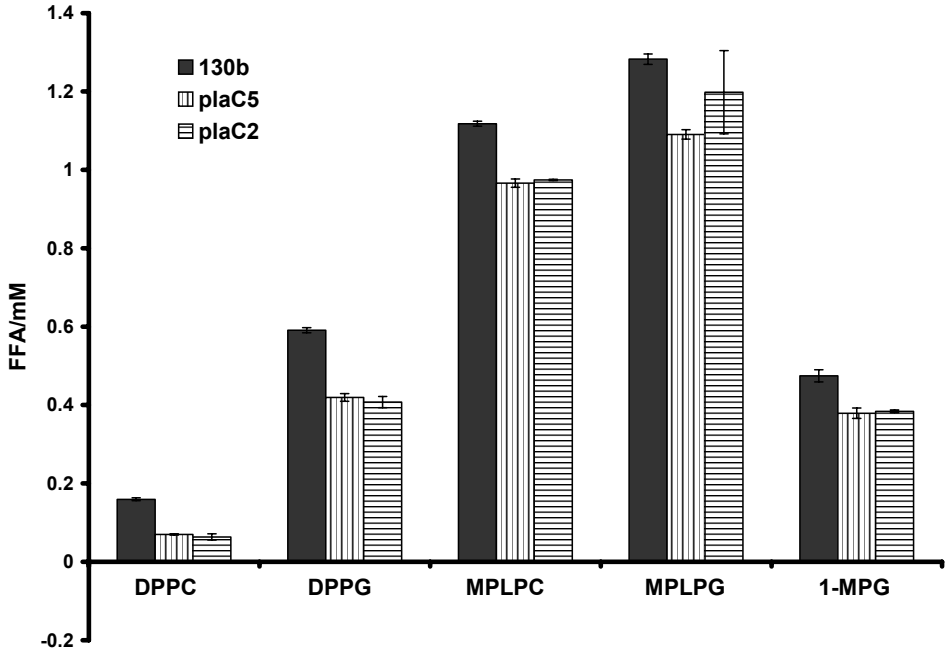

FIG.4.4. Secreted lipolytic activities of *L. pneumophila* wild type and a *plaC* mutant. Culture supernatants, obtained at late logarithmic growth phase (OD_{660}=2.0) of wild type and a *plaC* mutant were incubated with DPPC, DPPG, MPLPC, MPLPG, or 1-MPG for 5 h at 37°C. The release of FFA was quantified. Data are expressed as differences between the amount of FFA released by culture supernatants and the amount released by BYE broth. The results represent the means and standard deviations of duplicate cultures and are representative of three independent experiments. For all substrates lipolytic activities were significantly different from wild type ($P < 0.01$ for DPPC, DPPG, MPLPC and MPLPG, $P < 0.05$ for 1-MPG; Student`s t test).

Since PlaC showed homology to SatA from *A. salmonicida,* it was of interest to determine whether it is responsible for the GCAT activity observed in culture supernatants of *L. pneumophila* (75). In previous experiments, it was established that DPPG is the preferred substrate of *L. pneumophila* GCAT (75). In the presence of GCAT, a fatty acid residue from a phospholipid-donor molecule is transferred to cholesterol resulting in the formation of cholesterol ester which can be detected for example by TLC. Indeed, whereas the culture supernatant of *L. pneumophila* wild type incubated with DPPG and cholesterol showed GCAT activity, culture supernatant of the *plaC* mutants lacked GCAT activity (Fig. 4.5A), indicating that *plaC* is essential for the secreted GCAT activity of *L. pneumophila*. Interestingly, under the same reaction conditions, the *plaC* mutant also generated reduced amounts of an additional so far unidentified spot (Fig. 4.5A). Since this spot only occurs when cholesterol is

added to the lipid reaction mixture, it is likely representing an unknown cholesterol derivative (data not shown). Unlike the culture supernatants, the bacterial cell lysates of both wild type and *plaC* mutants, under the chosen reaction conditions, did not possess GCAT activity (data not shown). Thus, PlaC contributes not only to PLA and LPLA activities but is also the major secreted GCAT of *L. pneumophila*.

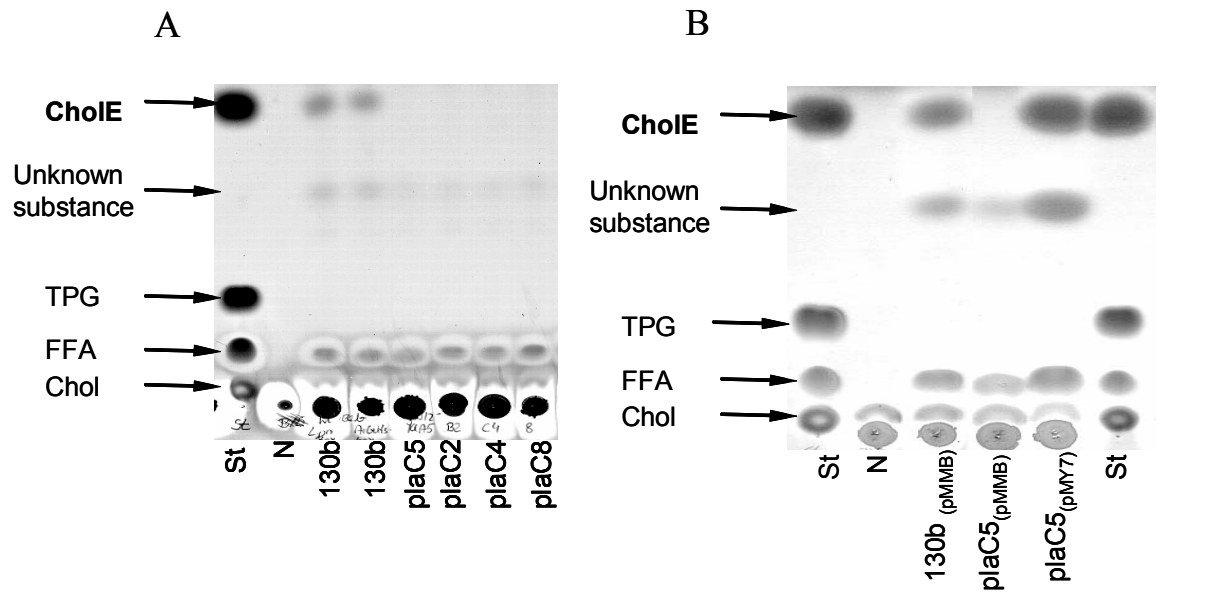

FIG.4.5. TLC analysis of secreted GCAT activity of *L. pneumophila* wild type and different mutants. Culture supernatant (obtained at OD_{660}=2.0) of wild type 130b (shown in duplicate), *plaC* mutants plaC5, plaC2, plaC4, and plaC8 were incubated with a mixture of DPPG and cholesterol for 23 h at 37°C, and then lipids were extracted and applied to TLC (Fig. A). Culture supernatant of wild type and the *plaC* mutant plaC5 harbouring the empty pMMB2002 vector and trans complemented plaC5 (harbouring pMY7) were incubated with a mixture of DPPG and cholesterol for 23 h at 37°C, and then lipids were extracted and applied to TLC (Fig. B). An apolar petroleum ether solvent mixture was employed for the separation of the apolar lipids, in particular for cholesterol ester. N: negative control, St: lipid standards, Number of independent experiments: 3.

4.1.3.4 Lipolytic activities of *trans* complemented *L. pneumophila plaC* mutants

Next it was assessed whether the introduction of *plaC* in *trans* could restore the missing lipolytic activities of the *L. pneumophila plaC* mutants, in particular the missing GCAT activity. Towards that end, an approximately 1.56 kb fragment containing *plaC* with its native promoter region was amplified from the *L. pneumophila* 130b genome using primers gdsl2_a1_f and gdsl2_b1_r and Pfu polymerase. The amplification product was cloned into pMMB2002 linearized with *Sma*I, resulting in pMY7 which was directly transformed into an *L. pneumophila plaC* mutant. Subsequently, culture supernatants of the wild type and the *plaC* mutant harbouring either the empty pMMB2002 vector or pMY7 were assessed for GCAT activity by incubation with cholesterol and DPPG. As expected, the wild type showed

GCAT activity indicated by the formation of cholesterol ester which was missing in the *plaC* mutant harbouring the empty pMMB2002 vector (Fig 4.5B). In contrast, the *plaC* mutant harbouring pMY7 with intact *plaC* showed GCAT activity thereby confirming that PlaC is indeed responsible for the secreted GCAT activity of *L. pneumophila* (Fig 4.5B). Next, culture supernatant of the wild type as well as the *plaC* mutant harbouring pMMB2002 or pMY7 was assessed for PLA, LPLA and lipase activities by monitoring the release of FFA from respective substrates. Again, the culture supernatant of plaC5 harbouring the empty pMMB2002 vector showed a reduced capacity to cleave FFA from DPPC, MPLPC and 1-MPG compared to the wild type (Fig 4.6). In contrast, plaC5 harbouring pMY7 exhibited a considerable increase in the release of FFA from DPPC and 1-MPG, verifying that PlaC contributes to the secreted PLA and lipase activities of *L. pneumophila* (Fig 4.6). The LPLA activity could not be restored by *trans* complementation (Fig 4.6). It is possible that the over expression of *plaC* might result in the formation of partially folded PlaC with restricted activity. Taken together, it was demonstrated that PlaC contributes to *L. pneumophila* PLA and lipase activities and is essential for GCAT activity of *L. pneumophila*.

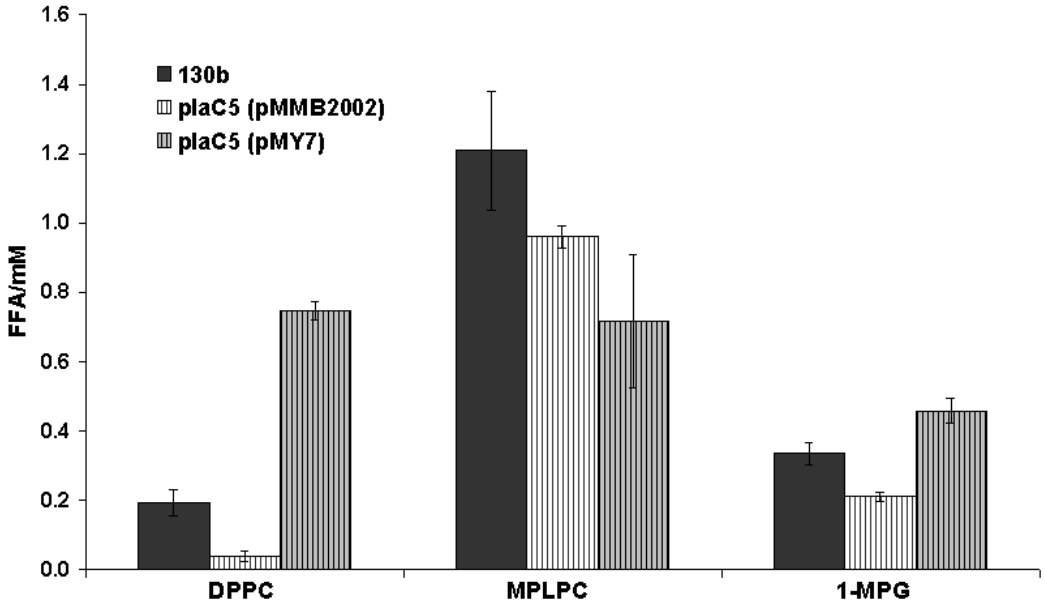

FIG.4.6. Secreted lipolytic activities of *L. pneumophila* wild type, *plaC* mutant, and complemented strain. Culture supernatants of wild type, the *plaC* mutant plaC5 harbouring the empty pMMB2002 vector and plaC5 harbouring pMY7 (obtained at OD_{660}=2.0) were incubated with DPPC, MPLPC, or 1 MPG for 5 h at 37°C. The release of FFA was quantified. Data are expressed as differences between the amount of FFA released by culture supernatants and the amount released by BYE broth. The results represent the means and standard deviations of duplicate cultures and are representative of three independent experiments. For all substrates except MPLPC lipolytic activities were significantly different from the plaC5 mutant ($P < 0.01$; Student`s t test).

4.1.3.5 Secretion and activation of PlaC by *L. pneumophila*

Since the *L. pneumophila plaC* mutants showed reduced lipolytic activities in their culture supernatant and since the PlaC protein possessed a predicted signal sequence and might therefore be type II secreted, a type II secretion mutant (*lspDE*) was examined for secretion of PlaC represented by its GCAT activity. The culture supernatant of the type II secretion mutant showed considerably decreased acyltransferase activity (Fig. 4.7). This indicates that either PlaC is exported by the type II system or that its activity is dependent on a type II secreted effector. Since the *lspDE* mutant also lacks the type II secreted zinc-metalloprotease (Msp or ProA) which has been shown to contribute to PLA and LPLA activities of *L. pneumophila* culture supernatants, the culture supernatant of an isogenic *proA* mutant was also tested for GCAT activity (9, 75, 82, 163). It was found that the culture supernatant of the *proA* mutant had also lost its GCAT activity, suggesting that ProA is directly or indirectly involved in PlaC activation (Fig. 4.7).

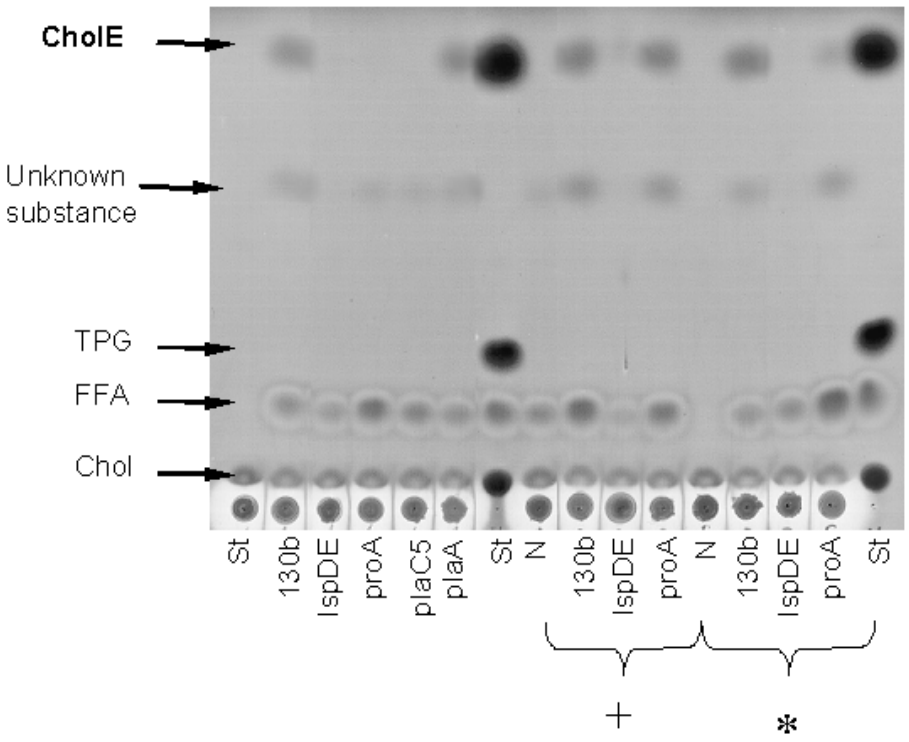

FIG.4.7. Secretion and activation of PlaC by *L. pneumophila*. Culture supernatant of wild type (130b), *lspDE* mutant, *proA* mutant, *plaC* mutant plaC5 and *plaA* mutant (obtained at OD_{660}=2.0) were either incubated with a mixture of DPPG and cholesterol or additionally to the lipid mixture incubated with supernatant from a *plaC* mutant (+) or partly purified ProA (*) for 20 h at 37°C, and then lipids were extracted and applied to TLC. An apolar petroleum ether solvent mixture was employed for the separation of the apolar lipids, in particular for cholesterol ester. N: negative control, St: lipid standards, Number of independent experiments: 2.

To exclude the possibility that the lack of GCAT activity in the culture supernatant of the *lspDE* mutant was simply due to the absence of ProA, the culture supernatant of the *lspDE* mutant was coincubated with a) the supernatant of a *plaC* mutant which still contains

protease activity and other type II secreted activities but lacks GCAT activity and b) with partially purified chromatography fractions containing ProA. For both incubations, the wild type showed GCAT activity whereas the type II secretion mutant still did not show GCAT activity confirming that PlaC itself is a candidate for a type II secreted effector (Fig. 4.7). In contrast, the GCAT activity could be recovered from culture supernatants of the *proA* mutant by incubation with the culture supernatant of a *plaC* mutant or partially purified ProA (Fig. 4.7). In conclusion, it was shown that PlaC is another candidate for export by the type II secretion system of *L. pneumophila* and is dependent on the presence of the zinc metalloprotease.

4.1.3.6 Enzymatic activities of *E. coli* clones harbouring the *plaC* gene

L. pneumophila plaC mutants showed reduced PLA, LPLA and lipase activities and a loss of acyltransferase activity in their culture supernatants. Since *L. pneumophila* possesses several lipolytic enzymes which may influence each other, the enzymatic activities of PlaC were additionally analyzed in recombinant *E. coli* clones. Therefore, a 1.3 kb fragment containing *plaC* without its putative promoter region was amplified from the *L. pneumophila* 130b genome using primers gdsl2_c1_f and gdsl2_e1_r and cloned into pGEMTeasy, resulting in pBH1. *plaC* from pBH1 was then subcloned into pBCKS, yielding pMY2. Further subcloning of *plaC* from pMY2 into the vector pMMB2002 generated pMY3 (Table 3.19). These constructs were transformed into *E. coli* DH5α yielding the desired clones with the intact *plaC* gene. Next, the recombinant *E. coli* clones harbouring pMY2 were assayed for PLA, LPLA, lipase, and acyltransferase activities in both culture supernatants and cell lysates (Fig. 4.8). Indeed, compared to the clone containing the empty pBCKS vector, the cell lysates from the *E. coli* clones harbouring pMY2 showed an increased capacity to cleave fatty acids from MPLPC and MPLPG indicating that PlaC, like PlaA, is an LPLA (Fig. 4.8). There was a small increase in the amount of FFA released from DPPC, which was not consistently reproducible in additional experiments and since no increased FFA release could be observed for DPPG, it is not yet clear whether PlaC also expresses PLA activity in *E. coli*. No increased release of fatty acids from any of the tested substrates could be detected in the culture supernatant, indicating that PlaC is not exported into the culture supernatant by *E. coli* (data not shown).

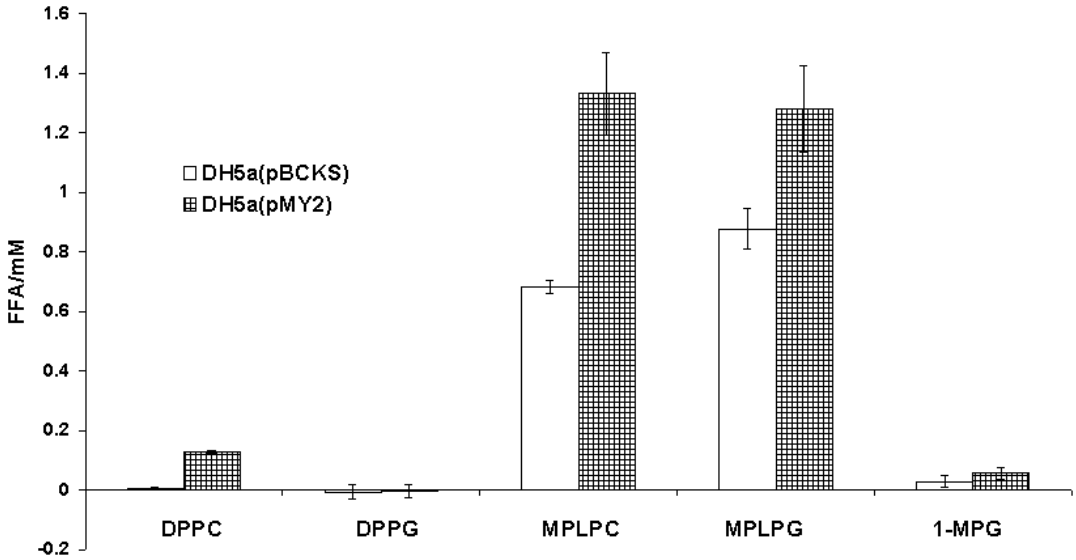

FIG.4.8. Cell-associated lipolytic activities of recombinant *E. coli* DH5α containing *L. pneumophila plaC*. Cell lysates of *E. coli* containing pBCKS or its derivative pMY2 (obtained at OD_{660}=2.0) were mixed with DPPG, DPPC, MPLPC, MPLPG, and 1-MPG. After 23h incubation at 37°C, the release of FFA was quantified. Data are expressed as differences between the amount of FFA released by cell lysate and the amount released by Tris-HCl buffer. The results represent the means and standard deviations of duplicate cultures and are representative of three independent experiments.

Additionally, it was of relevance to assess whether GCAT activity could also be detected in *E. coli* clones harbouring *plaC*. To this purpose, culture supernatants and cell lysates of the *E. coli* clones were assayed for acyltransferase activity. *E. coli* clones containing only pBCKS or pMMB2002 did not show acyltransferase activity in their culture supernatants and cell lysates. In contrast, GCAT activity could be detected in cell lysates but not in culture supernatants of *E. coli* clones containing *plaC* in pMMB2002 (pMY3) (Fig. 4.9). *E. coli* clones carrying the *plaC* gene in the pBCKS vector (pMY2) did not show GCAT activity in their culture supernatants or in the bacterial lysates (Fig. 4.9). As described above, in *L. pneumophila* the GCAT activity of PlaC was found to be dependent on a factor secreted by *L. pneumophila* which could either be the zinc metalloprotease ProA itself or a factor dependent on ProA. Therefore, the effect of culture supernatant of the *plaC* mutant (showing no GCAT but protease activity) on the acyltransferase activity of *plaC* cloned into *E. coli* was additionally investigated. In order to stimulate PlaC activity, culture supernatants and cell lysates of *E. coli* clones harbouring *plaC* as well as the respective clones harbouring the empty vector were coincubated with culture supernatant of an *L. pneumophila plaC* knockout mutant, DPPG, and cholesterol. Under these conditions, the cell lysates but not the culture supernatants of recombinant *E. coli* clones containing pMY2 or pMY3 both showed increased

GCAT activity confirming that *plaC* actually codes for an acyltransferase (Fig. 4.9 and data not shown). Taken together, these data corroborate that *plaC* confers LPLA and GCAT activities to *E. coli* and that the latter activity can be enhanced by a factor present in *L. pneumophila* culture supernatant.

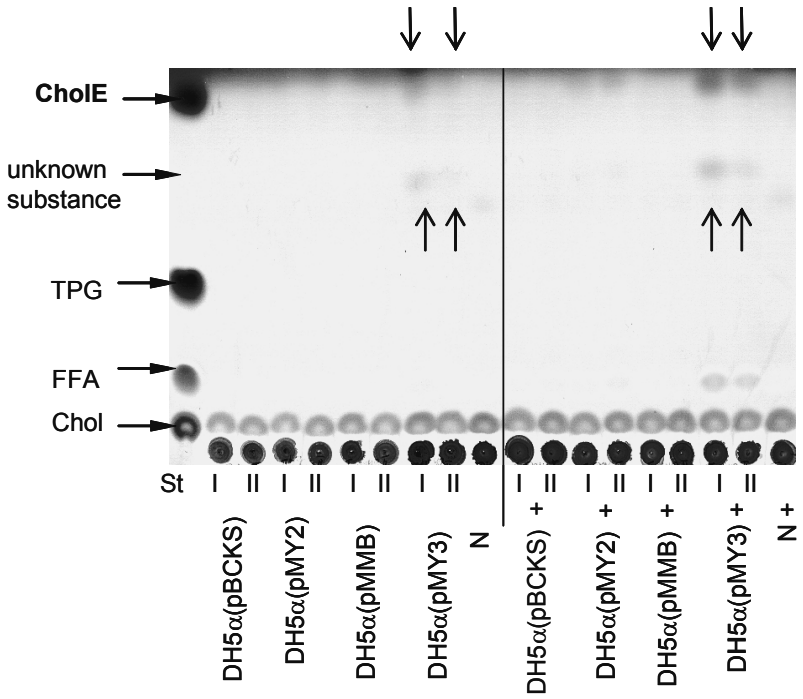

FIG.4.9. Cell-assocoated acyltransferase activities of recombinant *E. coli* DH5α containing *L. pneumophila plaC*. Cell lysates of *E. coli* containing pBCKS or its derivative pMY2 as well as pMMB2002 or its derivative pMY3 were incubated with a mixture of DPPG and cholesterol or additionally to the lipid mixture incubated with supernatant from a *plaC* mutant (+) for 20 h at 37 °C. Lipids were extracted and applied to TLC. An apolar petroleum ether solvent mixture was employed for the separation of the apolar lipids, in particular for cholesterol ester. The arrows denote the presence of cholesterol ester or the unknown substance related to cholesterol. N: negative control, St: lipid standards, Number of independent experiments: 3. I and II indicate duplicate cultures.

4.1.3.7 The role of *plaC* during intracellular infection of amoebae and macrophages

Since phospholipases are also known as virulence factors supporting intracellular survival of bacteria, the importance of PlaC for the infection of amoebae and macrophages was assessed in the following. To determine whether *plaC* is essential for *L. pneumophila* to infect its natural host, *A. castellanii* amoebae were inoculated with wild type *L. pneumophila* and *plaC* mutants and the CFU were counted at various time points. The *plaC* mutants showed the same increase in CFU during the whole infection period as the wild type

(Fig. 4.10). Namely, both the *plaC* mutants and *L. pneumophila* wild type multiplied about 100,000- to 1,000,000-fold by 72 h post inoculation. Additionally, the capability of the *plaC* mutants to infect U937 macrophages was investigated. Again, *L. pneumophila* wild type and *plaC* mutants displayed comparable replication rates (Fig. 4.10). In summary it was concluded that *plaC* is not essential for infection of and replication within *A. castellanii* amoebae and U937 macrophages. Its paralog PlaA was also found to be dispensable for the infection of host cells by *L. pneumophila* (75). However, since both enzymes possess LPLA activity and as there is a third GDSL enzyme present in *L. pneumophila* a functional redundancy might enable the GDSL enzymes to replace each other during the infection process.

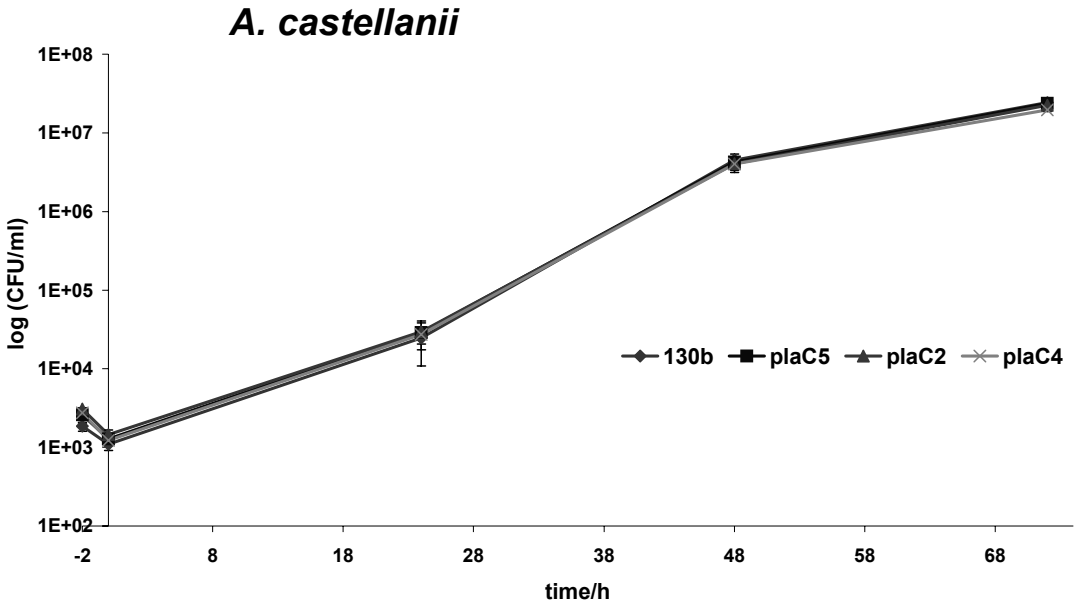

FIG.4.10a. Infection of A*canthamoebae castellanii* by wild type and *plaC* mutant *L. pneumophila*. Strains 130b and the *plaC* mutants plaC5, plaC2, and plaC4 were used to infect *A. castellanii* amoebae at a multiplicity of infection of 0.01. At various time points post inoculation, the number of bacteria was quantified by plating aliquots on BCYE agar. Results represent the means and standard deviations of triplicate samples and are representative of three independent experiments.

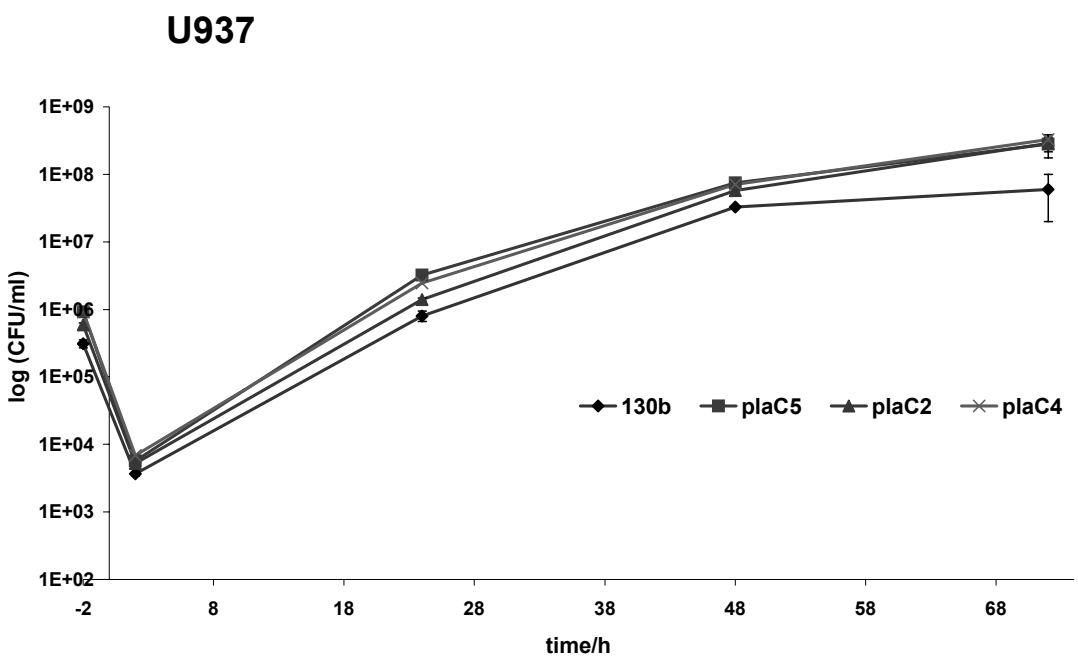

FIG.4.10b. Infection of U937 macrophages by wild type and *plaC* mutant *L. pneumophila*. Strains 130b and the *plaC* mutants plaC5, plaC2, and plaC4 were used to infect U937 macrophages at a multiplicity of infection of 1. At various time points post inoculation, the number of bacteria was quantified by plating aliquots on BCYE agar. Results represent the means and standard deviations of triplicate samples and are representative of three independent experiments.

4.1.3.8 Modification of host cell membrane sterols by *L. pneumophila* during infection

As *L. pneumophila* PlaC is a secreted enzyme which is able to modify cholesterol, it may be a means of the bacterium to alter the host membrane constituents. *L. pneumophila* and most other bacteria do not contain cholesterol in their membranes; however it is an important component of eukaryotic, in particular mammalian cells. Therefore, it was of interest to determine whether *L. pneumophila* modifies macrophage membrane cholesterol during infection and whether PlaC is involved in this process. To this purpose, U937 macrophages were infected with *L. pneumophila* 130b wild type or a *plaC* mutant with an MOI of 1, respectively for 72 h. As a control, U937 cells were incubated with medium (RPMI + 10 % FCS), only. After 72 h, the lipids including cholesterol and cholesterol esters from the pelleted macrophages were extracted with a mixture of chloroform and methanol and applied on a TLC plate. Figure 4.11 shows the lipid composition of U937 cells after 72 h of infection with *L. pneumophila.* As can be seen, the lipid extract of uninfected macrophages contains in addition to more polar lipids (which remain at the starting point), cholesterol,

fatty acids, and tripalmitoylglycerol but no cholesterol esters. Since it is known that mammalian cells produce cholesterol ester as a storage form for cholesterol, it is possible that the normal cholesterol ester level might be too low to be detectable by the applied staining method. Interestingly, cholesterol ester was detectable in macrophage extracts which had been infected with *L. pneumophila* (Fig. 4.11). But the formation of cholesterol ester was also visible when the macrophages were infected with a *plaC* mutant, indicating that the acylation of cholesterol is not or at least not exclusively dependent on *L. pneumophila* PlaC (Fig. 4.11).

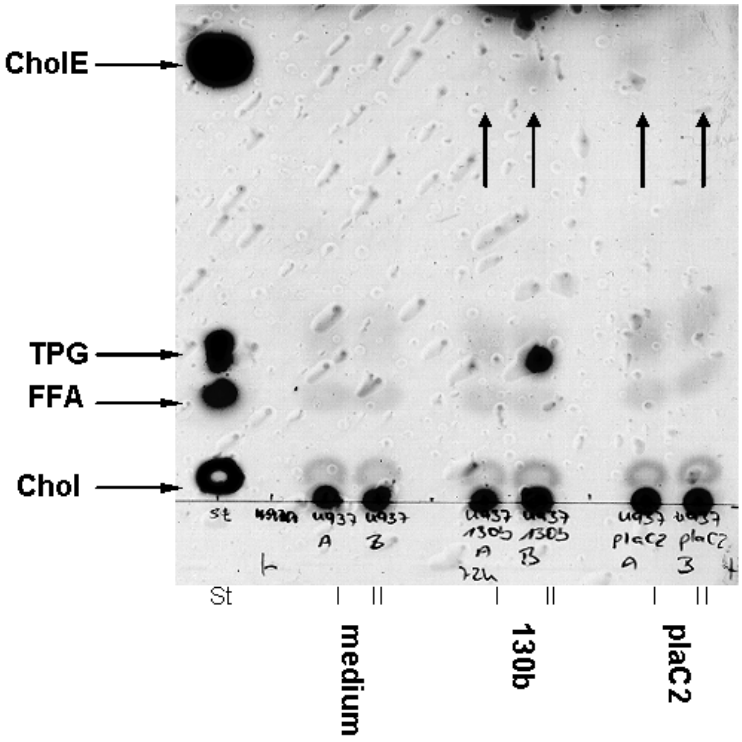

FIG.4.11. TLC analysis of lipids from U937 macrophages after infection with *L. pneumophila*. U937 macrophages were infected with *L. pneumophila* 130b wild type or a *plaC* mutant with an MOI of 1. As a control U937 cells were incubated with medium (RPMI + 10 % FCS), only. After 72 h, the lipids including cholesterol and cholesterol esters were extracted with a mixture of chloroform and methanol and applied on a TLC plate. An apolar petroleum ether solvent mixture was employed for the separation of the apolar lipids, in particular for cholesterol ester. N: negative control, St: lipid standards, Number of independent experiments: 2. I and II indicate duplicate cultures. The arrows denote the presence of cholesterol ester. Note: as the lipid extraction was carried out on a qualitative level, the extracts from the duplicate cultures show high variation in their lipid amounts.

Additionally, it was of interest to analyze whether the *A. castellanii* sterols were also modified during *L. pneumophila* infection. The *A. castellanii* membrane does not contain cholesterol but contains the related compound ergosterol (208). In order to determine whether the ergosterol of the *A. castellanii* membrane is also acylated during infection in a *Legionella*-dependent manner, amoebae were infected with *L. pneumophila* 130b wild type or *plaC* mutants with an MOI of 0.01, respectively for 18 h and 40 h. At the desired time points, either the whole infection sample (cells and supernatant) or only the pelleted amoebae were subjected to a lipid extraction (Fig. 4.12). Since no commercial ergosterol ester was available

at that time, cholesterol ester was used as a standard based on the assumption that ergosterol ester would be found in close proximity to the cholesterol ester. Figure 4.12 shows the extracted lipids from a 18 h- infection (comparable results were obtained after 40 h), the uninfected amoebal membrane (lanes marked p) mainly contained fatty acids but no cholesterol which is in accordance with the results reported by Ulsamer and colleagues (208). The ergosterol being slightly more polar than cholesterol was probably still located at the starting point as the employed solvent was not adequate for more polar compounds. When both the uninfected amoebal cells as well as the supernatant were used for lipid extraction (lane marked p+s), an additional spot running close to the cholesterol ester standard was visible indicating that the infection media contained some very non-polar lipid. However, the same lipids were observed for the infected amoebal extracts regardless whether the 130b wild type or *plaC* mutants were used. No additional spot appeared which could be correlated to ergosterol ester. In conclusion it appears that the ergosterol of amoebal membranes is not acylated by *L. pneumophila* suggesting that ergosterol might not be an adequate substrate for PlaC.

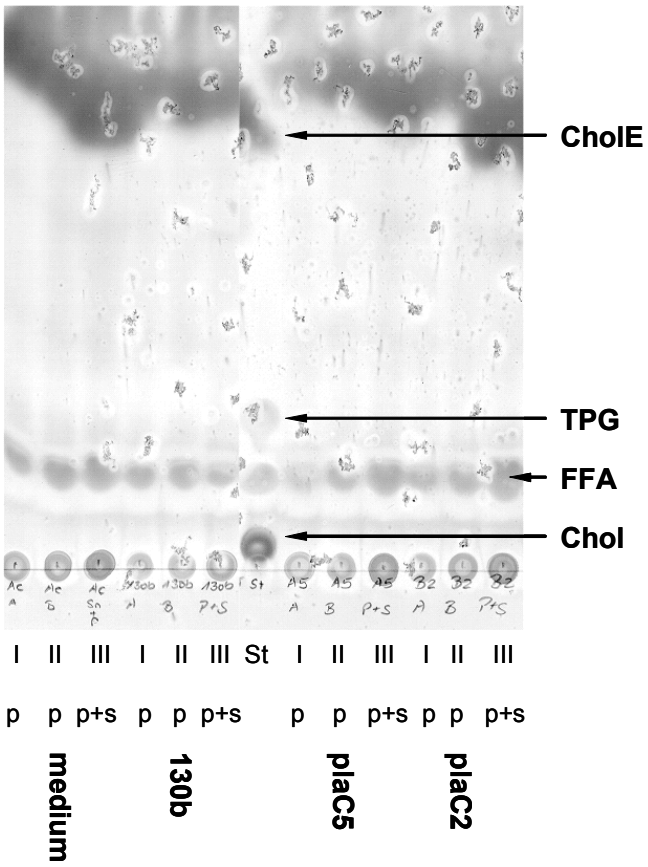

FIG.4.12. TLC analysis of lipids from *A. castellanii* after infection with *L. pneumophila*. *A. castellanii* amoebae were infected with *L. pneumophila* 130b wild type or two independent *plaC* mutants (plaC5 and plaC2) with an MOI of 0.01. As a control amoebae were incubated with infection medium (Table 3.6). After 18 h, the cells and the supernatant were mixed by pipetting and used for lipid extraction (marked as p+s) or alternatively only the cells were used for lipid extraction (marked as p). The lipids including ergosterol and ergosterol esters were extracted with a mixture of chloroform and methanol and applied on a TLC plate. An apolar petroleum ether solvent mixture was employed for the separation of the apolar lipids, in particular for cholesterol ester. N: negative control, St: lipid standards, Number of independent experiments: 2. I and II indicate duplicate cultures, III indicates pellet and supernatant mixture.

4.1.4 Characterization of the *L. pneumophila* GDSL protein PlaD

4.1.4.1 Genetic locus of *plaD* in *L. pneumophila* Philadelphila-1

Since both PlaA and PlaC were found to have lipolytic properties, it was of interest to investigate whether the third *L. pneumophila* GDSL protein possessed these properties as well. Although *plaD* was not found to be expressed under standard laboratory conditions in *L. pneumophila* strain 130b (Fig. 4.2), it was speculated that *plaD* might be expressed under special conditions (e.g. intracellular replication) or in another *L. pneumophila* strain. Therefore, the characterization of PlaD was chosen as the next step. The second paralog of *L. pneumophila* PlaA, designated PlaD (gi52842793) was a predicted protein of 516 amino acids and a molecular mass of 59.56 kDa with an isoelectric point of 8.1, which was encoded by an ORF of 1551 bp length. The putative protein did not contain a signal peptide, which makes it an unlikely substrate of the *L. pneumophila* type II secretion system. Interestingly, the region comprising the catalytical domains of GDSL hydrolases in the PlaD sequence extended from amino acids 11-345, resulting in a very large C-terminal extension of 170 amino acids (Figure 4.1). For comparison, the C-terminal extensions of the type II secreted proteins *L. pneumophila* PlaA, PlaC and *A. salmonicida* Sat A range from 24 to 30 amino acids and the type III secreted *Salmonella* effetor SseJ has a C-terminal extension of only 18 amino acids (Figure 4.1). Since the C-terminal region of a protein might be involved in type IVB secretion, PlaD represents a possible candidate for translocation by the Dot/Icm system (139). The PlaD sequence possesses 25 % identity and 42 % similarity to the PlaA protein sequence and 23 % identity and 43 % similarity to the PlaC protein sequence. The best characterized homolog was found to be SatA of *Aeromonas salmonicida* (gi9964017) (expect value=9×10^{-10}, 25 % identity, 43 % similarity) (33). However, these homologies were limited to the catalytic domains. The C-terminal part of PlaD (amino acids 346-516) did not possess homology to any known protein. The genetic locus of the *plaD* gene in *L. pneumophila* Philadelphia-1 consists of ORF1 (gi52842791) which is a putative d-alanyl-d-alanine dipeptidase, ORF2 (gi52842792) is a predicted papain c1 family cystein protease, and ORF3 which is a putative acid sphingomyelinase-like phosphodiesterase (Fig. 4.13). It is unlikely that ORF2 and *plaD* from an operon, because they are separated by 188 bp which includes putative -10 and -35 promotor sequences. Likewise, ORF3 and *plaD* cannot form an operon, as they are oppositely oriented.

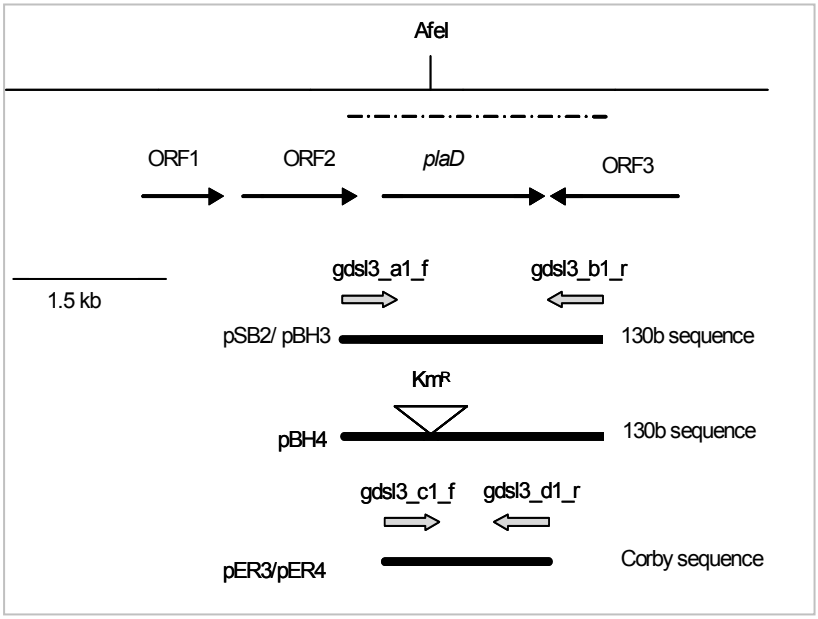

FIG.4.13. The *plaD* locus in *L. pneumophila* and recombinant *E. coli*. The upper line represents the *L. pneumophila* Philadelphia-1 chromosome region that contains the *plaD* gene, along with the location of the relevant *Afe*I restriction site which was utilized for introduction of a Km^R cassette. The dotted line below illustrates the region which was sequenced from 130b. The arrows below this line depict the relative location, size, and orientation of *plaD* and neighboring ORFs. The lines at the bottom of the figure represent the segments of *Legionella* DNA from strain 130b or Corby that were cloned into plasmid vectors. Plasmid pBH4 contained a Km^R gene cassette. The thick arrows represent primer pairs used for the amplification of the *plaD* gene and are not drawn to scale.

4.1.4.2 Expression kinetics of *plaD* in *L. pneumophila* strain Corby

As *plaD* was not expressed in *L. pneumophila* strain 130b, the *plaD* expression was additionally investigated in the pathogenic *L. pneumophila* strain Corby at four different optical densities (OD_{660}=1.0=early logarithmic growth phase, 1.6=mid logarithmic growth phase, 2.0=late logarithmic growth phase, 2.3=early stationary growth phase) during extracellular growth. Again, the isolated mRNA samples were used in a RT-PCR with *plaD* specific primers (gdsl3_s4_f and gdsl3_s3_r) and the expression of the gyrase gene (gyr) served as a control for the presence of mRNA (Fig. 4.14). Samples were found to be free of DNA contamination (Fig. 4.14, right picture). As shown in figure 4.14, *plaD* was indeed expressed in strain Corby when bacteria were grown in BYE broth. A *plaD* transcript could be detected from mid logarithmic (OD_{660}=1.6) until early stationary growth phase (OD_{660}=2.3). Since the *plaD* gene was expressed in strain Corby, the role of PlaD was further studied in this strain.

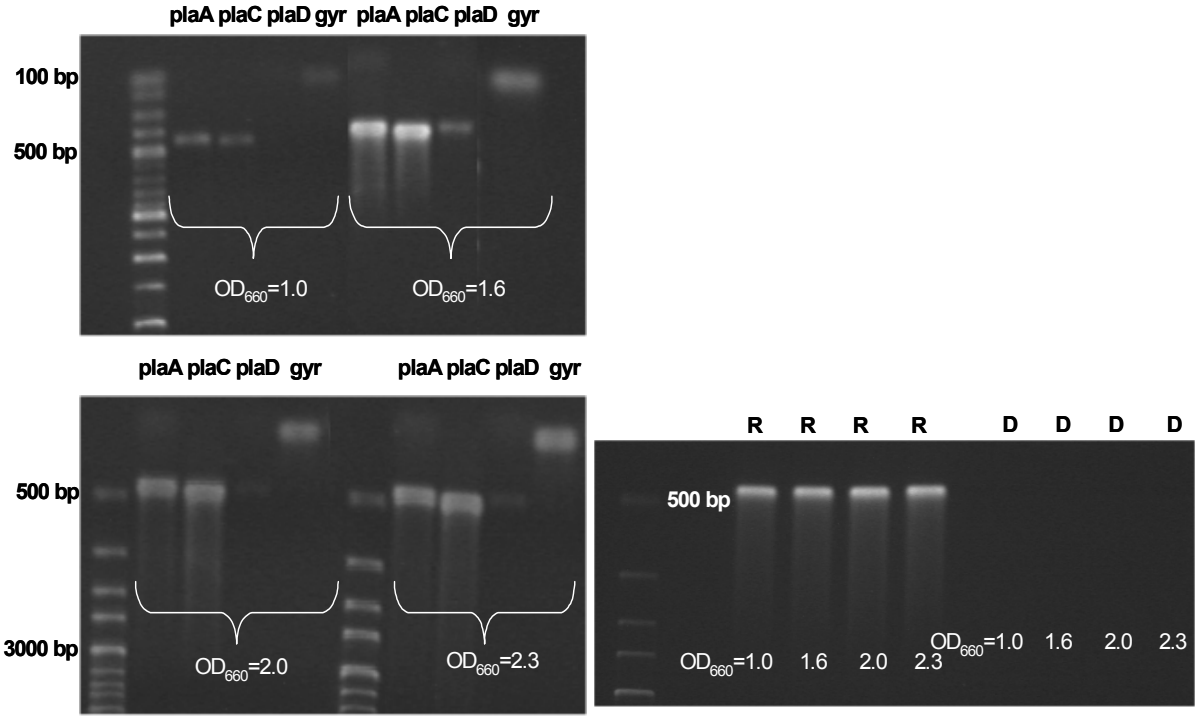

FIG.4.14. Expression kinetics of *L. pneumophila* Corby *plaA*, *plaC*, and *plaD*. RT-PCR of *L. pneumophila* Corby *plaA* using primers plaA_d1_f and plaA_e1_r (expected size: 444 bp), *plaC* using primers gdsl2_s2_f and gdsl2_s2_r (expected size: 462 bp), and *plaD* using primers gdsl3_s4_f and gdsl3_s3_r (expected size: 436 bp) from RNA templates isolated from bacterial liquid cultures at four different optical densities at 660 nm (OD_{660}=1.0, 1.6, 2.0, and 2.3) corresponding to different bacterial growth phases. The detection of the constitutively expressed gyrase gene (gyr) served as a control for the presence of RNA (GyrRTb_f and GyrRTb_r). Furthermore, the presence of RNA (lanes marked with R) and the absence of DNA (lanes marked with D) were checked using the primers plaA_d1_f and plaA_e1_r (right picture). Comparable results were obtained on one more occasion.

4.1.4.3 Isolation of *L. pneumophila* Corby *plaD* mutants

To study the enzymatic activities of PlaD in *L. pneumophila* and its importance for bacterial infection, knockout mutants of the *plaD* gene were generated. First, an approximately 1.9 kb fragment was amplified from the 130b genome (because the initial investigation was carried out in this strain) using the primers gdsl3_a1_f and gdsl3_b1_r (Fig. 4.13) and cloned into pGEMTeasy, yielding pSB2. The *plaD* gene from pSB2 was then subcloned into the plasmid pBCKS, yielding pBH3 (Table 3.19). Then a Km^R cassette was inserted into the *Afe*I restriction site of pBH3, resulting in pBH4. pBH4 was subsequently used to introduce a Km^R cassette into the chromosomal *plaD* gene of strain Corby by allelic exchange. Three independent *plaD* mutants (plaD- A4, plaD- C2, plaD- D8) were obtained. The mutation in the *plaD* gene was confirmed by PCR and Southern blot analysis (data not shown and see

Appendix). In the following experiments, results are shown mostly for plaD- A4, but plaD- C2 and plaD- D8 behaved similarly.

4.1.4.4 Lipolytic activities of *L. pneumophila* Corby *plaD* mutants

The *L. pneumophila* Corby *plaD* mutants were analyzed for lipolytic activities in the late logarithmic growth phase of the bacteria (OD_{660}=2.0) as the previous expression analysis indicated the presence of *plaD* transcript during this phase in the wild type (Fig. 4.14). Cell lysates as well as culture supernatants of *L. pneumophila* Corby wild type, two independent *plaD* mutants and for comparison two independent Corby *plaA* mutants were incubated with diacylphospholipids (DPPC and DPPG), monoacylphospholipids (MPLPC and MPLPG), or the lipid 1-MPG and the amount of released fatty acids was determined. The cell lysates of the Corby wild type, the *plaD* mutants, and the *plaA* mutants released comparable amounts of fatty acids from all employed substrates (data not shown). In contrast, the culture supernatants of the *plaD* mutants displayed a 50 % reduction in the hydolysis of the diacylphospholipids DPPG and DPPC, a 30 % reduction in hydrolysis of the monoacylphospholipid MPLPG, a 30 % reduction in the hydrolysis of 1-MPG, compared to wild type (Fig. 4.15). The Corby *plaA* mutants displayed an approximately 60 % reduction in the hydrolysis of the lysophospholipids MPLPG and MPLPC and an approximately 90 % reduction in the hydrolysis of 1-MPG (Fig. 4.15). This is similar to the activities of the *L. pneumophila* 130b *plaA* mutant, which is also reduced in LPLA and lipase activities (75). However, unlike the 130b *plaA* mutant, the corresponding mutants in strain Corby also displayed reduced hydrolysis of the diacylphospholipids DPPG and DPPC. Notably, the Corby *plaA* and *plaC* mutants show a comparable reduction in their secreted PLA activity whereas the LPLA and lipase activities display a stronger reduction in the *plaA* mutant than in the *plaD* mutant (Fig. 4.15). In conclusion, these data show that PlaD is a PLA and a LPLA which is secreted into the *L. pneumophila* culture supernatant.

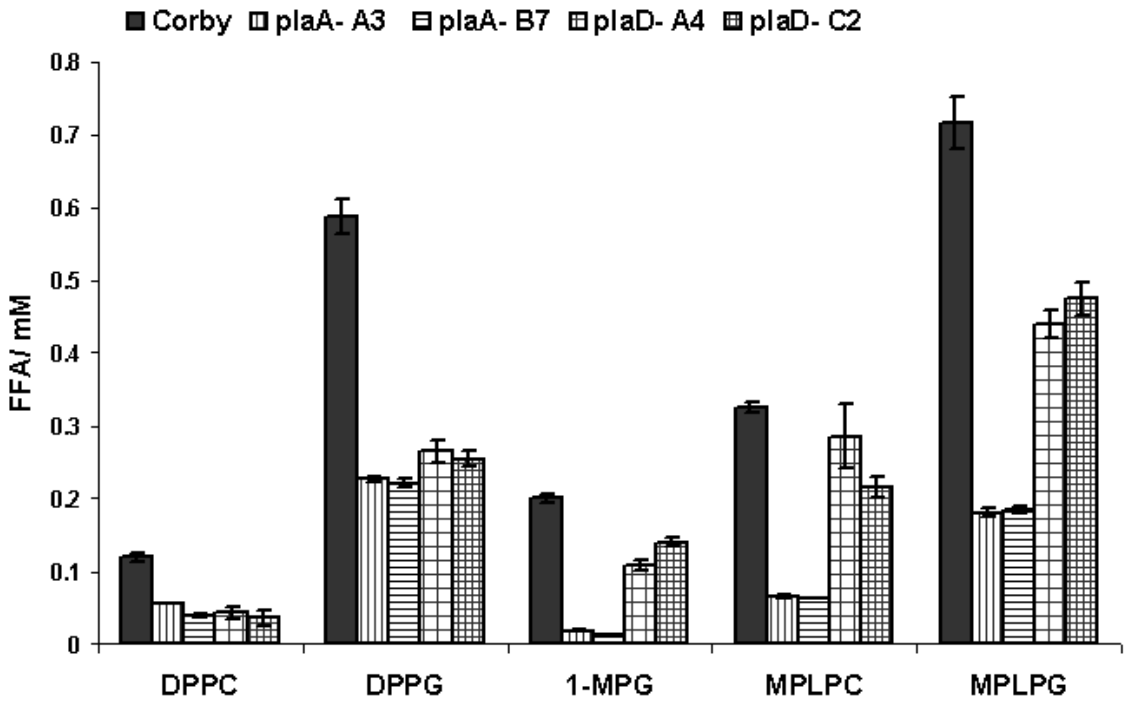

FIG.4.15. Secreted lipolytic activities of *L. pneumophila* Corby wild type, *plaA* mutants, and *plaD* mutants. Culture supernatants of Corby wild type, two independent *plaD* mutants and two independent *plaA* mutants were obtained during late logarithmic growth phase (OD_{660}=2.0) and incubated with DPPC, DPPG, MPLPC, MPLPG, or 1-MPG for 3 h at 37°C. The release of FFA was quantified. Data are expressed as differences between the amount of FFA released by culture supernatants and the amount released by BYE broth. The results represent the means and standard deviations of duplicate cultures and are representative of three independent experiments

4.1.4.5 Enzymatic activities of *E. coli* clones harbouring the Corby *plaD* gene

L. pneumophila Corby *plaD* mutants displayed a clear reduction in their secreted PLA and LPLA activities compared to Corby wild type. To investigate whether *plaD* could confer PLA and LPLA activities to *E. coli*, an approximately 1.56 kB fragment including the *plaD* gene without its putative promotor region was amplified from *L. pneumophila* Corby using primers gdsl3_c1_f and gdsl3_d1_r and cloned into the plasmid pGEMTeasy, resulting in pER3 (Fig. 4.13). The *plaD* gene from pER3 was then subcloned into the plasmid pBCKS, yielding pER4 (Table 3.19). The cell lysates as well as the culture supernatants from *E. coli* clones carrying pER4 were then examined for hydrolysis of PLA, LPLA, and lipid substrates. The culture supernatants from the *E. coli* clones harbouring pER4 released the same amount of fatty acids from all employed substrates as the clones carrying the pBCKS vector control (data not shown). The cell lysates of the *E. coli* clones harbouring *plaD* in *trans* showed the same hydrolysis of DPPC, DPPG and the lipid 1,2 DG but an increased hydrolysis of

monoacylphospholipids (MPLPC and MPLPG) compared to the clone carrying the empty vector (Fig. 4.16). Thus, these results show that *L. pneumophila* PlaD displays LPLA activity when expressed in *E. coli*. No PLA activity of PlaD was detectable in *E. coli* although the *L. pneumophila* Corby *plaD* mutants showed a high reduction in their PLA activity. Maybe the over expression of the *plaD* gene led to improper folding of the protein or some additional factor as is the case for PlaC was missing in *E. coli* resulting in restricted enzymatic activity of PlaD.

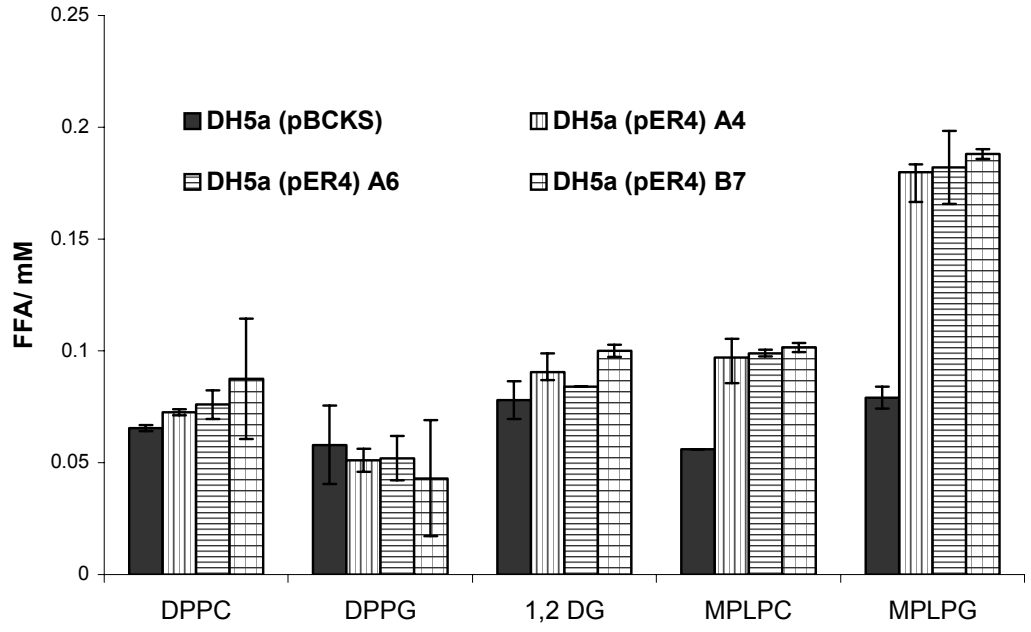

FIG.4.16. Lipolytic activities of recombinant *E. coli* DH5α containing *L. pneumophila* Corby *plaD*. Threefold concentrated cell lysates (obtained at OD_{660}=2.0) of *E. coli* containing pBCKS or its derivative pER4 were mixed with DPPG, DPPC, MPLPC, MPLPG, and 1,2-DG. After 3.5 h incubation at 37°C, the release of FFA was quantified. Data are expressed as differences between the amount of FFA released by cell lysate and the amount released by Tris-HCl buffer. The results represent the means and standard deviations of duplicate cultures and are representative of three independent experiments.

4.1.4.6 The role of *L. pneumophila* Corby PlaD during intracellular infection

To assess the importance of the GDSL enzyme PlaD during *Legionella* infection of host cells and compare it to the role of PlaA and PlaC in strain Corby, *L. pneumophila* Corby wild type as well as *plaA*, *plaC*, and *plaD* mutants were used to infect *Acanthamoeba castellanii*. The bacterial CFU were determined at various time points post infection. As can be seen in figure 4.17, the *plaD* mutants as well as the *plaA* and *plaC* mutants showed the same increase in CFU as the wild type, namely an increase of approximately three logarithmic units during

48 h of infection. Moreover, an infection of U937 macrophages demonstrated that PlaD as well as PlaA and PlaC were likewise dispensable for macrophage infection, as the *L. pneumophila* Corby *plaD*, *plaA*, and *plaC* mutants showed an increase in CFU of about five logarithmic units during 72 h of infection, comparable to Corby wild type (Fig. 4.17). Notably, *L. pneumophila* 130b *plaD* mutants were likewise found to be dispensable for the infection of *A. castellanii* amoebae and U937 macrophages (data not shown). In summary, these data show that none of the three GDSL enzymes alone is essential for intracellular replication in the two studied infection models.

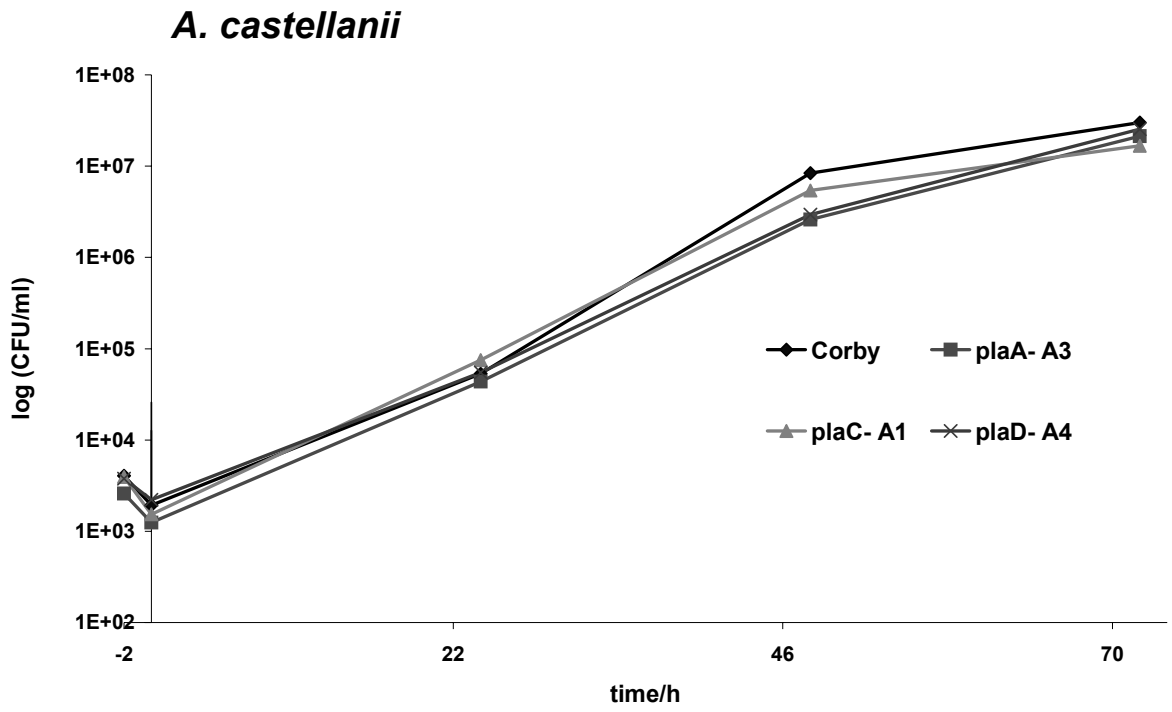

FIG.4.17a. Intracellular infection of *A. castellanii* by wild type Corby and *plaA*, *plaC*, and *plaD* mutant *L. pneumophila*. *Acanthamoeba castellanii* amoebae were inoculated with *L. pneumophila plaD*, *plaA*, and *plaC* knockout mutants as well as *L. pneumophila* Corby wild type (MOI of 0.01). At various time points post inoculation, the number of bacteria was quantified by plating aliquots on BCYE agar. Results represent the means and standard deviations of triplicate samples and are representative of three independent experiments.

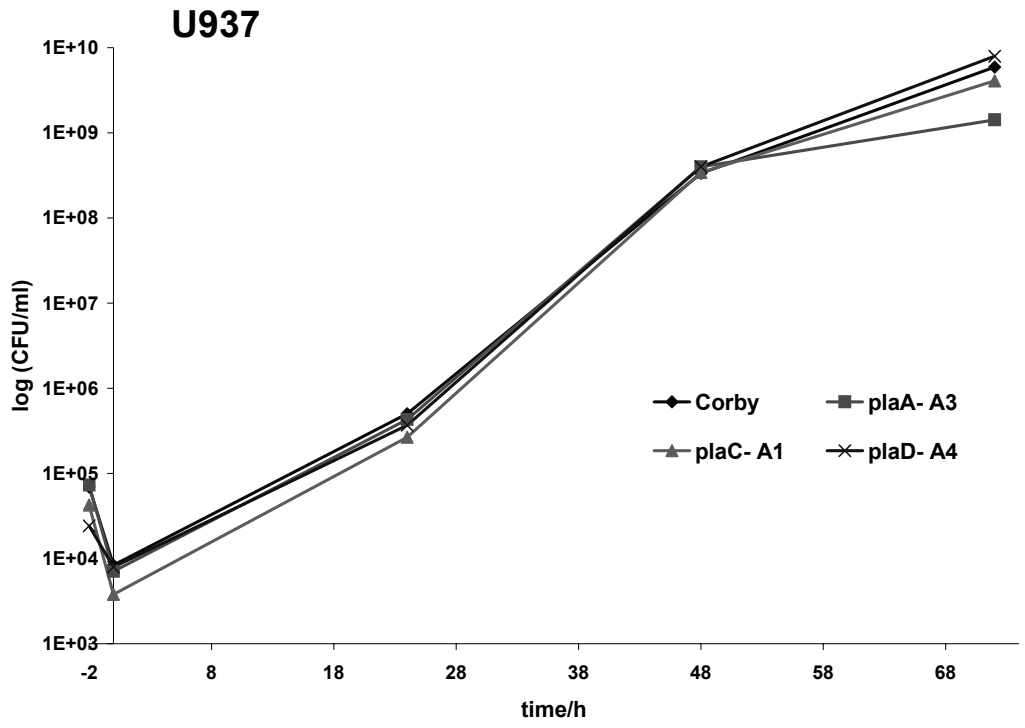

FIG.4.17b. Intracellular infection of U937 macrophages by wild type Corby and *plaA*, *plaC*, and *plaD* mutant *L. pneumophila*. U937 macrophages were inoculated with *L. pneumophila plaD*, *plaA*, and *plaC* knockout mutants as well as *L. pneumophila* Corby wild type (MOI of 1). At various time points post inoculation, the number of bacteria was quantified by plating aliquots on BCYE agar. Results represent the means and standard deviations of triplicate samples and are representative of three independent experiments.

In summary, two paralogs of the *L. pneumophila* lysophospholipase A, PlaA, were identified in the *L. pneumophila* genome and named PlaC and PlaD. All three Proteins belong to a group of lipolytic enzymes containing the characteristic conserved amino acid sequence GDSL. PlaC was shown to possess acyltransferase activity which transfers fatty acids from DPPG to cholesterol as well as phospholipase A and lysophospholipase A activities. PlaC is exported by the type II secretion system of *L. pneumophila* into the bacterial culture supernatant and requires the *L. pneumophila* zinc metalloprotease ProA for its activity. The third GDSL enzyme, PlaD, is likewise exported into the bacterial culture supernatant, as *L. pneumophila plaD* mutants possess reduced lipolytic activities in their culture supernatant but not in their cell lysates. The lack of a signal peptide suggests that PlaD is not exported by the type II secretion system and might therefore be a candidate for type IVB secretion. PlaD possesses LPLA activity and contributes to PLA activity in *L. pneumophila*. Thus, all three *L. pneumophila* GDSL enzymes have overlapping enzymatic activities, in particular in

their LPLA activity. Finally, the role of PlaC, PlaD, and PlaA during intracellular infection was assessed in strain Corby and all enzymes were found to be dispensable for infection of amoebae and macrophages. It seems likely that the dispensability of any one of the three GDSL enzymes for *L. pneumophila* infection is based on their ability to replace each other functionally.

4. 2. Screening an *L. pneumophila* genomic library in *E. coli* for hemolytic activities

Towards identifying novel virulence factors of *L. pneumophila*, the group of Klaus Heuner (University of Würzburg) screened an *L. pneumophila* Corby gene library in *E. coli* for hemolysis of human blood (76). From a pool of 8000 screened *E. coli* clones representing the *L. pneumophila* genome, three clones were found to be hemolytic, all of which contained the same gene (76). Since the protein encoded by this gene displayed partial sequence homology to the *L. pneumophila* lipase LipB (10) and possessed a lipase-like motif, its lipolytic properties were investigated in this study.

4.2.1 The genetic locus of *plaB* in *L. pneumophila* strain Philadelphia-1

The protein PlaB (gi52841831), for phospholipase A protein B, was predicted to consist of 474 amino acids with an isoelectric point of 8.75. The protein with the highest percentage of sequence identitiy to PlaB was a phospholipase (gi78365560) of *Shewanella* sp. (41% identity and 59% similarity). A paralog of PlaB is *L. pneumophila* LipB (gi21666984) with an expect value of 1.2, 25% identity and 41% similarity. The high expect value is due to the fact that the homology between the two protein sequences is limited to specific regions (Fig. 4.18). These regions therefore probably comprise the active site residues. Both proteins contain a lipase-like amino acid motif, namely TXSXG (Fig. 4.18). Notably, the LipB sequence owns a PFAM domain of PGAP-1 like proteins (www.sanger.ac.uk/Software/Pfam/) which is a group of proteins with glycosylphosphatidylinositol deacylase activity. An alignment of PlaB with LipB and human PGAP1 (gi46240862) showed that the PlaB sequence also possesses similar conserved amino acid regions to the other two proteins (Fig. 4.18).

	Organism	Gi No.	Name	Function	Δ	Block I	Δ	Block II
A)	*Legionella pneumophila*	52841831	PlaB	PLA, LPLA	4	VIFVH**G**WSVT	69	T**HS**T**GG**PIV**R**
B)	*Legionella pneumophila*	21666984	LipB	lipase	56	IVLIH**G**LMRT	56	T**HS**L**GG**IIV**R**
C)	*Homo Sapiens*	46240862	PGAP1	GPI deacylase	87	VLFLP**G**NAGS	73	G**HS**M**GG**LVA**R**

	Δ	Block III	Δ	Block IV	Δ
A)	18	**LIM**L**A**PANHGSALAQL	34	LNESWL**DY**	306
B)	16	**LIM**L**A**PPNQGSKLAKL	43	DAKVPP**DY**	39
C)	15	**LI**TQ**A**TPHVAPVMPLD	52	VAGGFR**DY**	675

FIG.4.18. Alignment of homologous amino acid blocks of *L. pneumophila* PlaB, LipB and human PGAP1. *L. pneumophila* PlaB, LipB, and human PGAP1 were aligned and the conserved blocks of amino acids are shown. Possible members of a putative catalytic dyad are underlined. Alignments were performed with the web-based program MaliP (www.softberry.com).

The PlaB protein did not contain a predicted N-terminal signal sequence which makes it unlikely to be secreted by the *L. pneumophila* type II secretion system. Due to the large C-terminal extension, PlaB might be secreted by the *L. pneumophila* type IVB secretion system (Fig. 4.18). Two open reading frames flank *plaB* both of which are oppositely oriented to *plaB* (Fig. 4.19). The upstream ORF1 encodes a protein named FLJ00180 containing a leucine rich domain with no homology to any characterized protein. The downstream ORF2 represents a protein of unknown function with homology to a hypothetical protein (gi67156042) of *Azotobacter vinelandii*.

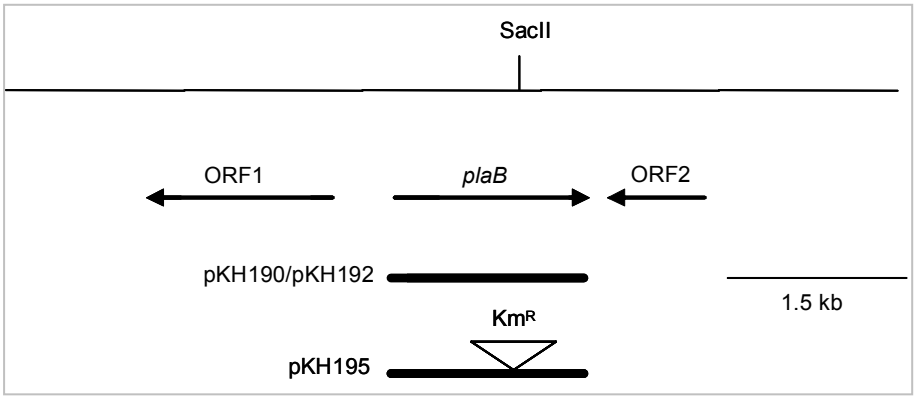

FIG.4.19. The *plaB* locus in *L. pneumophila* and recombinant *E. coli.* The upper line represents the *L. pneumophila* Philadelphia-1 chromosome region that contains the *plaB* gene, along with the location of the relevant *Sac*II restriction site which was utilized for introduction of a Km^R cassette. The arrows below this line depict the relative location, size, and orientation of *plaB* and neighboring ORFs. The lines at the bottom of the figure represent the segments of *Legionella* DNA from strain Corby that were cloned into plasmid vectors. Plasmid pKH195 contained a Km^R gene cassette (76).

4.2.2 Isolation of *L. pneumophila* Corby *plaB* mutants

In order to determine the degree to which *plaB* is responsible for lipolytic activities in *Legionella, plaB* mutants were generated in strain Corby by Klaus Heuner (Universität Würzburg) and Kerstin Rydzewski (Robert Koch-Institut). First, the *plaB* gene was amplified by using the primers pla1 and pla2 and cloned into plasmid pUC18, yielding pKH190. Then the *plaB* gene was disrupted by the insertion of a Km^R cassette into the *Sac*II restriction site of the gene. The mutants were produced by cloning the interrupted *plaB* gene of pKH194 into pBOC20 and by subsequent allelic exchange forced by the counter selectable *sacB* gene present in pBOC20 (63, 143) or by directly using pKH194 for allelic exchange. Two *plaB* mutants (plaB60 and plaB1) were obtained and confirmed by southern blot analysis (76).

4.2.3 Lipolytic activities of *L. pneumophila* Corby *plaB* mutants

L. pneumophila has been shown to secrete several lipolytic activities into the culture supernatant as well as to possess lipolytic activities associated with the bacterial cell (9, 10, 72, 73, 75, 135). To assess the *plaB* mutants with respect to lipid hydrolysis, the bacterial culture supernatants and cell lysates were examined for the ability to release fatty acids from DPPG, DPPC, MPLPG, MPLPC, and 1-MPG. The culture supernatant of wild type *L. pneumophila* and the mutants plaB60 and plaB1 showed comparable hydrolysis of all the tested substrates, suggesting that PlaB is not secreted into the culture supernatant of *L. pneumophila* (Fig. 4.20, upper part). However, the cell-associated activities hydrolyzing DPPG, DPPC, MPLPG, and MPLPC were dramatically reduced in the *plaB* mutants (Fig. 4.20, lower part). When the plasmid pKH192 containing the *plaB* gene was introduced into the mutant plaB60 (complemented strain received from Klaus Heuner), the cell-associated lipolytic activities were not only restored to the wild type level, but were even higher than in the wild type. These data show that *plaB* is the gene for the major cell-associated PLA and LPLA activities of *L. pneumophila*.

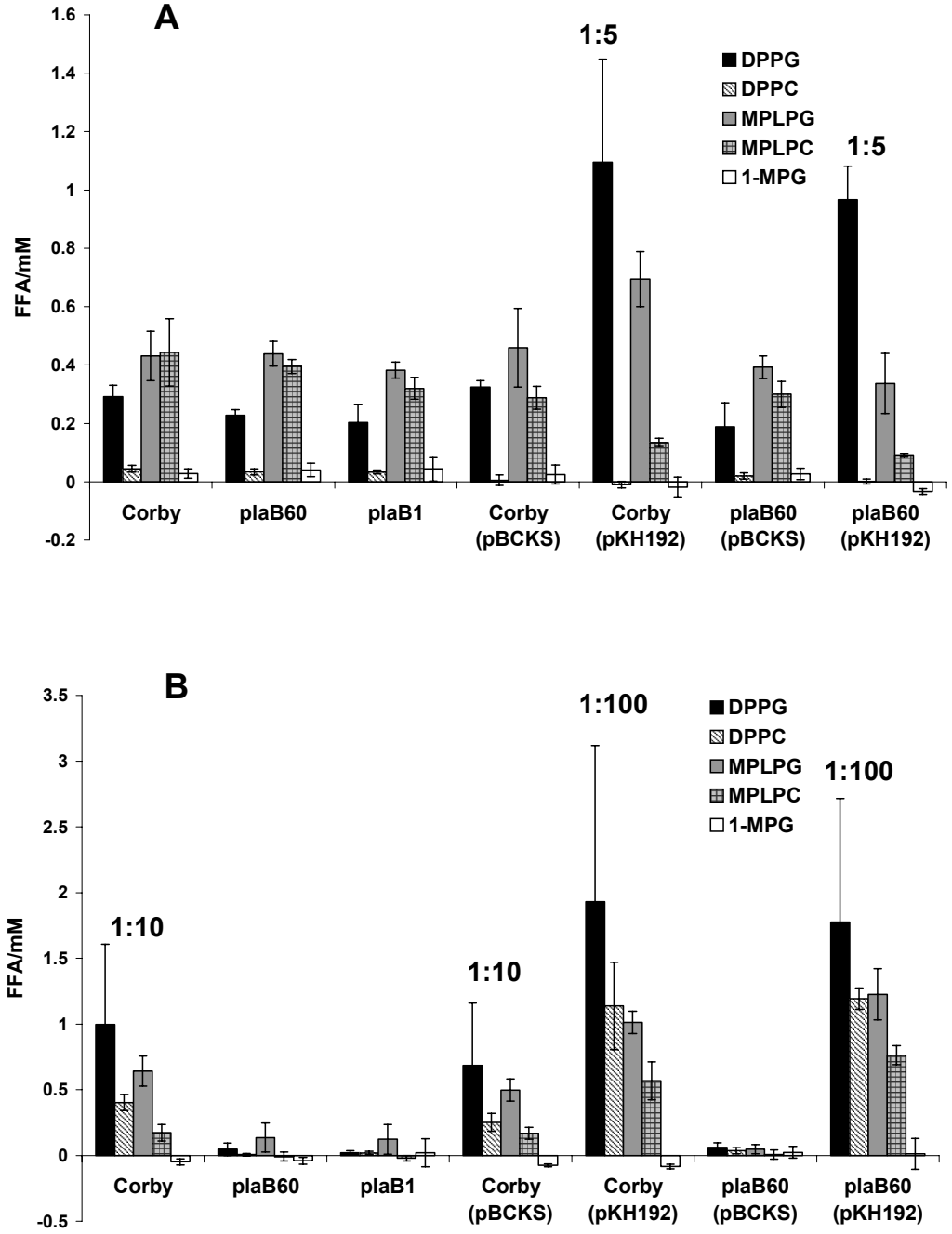

FIG.4.20. Lipolytic activities of wild type, *plaB* mutant, and genetically complemented *L. pneumophila* Corby strains. Culture supernatants (A) and cell lysates (B) of wild type, mutants plaB60 and plaB1, and genetically complemented *L. pneumophila* strains were incubated with the indicated lipids for 2h (A) or 30 min (B), and then the release of FFA was quantified. In some cases, culture supernatants or cell lysates were diluted as indicated prior to incubation. Data are expressed as differences between the amount of FFA released by the culture supernatant or cell lysate and the amount released by uninoculated BYE broth or Tris-HCl buffer, respectively. Results are means and standard deviations from duplicate cultures and are representative of three independent experiments.

To confirm that *plaB* mutants possessed reduced cell-associated lipolytic properties, lipid hydrolysis was examined by TLC as well. As shown in figure 4.21, the cell lysates of Corby wild type almost completely hydrolyzed the diacylphospholipids DPPC and DPPG (Fig. 4.21a, left part) releasing fatty acids from these substrates (Fig. 4.21a, right part). The hydrolysis of 1-MPG was also observed; however, fatty acid release from more non-polar substrates, e.g. 1,2-DG and TPG was not detectable in wild type (Fig. 4.21b). In contrast, the cell lysates of plaB60 and plaB1 did not release fatty acids from any of the substrates tested (Fig. 4.21a and b) corroborating the former results. The phenotype of the *L. pneumophila* plaB60 mutant was fully complemented by a plasmid copy of *plaB* (Fig. 4.21a and b). In summary, *L. pneumophila* PlaB is a cell-associated PLA and LPLA.

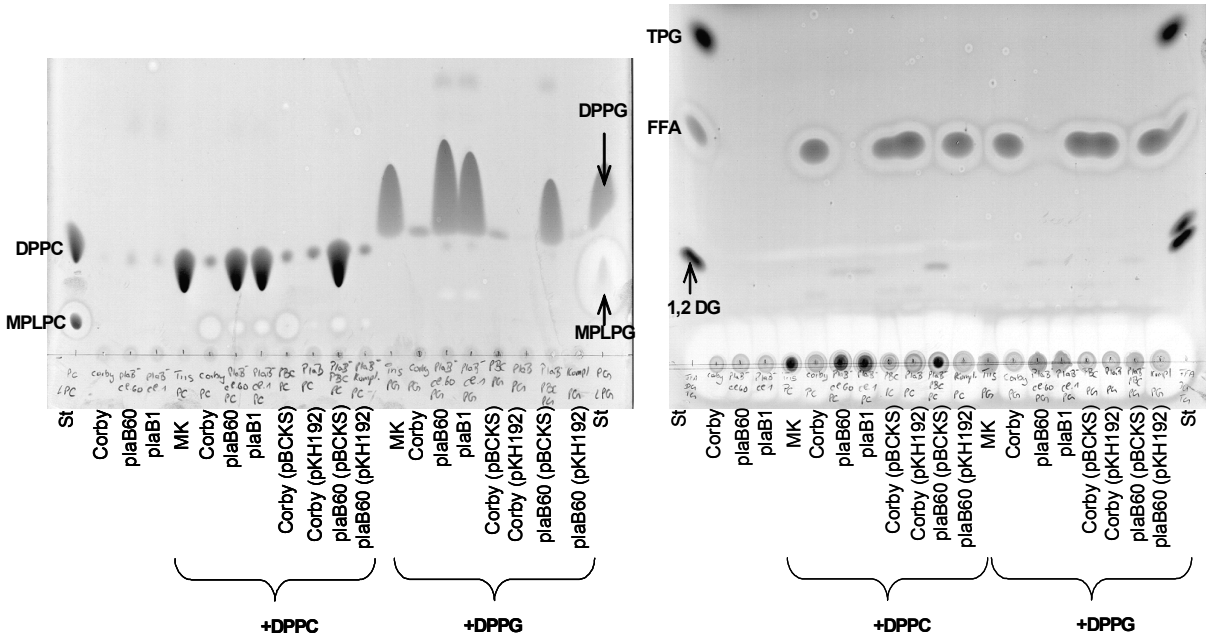

FIG.4.21a. TLC analysis of lipid hydrolysis by *L. pneumophila* Corby cell lysates. Cell lysates (obtained at OD_{660}=2.0) of Corby wild type, mutants plaB60 and plaB1, and genetically complemented *L. pneumophila* strains were incubated with the indicated lipids or as a background control with buffer, only for 24 h at 37 °C, and then lipids were extracted and subjected to TLC. A polar or apolar solvent mixture was used for the separation of the polar (left panel) or apolar (right panel) lipids, respectively. A mixture of Tris-HCl buffer and the lipids was also incubated and served as a negative control (MK). For qualitative identification of the lipid spots, lanes containing lipid standards (St) were included. The observations depicted here were made on one more occasion.

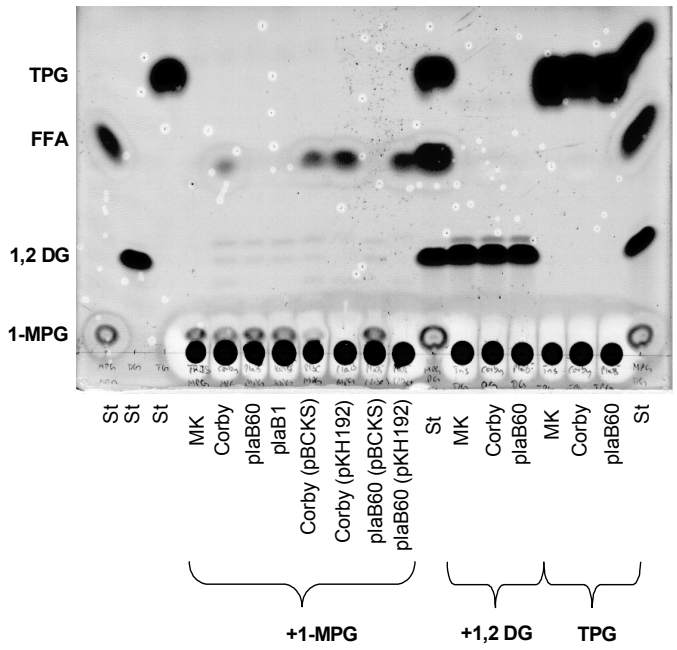

FIG.4.21b. TLC analysis of lipid hydrolysis by *L. pneumophila* Corby cell lysates. Cell lysates (obtained at OD_{660}=2.0) of Corby wild type, mutants plaB60 and plaB1, and genetically complemented *L. pneumophila* strains were incubated with the indicated lipids or as a background control with buffer, only for 24 h at 37 °C, and then lipids were extracted and subjected to TLC. A polar or apolar solvent mixture was used for the separation of the polar (A) or apolar (B and C) lipids, respectively. A mixture of Tris-HCl buffer and the lipids was also incubated and served as a negative control (MK). For qualitative identification of the lipid spots, lanes containing lipid standards (St) were included. The observations depicted here were made on one more occasion.

4.2.4 Enzymatic activities of *E. coli* harbouring *L. pneumophila* Corby *plaB*

L. pneumophila plaB mutants almost completely lack cell-associated PLA and LPLA activities. Therefore it was of interest to examine whether PlaB expressed these activities in *E. coli*. *E. coli* clones carrying the *plaB* gene in *trans* in the vector pBCKS were provided by Klaus Heuner (to this purpose, he subcloned the *plaB* gene from pKH190 into the vector pBCKS, yielding pKH192 which he transformed into *E. coli*). Then, the culture supernatants and cell lysates of *E. coli* clones carrying the *plaB* gene were assayed for fatty acid release from diacylglycerophospholipids (DPPG and DPPC), from 1-monoacylphospholipids (MPLPG and MPLPC), and from monoacylglycerol (1-MPG). Both culture supernatants and cell lysates of the hemolytic *E. coli* clones containing either pKH190 (pUC18+*plaB*) or pKH192 (pBCKS+*plaB*) released significantly more FFA from all of the tested lipid substrates than *E. coli* harboring the corresponding control vectors (Fig. 4.22). Clones containing *plaB* hydrolyzed predominantly the diacyl- and lysophospholipid substrates, showing that the respective protein product is both a phospholipase A and a lysophopholipase A. Moreover, the clone harboring pKH194 which contained the *plaB* gene disrupted by a Km^R cassette did not liberate increased amounts of FFA from the different lipids (Fig. 4.22). These results corroborate that *L. pneumophila* PlaB has PLA and LPLA activities both of which can be expressed in *E. coli*.

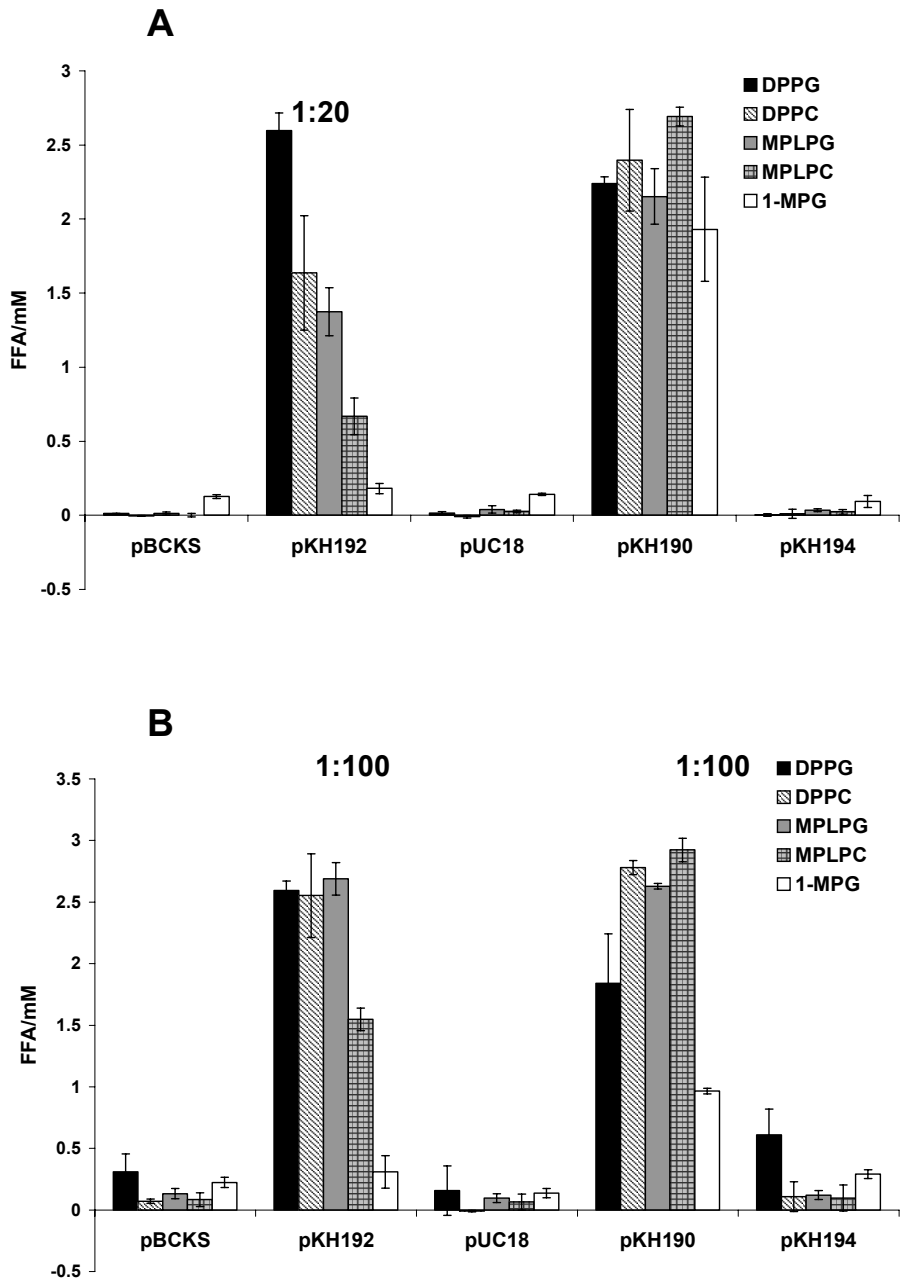

FIG.4.22. Lipolytic activities of recombinant *E. coli* DH5α containing *L. pneumophila* Corby *plaB*. Culture supernatants (A) and cell lysates (B) of *E. coli* containing pBCKS or its derivative pKH192, or pUC18, or its derivative pKH194, were incubated with the indicated lipids at 37 °C for 2h (A) or 50 min (B), respectively, and then the release of FFA was quantified. As indicated, in some cases the culture supernatants or cell lysates were diluted prior incubation. Data are expressed as differences between the amount of FFA released by the culture supernatant or cell lysates and the amount released by uninoculated LB broth or Tris-HCl buffer, respectively. Results are means and standard deviations of duplicate cultures and are representative of three independent experiments.

4.3. Screening the *L. pneumophila* genome for patatin-like protein genes

Patatins are a group of plant storage glycoproteins showing lipid acyl hydrolase-activity, e.g. phospholipase A activity (6). The patatin-associated lipolytic activity can be a means of defence against plant parasites or be involved in signal transduction pathways of the plant (94, 196). The first characterized bacterial protein with a patatin domain is the *Pseudomonas aeruginosa* type III secreted cytotoxin and virulence factor ExoU (174). Interestingly, *P. aeruginosa* ExoU possesses PLA, LPLA, and lipase activities (148, 150, 174). Since proteins with a patatin domain are potential PLAs, it was of interest to analyze the *L. pneumophila* genome for such proteins. Furthermore, as *P. aeruginosa* had been the only reported bacterium to own a protein with a patatin domain at that time, the occurrence of such proteins among bacteria in general was examined additionally.

4.3.1 Screening the genomes of completely sequenced bacteria for patatin-like protein genes

In order to find out whether patatin-like proteins (PLP) exist in bacteria other than *P. aeruginosa* and especially in *L. pneumophila*, all available bacterial genomes were searched for encoded proteins with homology to patatin B2 and *P. aeruginosa* ExoU by means of the BLAST algorithm (http://www.ncbi.nlm.nih.gov/sutils/genom_table.cgi) (5). However, with help of the Blast alorithm only a minimal number of hits for PLP in bacteria were obtained (< 20 for patatin B2 or ExoU, expect value $\leq$ 1). Therefore, another approach was conducted which was to apply the key word 'patatin' to screen the 216 accessible completed bacterial genomes (May 2005) using the text search tool of the pedant server (http://pedant.gsf.de). The pedant server provides extensive data from computational analysis of genome sequences by algorithms like PROSITE, PFAM, BLAST, and others. This time, a high number of hits were found (> 200) by means of the pedant server text search. In 326 proteins, text search hits for 'patatin' originated from the detection of the patatin domain (expect value $\leq$ 0.5) by the PFAM algorithm (19). These findings indicate that only short amino acid sequences of homology exist within related proteins. This might also explain why the application of the BLAST algorithm did not lead to adequate results. Genes encoding PLPs were detected in 116 of the 216 completed bacterial genomes including a wide range of Gram-positive and Gram-negative bacteria, such as *Bacillus* sp., *Brucella* sp., *Rickettsia* sp., *Staphylococcus aureus*, *Yersinia pestis* and many others. The average number of PLP genes among the genomes which coded for at least one PLP gene was 2.65.

Table 4.1 gives an overview of completely sequenced bacterial species which possess at least 0.5 PLP genes per 1000 ORFs. Notably, for *L. pneumophila*, eleven genes were detected in the case of strains Philadelphia-1 and Paris and ten genes in the case of strain Lens coding for proteins containing characteristic domains of patatin. It is noticeable that among the 216 accessible completed bacterial genomes of the pedant database, *L. pneumophila* Philadelphia-1 possessed with eleven PLP genes by far the highest number of PLP genes per 1000 ORFs, namely 3.74, followed by *Rickettsia prowazekii* Madrid and *Rickettsia typhi* Wilmington with two PLP genes each (2.39 and 2.04 PLP genes, respectively/ 1000 ORFs) and *Mycobacterium bovis* and *Mycobacterium tuberculosis* with eight PLP genes each (2.04 PLP genes/ 1000 ORFs).

4.3.2 Correlation of the number of patatin-like proteins with bacterial pathogenicity

It was found that particularly some animal pathogen and plant pathogen/symbiont genomes contained a high number of PLP genes, e.g. *Legionella pneumophila* (n=10 or 11), *Bradyrhizobium japonicum* (n=8), *Burkholderia pseudomallei* (n=7), *Mesorhizobium loti* (n=6), *Mycobacterium tuberculosis* (n=8), *Mycobacterium bovis* (n=8), and *Ralstonia solanacearum* (n=5) (Table 4.1). Therefore it was of interest to examine whether animal pathogens and plant pathogens/symbionts possessed more PLP genes than non-pathogens. Thus, the number of PLP genes present per 1000 open reading frames (ORFs) in the two groups was compared and it was found that the genomes of the pathogens/symbionts showed a significantly higher number of PLP genes than the genomes of non-pathogens, more precisely 0.82±0.68 and 0.49±0.29 ($P \leq 0.005$, Student's t-test), respectively. The number of PLP genes also varied between different species of a genus. For example, the genome of *Mycobacterium leprae* included only one PLP gene, whereas the genome of *M. tuberculosis* contained eight corresponding genes (Table 4.1). This finding is in agreement with a previous report which stated that *M. leprae* originated by a process of reductive evolution resulting in a minimal gene set sufficient for survival in its highly specialized niche (47). In contrast, 52% of the proteome of *M. tuberculosis* was derived from gene duplication (203), leading to a higher flexibility in utilizing nutrients. Furthermore, the genome of pathogenic *Escherichia coli* O157:H7 encoded a higher number of PLP genes (n=4) than the genome of non-pathogenic strain *E. coli* K-12 (n=2), which again implies a correlation between the number of PLP genes and virulence. Hence, a high number of PLP genes might confer an advantage to the bacterium in (i) interaction with the host, (ii) adaptation to various environments and (iii) competition with other microorganisms.

Table 4.1 Number of patatin-like genes found in completely sequenced bacterial genomes. To identify the number of patatin-like protein genes, 216 completely sequenced bacterial genomes from the pedant server (www.pedant.gsf.de) were searched by using the keyword 'patatin'. Only sequences containing a PFAM domain of patatin with an expect value ≤ 0.5 and containing at least 0.5 PLP genes per 1000 ORFs are listed (19). The number of PLP genes per 1000 ORFs, the number of PLP genes and the total number of ORFs found in the genomes are shown. The bacteria are listed according to decreasing number of PLP genes per 1000 ORFs.

Bacterial species	PLP genes /1000 ORFs	PLP	Total ORFs
Legionella pneumophila Philadelphia-1	3.74	11	2942
Legionella pneumophila Paris	3.47	11	3166
Legionella pneumophila Lens	3.41	10	2934
Rickettsia prowazekii Madrid E	2.40	2	834
Rickettsia typhi Wilmington	2.39	2	838
Mycobacterium bovis AF2122/97(spoligotype9)	2.04	8	3920
Mycobacterium tuberculosis H37Rv	2.04	8	3924
Mycobacterium tuberculosis CDC1551	1.91	8	4187
Chromobacterium violaceum ATCC12472	1.82	8	4407
Photobacterium profundum SS9	1.64	9	5480
Rickettsia conorii Malish 7	1.46	2	1374
Leptospira interrogans serovar Copenhageni Fiocruz L1-130	1.37	5	3660
Bacteroides fragillis YCH46	1.30	6	4625
Burkholderia mallei ATCC23344	1.26	6	4764
Burkholderia pseudomallei K96243	1.22	7	5729
Acinetobacter ADP1	1.20	4	3325
Symbiobacterium thermophilum IAM 14863	1.20	4	3337
Ehrlichia ruminantium Welgevonden (Uni Pretoria)	1.13	1	888
Bdellovibrio bacteriovorus HD100	1.12	4	3583
Vibrio cholerae N16961chr. I	1.10	3	2736
Caulobacter crescentus CB15	1.07	4	3737
Bradyrhizobium japonicum USDA110	1.06	8	7549
Leptospira interrogans serovar 56601	1.06	5	4727
Anaplasma marginale St Maries	1.05	1	949
Ehrlichia ruminantium Gardel	1.05	1	950
Vibrio fischeri ES114	1.05	4	3802
Porphyromonas gingivalis W83	1.05	2	1909
Bacteroides thetaiotaomicron VPI-5482	1.05	5	4778
Ehrlichia ruminantium Welgevonden (CIRAD)	1.04	1	888
Rhodopseudomonas palustris CGA009	1.04	5	4814
Thermus thermophilus HB27	1.01	2	1982
Ralstonia solanacearum + megaplasmid	0.98	5	5116
Treponema pallidum Nichols	0.97	1	1031
Brucella melitensis 16M (chr. I+II)	0.94	3	3198
Brucella suis 1330 (chr. I+II)	0.92	3	3264
Thermus thermophilus HB8	0.89	2	2238
Mannheimia succiniciproducens MBEL55E	0.84	2	2384
Shewanella oneidensis MR-1 (+megaplasmid)	0.84	4	4778
Neisseria meningitidis serogroup B (MC58)	0.50	1	1989
Neisseria gonorrhoeae FA 1090 (ATCC700825)	0.50	1	2002
Yersinia pseudotuberculosis IP32953	0.50	2	4021
Wolbachia endosymbiont of Drosophila melanogaster	0.84	1	1195
Vibrio parahaemolyticus O3:K6	0.83	4	4832
Mesorhizobium loti MAFF 303099+pMLa +pMLb	0.82	6	7275
Nitrosomonas europaea (ATCC19718)	0.81	2	2461
Bacillus thuringiensis serovar konkukian str 97-27	0.78	4	5117
Bacillus cereus ZK	0.78	4	5134
Bacillus cereus ATCC14579 (+pBClin15)	0.76	4	5255
Idiomarina loihiensis L2TR	0.76	2	2628
Eschericha coli O157:H7 EDL933 (ATCC 700927)	0.75	4	5349
Escherichia coli O157:H7 (RIMD 0505952)	0.75	4	5361
Escherichia coli CFT073	0.74	4	5379
Clostridium perfringens 13+pCP13	0.73	2	2723
Bacillus subtilis 168	0.73	3	4112
Bacillus cereus ATCC10987	0.71	4	5603
Vibrio vulnificius CMCP6 (chr. I+II)	0.66	3	4537
Aquifex aeolicus VF5	0.66	1	1522
Azoarcus sp EbN1	0.65	3	4599
Mycobacterium leprae TN	0.62	1	1605
Sinorhizobium meliloti 1021	0.60	2	3341
Vibrio vulnificius YJ016 (chr. I+II)	0.60	3	5024
Haemophilus ducreyi 35000HP	0.58	1	1717
Geobacter sulfurreducens PCA	0.58	2	3445
Bifidobacterium longum NCC2705	0.58	1	1729
Bacillus anthracis Sterne	0.57	3	5287
Geobacillus kaustrophilus HTA426	0.56	2	3540
Bacillus anthracis Ames	0.56	3	5311
Pseudomonas putida KT2440	0.56	3	5350
Lactobacillus johnsonii NCC533	0.55	1	1821
Bacillus anthracis Ames 0581 (+pX01+pX02)	0.54	3	5558
Thermotoga maritima MSB8	0.54	1	1846
Pseudomonas aeruginosa PAO1	0.54	3	5565
Lactobacillus acidophilus NCFM	0.54	1	1864
Streptococcus thermophillus LMG18311	0.53	1	1889
Streptococcus thermophillus CNRZ1066	0.52	1	1915
Yersinia pestis biovar Mediaevalis 91001	0.51	2	3895

4.3.3 Characteristic features of bacterial patatin-like proteins

Subsequently, the bacterial PLP sequences were analyzed for conserved motifs which were then compared with the characteristic domains of their eukaryotic counterparts. Towards this end, 60 bacterial PLP were aligned by the ClustalW method (205). It was found that bacterial PLP possess four conserved domains (block I-IV), similar to those found in potato patatin B2 (data not shown). Block I consists of a glycine-rich region with a conserved arginine or lysine residue. In the potato patatin isozyme Pat17, this region has been suggested to serve as an oxyanion hole formed by the backbone amides of the successive glycine residues which stabilizes the oxyanion generated during the transition state (168). The ammonium group of the conserved arginine/lysine residues may be necessary for electrostatic interaction with the phosphate moiety of a phospholipid substrate (57, 168). Block II is located in proximity to block I (about 10-20 amino acids distance) and comprises the hydrolase motif G-X-S-X-G with the putative active site serine (176). Block III contains a conserved serine, which may be an important structural element as a potential phosphorylation site or due to its capacity to form hydrogen bonds. The adjacent highly conserved proline residues (in block III and IV) may be important for the proper conformation of the protein. In addition to many structural features shared both by eukaryotic and bacterial PLP, it was observed that in block III bacterial and eukaryotic PLP show different conserved motifs. While bacterial PLPs possess the conserved sequence A-S-X-X-X-P, eukaryotic PLPs contain the conserved amino acids A-A-P, as seen by ClustalW alignment of 20 eukaryotic PLP (data not shown) (Table 4.2). Block IV includes the putative active site aspartate which is the second member of the catalytic dyad in patatin Pat17 (168). Dessen et al. (1999) have proposed a catalytic mechanism for the human $cPLA_2$ in which the active site aspartate abstracts a proton from the active site serine thereby activating it for its nucleophilic attack at the sn-2 ester. Successive to the domain with the active site aspartate, Hirschberg et al. (2001) have defined an additional region of protein homology for potato patatin B2 and human $cPLA_2$ containing a conserved serine. It was found that this domain was present in at least 15 other eukaryotic PLPs (data not shown) but was not conserved in the respective prokaryotic proteins (Table 4.2). Therefore it was concluded that eukaryotic and bacterial PLP share many but not all structural features, suggesting that they originated from a common ancestor and were modified to support/expand the specific life-style of an organism.

4.3.4 Classification of *L. pneumophila* Philadelphia-1 patatin-like proteins

The genome of *L. pneumophila* Philadelphia-1 was found to encode 11 PLP, which were designated PatA, PatB to PatK. All eleven *L. pneumophila* Philadelphia-1 PLPs possess the four conserved blocks of amino acid homology of bacterial PLPs, indicating their affiliation to this new protein group (Table 4.2). Furthermore, it was found that none of the eleven *L. pneumophila* Philadelphia-1 PLPs possessed a signal sequence, prerequisite for transport across the inner membrane by the sec or tat system, indicating that probably none of them is type II secreted (Table 4.2). Since *L. pneumophila* possesses a putative Lss type I and a Dot/Icm type IVB secretion system, the substrates of which do not require export by the sec or tat system, it is possible that some *L. pneumophila* Philadelphia-1 PLPs might be exported by the type I or type IVB apparatus (Jacobi & Heuner, 2003; Segal *et al.*, 1998; Vogel *et al.*, 1998). Indeed, a recent study by Shohdy and colleagues identified an *L. pneumophila* JR32 protein VipD (identical to PatA) with a patatin-like phospholipase domain and with homology to *P. aeruginosa* ExoU, as a substrate of the type IVB (Dot/Icm) secretion system (187). The patatin domain of *L. pneumophila* Philadelphia-1 and other bacterial PLPs is predominantly located at the N-terminal region of the protein (Table 4.2 and data not shown). All *L. pneumophila* PLPs have a C-terminal region after the patatin domain consisting of at least 126 amino acids. Depending upon the protein length, the *L. pneumophila* PLPs can be divided into two groups, group I and II, without or with a C-terminus appending after the PLP block IV of larger than 200 amino acids, respectively. PatA, PatC, PatF and PatG belong to group II. A recent study by Nagai and colleagues identified a conserved hydrophobic residue at the -3 or -4 position of the C-terminus of known *L. pneumophila* type IVB substrates (139). Notably, the C-terminus of VipD/PatA which was found to be essential for type IVB translocation also features a hydrophobic phenylalanine residue at the -4 position (187). Some of the *L. pneumophila* PLPs have an N-terminal extension as well (≥20 amino acids), including PatA, PatC, PatD, PatF, PatJ and PatK (Table 4.2). Noticeably, the N-terminal extension of PatF is extraordinary large (> 300 amino acids).

Table 4.2 Alignment of all *L. pneumophila* Philadelphia-1 proteins with patatin domains.
Eleven *L. pneumophila* Philadelphia-1 proteins with patatin-like domains were aligned by the ClustalW Method (205) using the program MEGALIGN (DNASTAR). Residues which were conserved in more than eight of the eleven aligned proteins are marked bold and an arrow designates the putative members of the catalytic dyad. Conserved regions of *Pseudomonas aeruginosa* PA103 ExoU and of *Solanum tuberosum* patatin B2 modified from (92) are shown for comparison.
A prediction of the protein function was provided by the NCBI Entrez *Legionella* database (www.ncbi.nlm.nih.gov/genomes/altik.cgi?gi=504&db=genome). For a prediction of the subcellular localization of the *L. pneumophila* Philadelphia-1 PLPs, the precomputed *L. pneumophila* Philadelphia-1 genome using PSORTb version 2.0 provided at the psort website (http://www.psort.org) was used and the predictions are marked (p). The sequences were also analyzed for the presence of a hydrophobic C-terminal residue at the -3 or -4 C-terminal position which might be conserved in substrates of the *L. pneumophila* type IVB secretion system (139). Delta designated the length of N-or C-terminus or number of amino acids between two blocks.

Nr.	Organism	Lpg No.	Gi No.	Name	Function	Predicted Localization
1	*P. aeruginosa*	-	2429143	ExoU	PLA/LPLA	
2	*L. pneumophila*	Lpg2831	52843027	PatA	PLA/LPLA	unknown
3	*L. pneumophila*	Lpg2807	52843003	PatB	Patatin family protein (p)	unknown
4	*L. pneumophila*	Lpg2410	52842619	PatC	Patatin-like phospholipase (p)	unknown
5	*L. pneumophila*	Lpg2317	52842527	PatD	Transmembrane protein (p)	cytoplasmic membrane
6	*L. pneumophila*	Lpg1944	52842161	PatE	Hypothetical protein (p)	cytoplasmic membrane
7	*L. pneumophila*	Lpg1426	52841656	PatF	Hypothetical protein (p)	outer membrane
8	*L. pneumophila*	Lpg1227	52841459	PatG	Hypothetical protein (p)	unknown
9	*L. pneumophila*	Lpg0952	52841187	PatH	Phosphoesterase (p)	cytoplasm
10	*L. pneumophila*	Lpg0670	52840907	PatI	Hypothetical protein (p)	cytoplasmic membrane
11	*L. pneumophila*	Lpg0290	52840545	PatJ	Lipoprotein (p)	cytoplasmic membrane
12	*L. pneumophila*	Lpg0014	52840270	PatK	Transmembrane protein (p)	cytoplasmic membrane
13	*Solanum tuberosum*	-	21510	Patatin B2	Lipid acyl hydrolase	

Table 4.2 Alignment of all *L. pneumophila* Philadelphia-1 proteins with patatin domains (continued)

Nr.	Name	Δ	Block I (oxyanion hole)	Δ	Block II (serine hydrolase motif) ↓	Δ	Block III (conserved proline)	Δ	Block IV (active site aspartic acid) ↓	Δ	Hydro-phobic C-terminal residue?
1	ExoU	109	S**GGG**AK**G**AAYP**G**AMLA	14	**G**S**S**A**G**GIT**A**ALLASGMSPAA	149	VAQAAHI**S**GSF**P**GVFQK	15	EFQ**DGG**VMINV**P**	335	-
2	VipD/ PatA	40	S**GGG**AK**G**ISYL**G**MIQA	14	**G**A**S**A**G**AMT**A**SILAVGMDIKD	175	IAQVVQW**S**GAH**P**VLFVP	7	YIA**DGG**ILDNM**P**	325	yes
3	PatB	9	A**GGG**AR**G**AYQA**G**VLKA	16	**G**V**S**V**G**SVN**A**AVLAENANDFP	116	NAQHILA**S**SAL**P**LFFPP	6	HYG**DG**SIGLVA**P**	158	yes
4	PatC	59	S**GGG**SRILAHI**G**ALDE	12	**G**S**S**A**G**AMV**A**AFAYLGYNCSE	128	LADAIII**S**ANL**P**IAFER	6	VYS**DGG**ISNNL**P**	395	no
5	PatD	20	Q**GGG**AL**G**AYQA**G**VLHA	12	**G**T**S**I**G**AIN**A**AIAAGNSDKER	118	GPEHIMA**S**GAL**P**PGFPA	6	YYW**DGG**ISSNS**P**	166	no
6	PatE	8	Q**GGG**AL**G**AYEL**G**VLKY	13	**G**V**S**I**G**AIN**A**AALIGAKDEPI	111	TPLHVLA**S**GSL**P**PGFPM	6	YYW**DGG**LFSNT**P**	141	no
7	PatF	306	C**GGG**AKIFAHV**G**VWKA	12	**G**S**S**A**G**AIMSLMCYLGYTADE	102	VSEAVKI**S**ASF**P**VLYRD	6	EHN**DGG**ILSNF**P**	572	no
8	PatG	9	R**GGG**SK**G**IAYV**G**ALQS	14	**G**S**S**A**G**AMT**A**AIVACGGSADL	207	VSIAVRI**S**ASL**P**GVFDP	6	KYI**DGG**AANNL**P**	277	yes
9	PatH	12	GSGSAR**G**WAHI**G**VIQS	12	**G**C**S**I**G**ALVGAIYACGTLDLF	70	LELAIRS**S**MSL**P**GLFTP	6	WLV**DGG**LVNPV**P**	126	yes
10	PatI	12	Q**GGG**AH**G**ALAW**G**IIDR	13	AT**S**A**G**AMN**A**AVLAYGFATGG	108	SADAVMA**S**ACL**P**FMFQA	6	YFW**DGG**YMGNPA	137	no
11	PatJ	84	S**GGG**DY**G**AFGA**G**LLNG	14	**G**I**S**T**G**ALI**A**PLAFAGPKYDA	94	FRKILLA**S**ASI**P**VVMPP	14	MHV**DG**STTFAVF	130	yes
12	PatK	37	Q**GGG**SL**G**AYQF**G**VVKG	12	AT**S**I**G**AIQ**A**AIIVGNPPEKR	115	EVEHIMA**S**AAL**P**PGFPA	6	LYW**DGG**VHSNT**P**	172	no
13	Patatin B2	34	D**GGG**IK**G**IIPAIILEF	24	**G**T**S**T**G**GLLTAMITTPNENNR	85	MYDICYSTAAA**P**IYFPP	15	NLV**DG**AVATVGDP	123	-

4.3.5 Identification of an *Legionella pneumophila* PLP possessing protein homology to ExoU

L. pneumophila Philadelphia-1 possesses eleven PLP genes. Four of these PLPs, PatA (gi52843027), PatC (gi52842619), PatF (gi52841656), and PatG (gi52841459) were particularly considered to be likely orthologs of *P. aeruginosa* ExoU based on the relatively low expect values of 1×10^{-16}, 3×10^{-08}, 3×10^{-08} and 3×10^{-15}, respectively, resulting from a BLAST search. Interestingly, all of these PLPs belonged to group II showing a C-terminal extension of larger than 200 amino acids (Table 4.2). The homologous regions only included the bacterial PLP domains whereas the C-terminal extensions were not homologous to each other or to ExoU. The *L. pneumophila* Philadelphia-1 PLP with the highest protein sequence similarity to ExoU among the paralogs (27% identity, 44% similarity, Expect value: 1×10^{-16}) was PatA. PatA is coded by an ORF of 1866 bp length and was predicted to represent a protein of 621 amino acids with a molecular mass of about 69.3 kDa and an isoelectric point of 5.8. Next, the genetic *patA* locus was examined. Two uncharacterized genes flank *L. pneumophila* Philadelphia-1 *patA* (Fig. 4.22). The upstream ORF1 which is oriented oppositely to *patA* encodes a protein with a PFAM domain of the conserved ubiquitin conjugation factor E4 family (U-box) which so far has been only found in eucaryots, e.g. human and yeast (35). Because of its U-box domain, this protein might be able to interfere with host protein ubiquitylation processes, which normally tag proteins for degradation (86). Interestingly, *sidH*, encoding another recently identified type IVB translocated protein is located further upstream, next to ORF1 (Fig. 4.22) (123). The oppositely oriented downstream ORF2 shows homology to a hypothetical protein y4LR of *Rhizobium* sp. (77). ORF3 is a predicted acyl-coA thioester hydrolase possessing a PFAM domain of the thioesterase superfamily (www.sanger.ac.uk/Software/Pfam/) (19). ORF4 encodes a protein of unknown function whereas ORF5 codes for a protein with a PFAM domain of amidinotransferases. Remarkably, *plaC* encoding the major secreted glycerophospholipid:cholesterol acyltransferase of *L. pneumophila* is located six ORFs downstream of *patA*. It is impossible that *patA* forms an operon with ORF1 or ORF2 as both are oppositely oriented to it (Fig. 4.23). The *patA* locus in *L. pneumophila* strain Paris was found to be similar to the locus of strain Philadelphia-1, but with the difference of an insertion of two genes encoding proteins with homology to transposases of the IS21 family interrupting *sidH* (Fig. 4.23) (35). Notably, *L. pneumophila* strain Lens lacks the whole genomic region containing *patA*, ORF1 and *sidH* (Fig. 4.23).

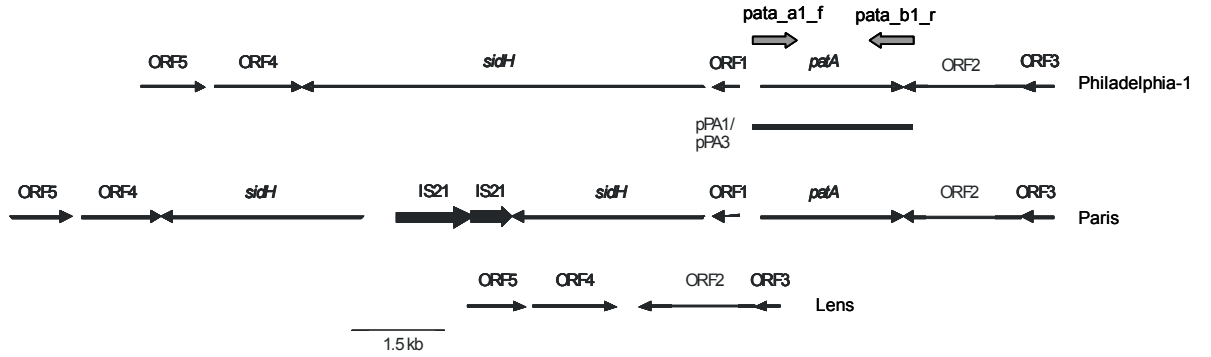

FIG. 4.23. The *patA* locus in different *L. pneumophila* strains. The *pat* locus in *L. pneumophila* sg1 strain Philadelphia-1 ist shown in the upper part, and the line below represents the segment of *Legionella* DNA that was cloned into the plasmid vectors pPA1 (=pGEMTez+*patA*) and pPA3 (=pBCKS+*patA*). The middle part represents the sg1 strain Paris, where the *sidH* gene is disrupted by two IS elements. The lower part shows the sg1 strain Lens where *patA*, *sidH* and ORF1 are not found. The arrows depict the relative location, size and orientation of *patA* and neighboring ORFs. The two thick arrows (not drawn to scale) represent the primers which were used for the amplification of the *patA* gene from strain Philadelphia-1. Abbreviations: IS=insertion element.

4.3.6 Lipolytic activities of PatA expressed in *E. coli* DH5α

The ortholog of *L. pneumophila* PatA, ExoU of *P. aeruginosa*, expresses phospholipase A and lysophospholipase A activities after contact with an eukaryotic factor which activates ExoU (150, 173, 174, 201). Therefore, recombinant *E. coli* clones harbouring *patA* were assessed for lipolytic activities. To this purpose, the *patA* gene with its putative promoter region was amplified from the *L. pneumophila* Philadelphia-1 genome by means of the primers patA_a1_f and patA_b1_r and cloned into pGEMTez, yielding pPA1. The *patA* gene from pPA1 was then subcloned into the vector pBCKS which generated pPA3. The culture supernatant and cell lysates of clones harbouring pPA3 (pBCKS+*patA*) as well as the empty pBCKS vector were incubated with phospholipase A substrates (DPPG, DPPC), lysophospholipase A substrates (MPLPG, MPLPC), and a lipase substrate (1-MPG). As displayed in figure 4.24, the cell lysate of the *E. coli* clone carrying *patA* in *trans* displayed lysophospholipase A activity as it possessed an increased capacity to release free fatty acids from MPLPG compared to the clone carrying the empty vector. However, there was no distinct increase in the hydrolysis of MPLPC showing that MPLPG was the preferred substrate of PatA. There was also a tendency of increased DPPG hydrolysis which was not consistently reproducible in additional independent experiments. No increased lipase activity could be detected in the clones harbouring pPA3 (Fig. 4.24). The culture

supernatant of recombinant *E. coli* clones harbouring pPA3 showed the same low level of capacity to cleave the respective substrates as the clone carrying the empty vector (data not shown), implying that recombinant PatA remains associated with the *E. coli* cell. In summary, the data show that *patA* expressed in *E. coli* possesses lysophospholipase A activity.

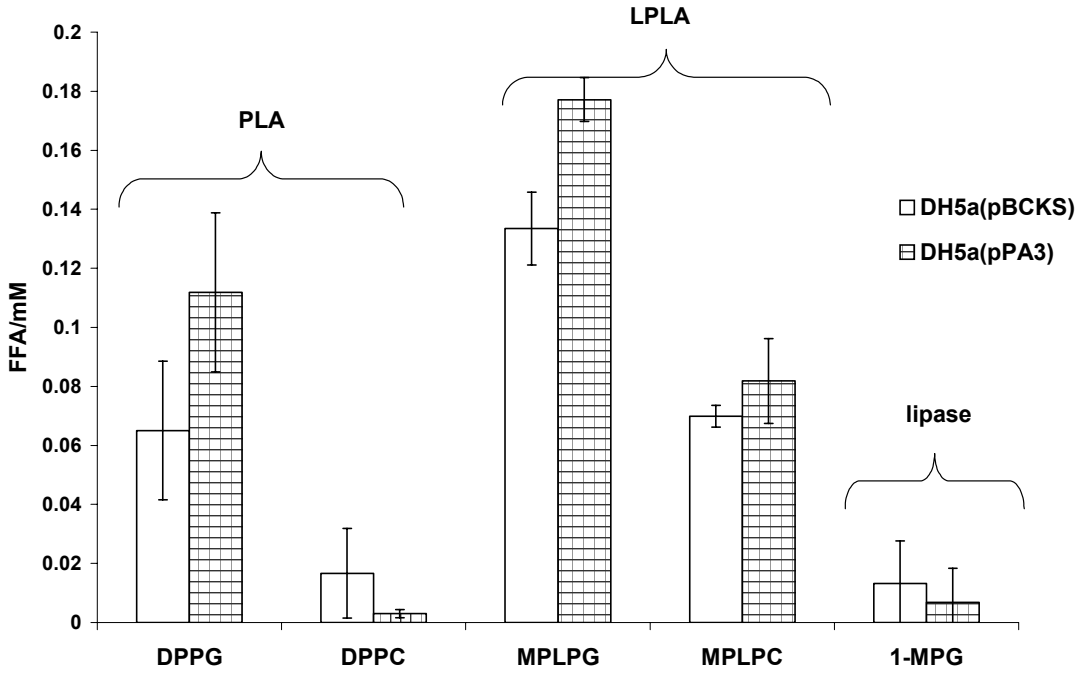

FIG.4.24. Cell-associated lipolytic activities of recombinant *E. coli* DH5α containing *L. pneumophila patA*. Cell lysates from *E. coli* clones (obtained at OD_{660}=2.0) carrying pBCKS or its derivative pPA3 (pBCKS+ *patA*) were incubated with DPPG, DPPC, MPLPG, MPLPC, or 1-MPG for 4.5 h incubation at 37°C, the release of FFA was quantified. Data are expressed as differences between the amount of FFA released by cell lysate and the amount released by Tris-HCl buffer. The results represent the means and standard deviations of duplicate cultures and are representative of three independent experiments.

After having established that recombinant PatA possessed predominantly LPLA activity, it was of interest to determine at with pH the highest activity occurred, as it known from plant patatin that higher phospholipase A activity occurs at basic pH values (6, 196). To this purpose the hydrolysis of MPLPG by the cell lysates of *E. coli* clones carrying pPA3 or pBCKS only, was assessed at pH 4, pH 7, and pH 9. As shown in figure 2.25, the highest LPLA activity of PatA expressed in *E. coli* occurred at pH 7 whereas almost no activity could be detected at pH 4. Thus it was found that the LPLA activity of PatA is highest at neutral pH.

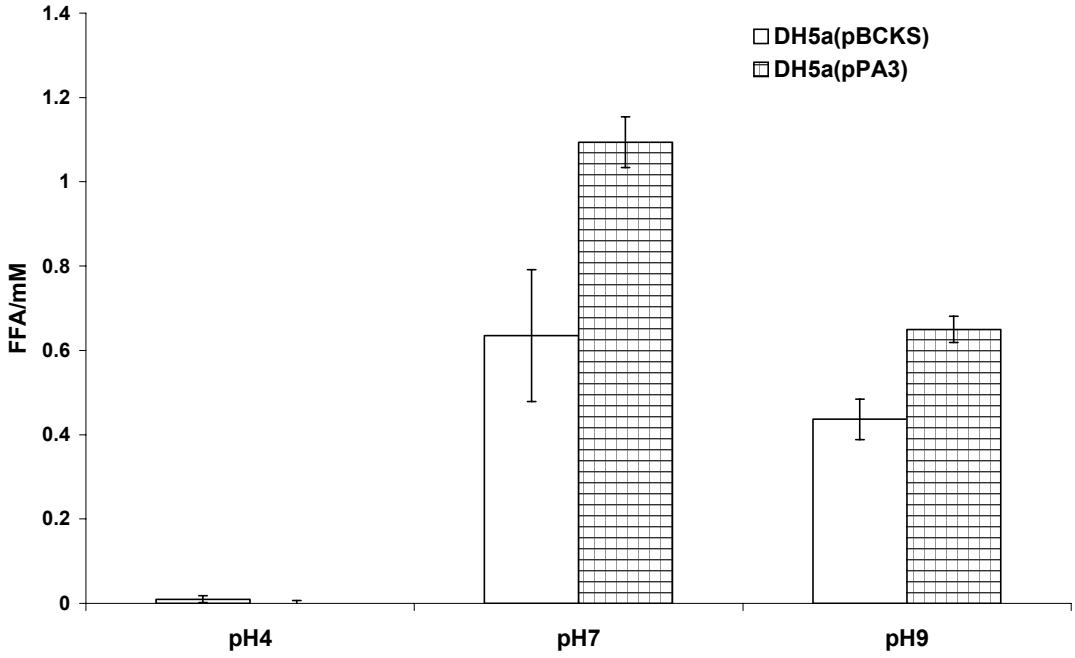

FIG.4.25. Cell-associated LPLA activity of recombinant *E. coli* DH5α containing *L. pneumophila patA* at different pH values. Cell lysates from *E. coli* clones (obtained at OD_{660}=2.0) carrying pBCKS or its derivative pPA3 (pBCKS+ *patA*) were incubated with MPLPG at pH 4, 7, and 9 for 17 h at 37°C, the release of FFA was quantified. Data are expressed as differences between the amount of FFA released by cell lysate and the amount released by Tris-HCl buffer. The results represent the means and standard deviations of duplicate cultures and are representative of three independent experiments.

Since the PLA and LPLA activities of ExoU are activated by an unknown eukaryotic factor it was of interest to determine whether the LPLA activity of PatA was enhanced by a eukaryotic factor as well. To this purpose bacterial cell lysates were incubated with lysates of U937 monocyte cells, which are *L. pneumophila* host cells, prior to incubation with MPLPG. As shown in figure 4.26, the LPLA activities were comparable with or without the addition of monocyte lysates, suggesting that the LPLA activity of PatA is not enhanced by a eukaryotic factor.

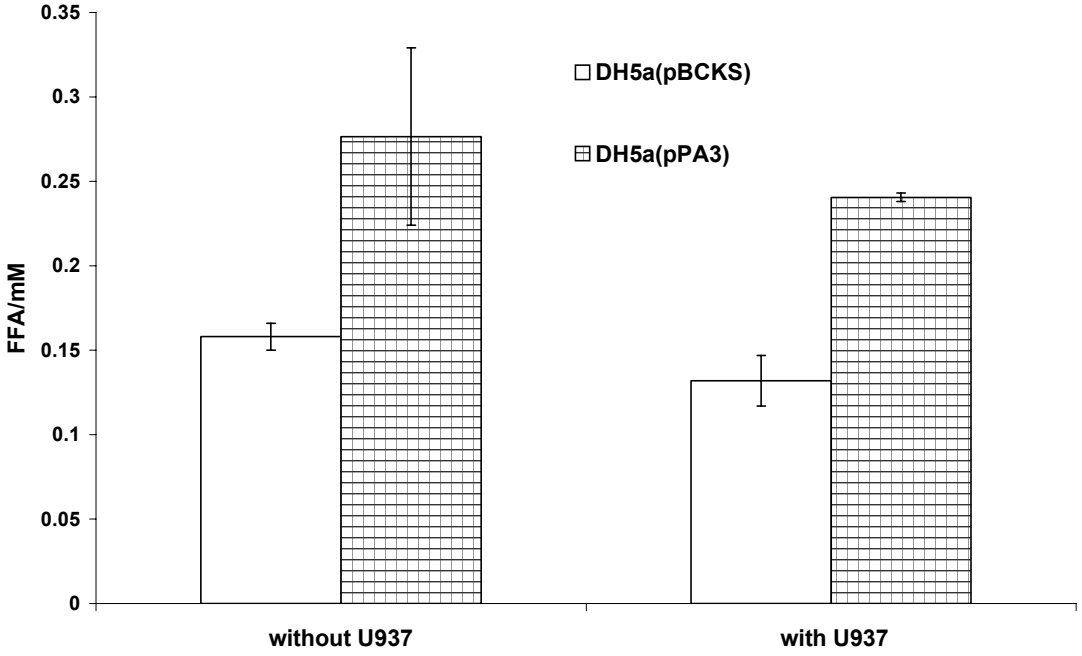

FIG.4.26. Cell-associated LPLA activity of recombinant *E. coli* DH5α containing *L. pneumophila patA* after incubation with U937 cell lysate. Cell lysates from *E. coli* clones (obtained at OD_{660}=2.0) carrying pBCKS or its derivative pPA3 (pBCKS+ *patA*) were first incubated with the same volume of U937 monocyte cell lysate for 1h and then an aliquot of the mixture was incubated with MPLPG for 5 h at 37°C, the release of FFA was quantified. Data are expressed as differences between the amount of FFA released by cell lysate and the amount released by Tris-HCl buffer. The results represent the means and standard deviations of duplicate cultures and are representative of three independent experiments.

4.3.7 Lipolytic Activities of PatA expressed in *L. pneumophila*

PatA confers enhanced LPLA activity to *E. coli* clones. Its ortholog, the *P. aeruginosa* cytotoxin ExoU, possesses PLA and LPLA activities which is also the case for the eukaryotic potato patatin B2. In order to determine whether a *Legionella* factor leads to a broader substrate variability of PatA and whether PatA is secreted or cell-associated, additional copies of the *patA* gene were introduced into *L. pneumophila* 130b wild type. Subsequently, the culture supernatant and cell lysates *of L. pneumophila* 130b clones harbouring pPA3 or the vector control were incubated with phospholipase A substrates (DPPG and DPPC), the lysophospholipase A substrate MPLPG, and the lipase substrate (1-MPG). Additionally, in order to assess whether PatA expressed in *L. pneumophila* was activated by a eukaryotic factor present in yeast, bacterial culture supernatants or cell lysates were incubated with lysates of the yeast *Candida albicans*. As can be

derived from figures 4.27 A and B, culture supernatants and cell lysates of *L. pneumophila* clones carrying multiple copies of the *patA* gene possessed an enhanced ability to cleave the LPLA substrate MPLPG thereby confirming the LPLA activity of PatA. Notably, PatA expressed in *L. pneumophila* also showed PLA activity represented by the enhanced hydrolysis of DPPG and DPPC, implying that a factor present in *L. pneumophila* but not in *E. coli* might activate PatA (Fig. 4.27). Since both culture supernatants as well as cell lysates of *L. pneumophila* clones over-expressing *patA* showed enhanced PLA and LPLA activities, it was not possible to derive from this experiment whether PatA is exported into the bacterial culture supernatant or remains associated to the bacterial cell under wild type conditions (Fig. 4.27). Since PatA/VipD has been identified as a type IVB secreted effector, it appears that the over-expression of PatA resulted in improper secretion and to an accumulation in the bacterial cell. The addition of *C. alibans* cell lysate did not lead to enhanced lipolytic properties of the *L. pneumophila* clone carrying *patA* in trans, it rather lead to reduced hydrolysis of MPLPG (Fig. 4.27 A and B, right). Thus this result corroborates the former observation that PatA does not require activation by a eukaryotic factor. In conclusion, it was shown that PatA is a PLA and LPLA which does not require activation by a eukaryotic factor but might require activation by some unknown *Legionella* factor.

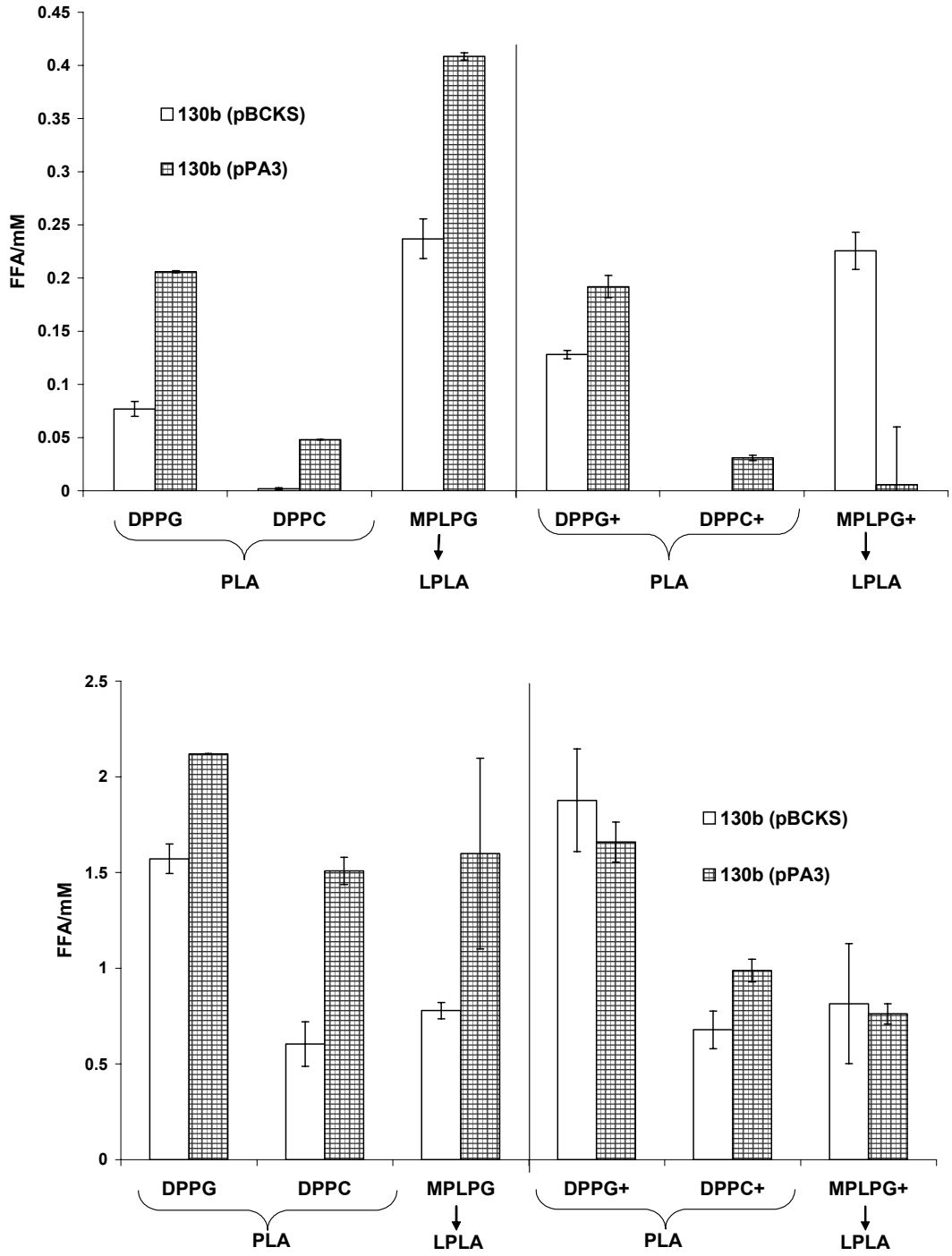

FIG.4.27. Secreted and cell-associated PLA/LPLA activities of *L. pneumophila* harbouring *patA* in *trans*. Culture supernatant (upper picture) or cell lysates (lower picture) of *L. pneumophila* 130b carrying *patA* in *trans* or the pBCKS vector were incubated with DPPG, DPPC, or MPLPG for 3 h at 37 °C and the release of FFA was quantified. Additionally to check for activation by a yeast factor, the samples were pre-incubated for 1h with cell lysates of *Candida albicans* (marked with +). The results represent the means and standard deviations of duplicate cultures and are representative of two independent experiments (activation only performed once).

4.3.8 Characterization of *L. pneumophila patA* mutants

As *L. pneumophila* PatA shows homology to *P. aeruginosa* ExoU and like ExoU possesses PLA and LPLA activities, it was of particular interest to determine the role of PatA during intracellular infection of host cells. Therefore, *L. pneumophila patA* mutants were constructed in strain 130b. Towards this end, the *patA* gene was amplified from the Philadelphia-1 genome and introduced into the vector pGEMTez, yielding pPA1. The *patA* gene of pPA1 was disrupted by the insertion of a kanamycin resistence cassette at its *Sfo*I site (base pair position 606) thereby generating pPA5 (Table 3.21). pPA5 was then used for creating *L. pneumophila patA* mutants by taking advantage of the natural competence of the bacteria when grown at 30 °C. Several independent mutants were obtained (e.g, patA2, patA4, patA5).

4.3.8.1 Intracellular replication of *L. pneumophila* 130b *patA* mutants

In order to assess the importance of *L. pneumophila patA* for the intracellular infection of *L. pneumophila*, the 130b wild type and two independent *L. pneumophila* 130b *patA* mutants were used for the infection of *A. castellanii* amoebae and U937 macrophages (Fig. 4.28). In the amoebal model, the 130b wild type displayed a typical four-log increase in CFU. In contrast, the two independent *patA* mutants did not show any intracellular replication but their CFU rather decreased over the time-course of the infection possibly because the infection medium does not support extracellular replication of *L. pneumophila* (Fig. 4.28, upper part). Likewise, while the wild type showed a thirtyfold increase in CFU in the macrophage model the two independent *patA* mutants did not show any replication, again suggesting an essential role for PatA in the infection process (Fig. 4.28, lower part). However, introduction of *patA* in *trans* into the *L. pneumophila patA* mutant did not restore the wild type phenotype during amoebal infections (Fig. 4.28, upper part). Since the infections were carried out without the addition of antibiotics and since the pBCKS vector is not well kept by the bacteria in the absence of chloramphenicol, the *patA* gene was amplified from the Philadelphia-1 genome and introduced into the better persistent vector pMMB2002 (164). Yet, *patA* mutants carrying pSB13 (pMMB2002+*patA*) were still unable to replicate intracellularly (data not shown). The lack of *trans* complementation either suggests a directed second-site mutation, because all of the *patA* mutants displayed the described growth defects or a specific PatA dosage is required for a complementation which was not achieved with the two employed vectors. It is however striking that the absence of PatA

leads to such a dramatic intracellular growth defect of *L. pneumophila* which mirrors the effect of a type IVB secretion mutant.

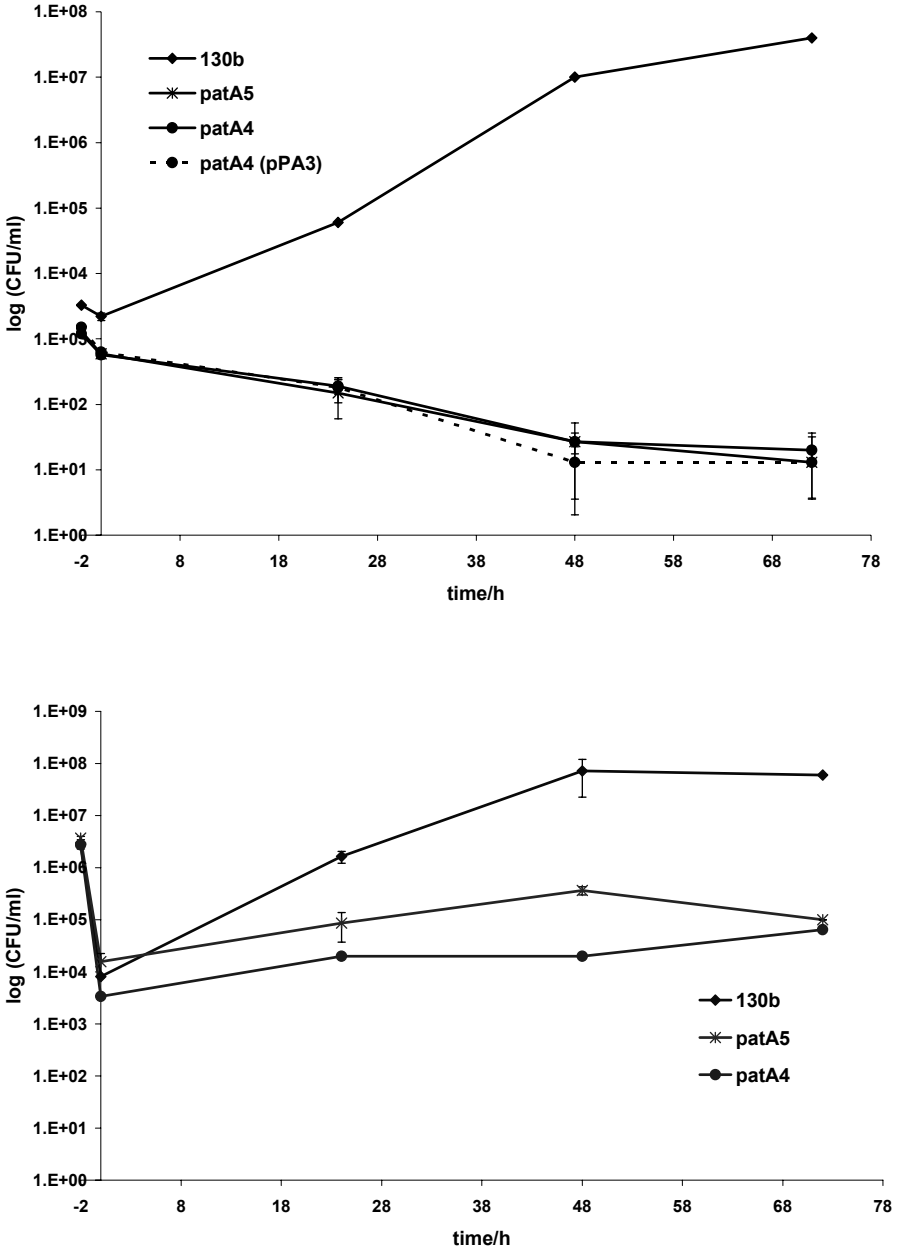

FIG.4.28. Intracellular infection of host cells by wild type 130b and *patA* mutant *L. pneumophila*. *Acanthamoeba castellanii* amoebae and U937 macrophages (upper and lower figures, respectively) were inoculated with *L. pneumophila patA* knockout mutants as well as *L. pneumophila* wild type (MOI of 0.1 and 1, respectively). At various time points post inoculation, the number of bacteria was quantified by plating aliquots on BCYE agar. Results represent the means and standard deviations of triplicate samples and are representative of two independent experiments.

4.4. Identification of novel *L. pneumophila* phospholipases A by biochemical protein purification

4.4.1 Biochemical purification of secreted *L. pneumophila* PLA activity

An additional approach of identifying novel secreted phospholipases A of *L. pneumophila* was a partial biochemical purification of proteins with PLA-activity from bacterial culture supernatant followed by N-terminal protein sequencing. First, the secreted PLA and LPLA activities of *L. pneumophila* were determined at different bacterial growth phases in order to estimate the point of highest PLA activity. Figure 4.29 shows the hydrolysis of two groups of lipids by *L. pneumophila* culture supernatant, namely diacylglycerophospholipids (DPPC and DPPG), representing PLA substrates and monoacylphospholipids (MPLPC, MPLPG and MPLPE) representing LPLA substrates. As shown in figure 4.29 the PLA activity (marked by the left arrow) peaks at the mid to late logarithmic bacterial growth phase with a bacterial OD_{660} of 1.6-1.8, while the LPLA activity (marked by the right arrow) peaks at early stationary growth phase when the bacteria have reached an OD_{660} of approximately 2.1.

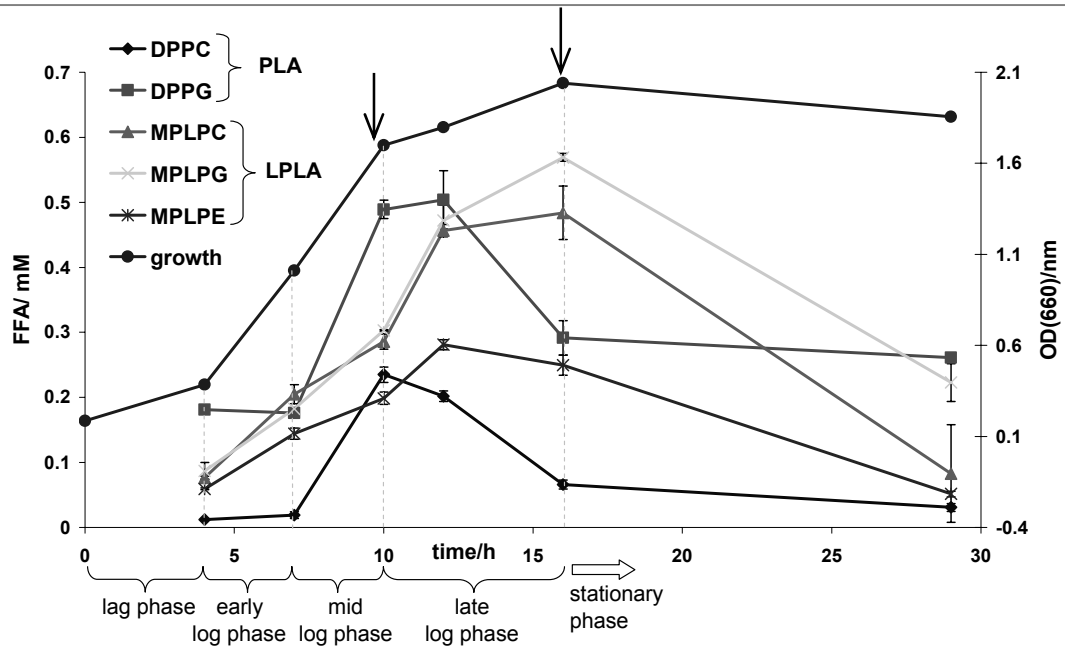

FIG.4.29. Kinetics of PLA and LPLA secretion into the culture supernatant by *L. pneumophila* 130b. *L. pneumophila* culture supernatant was obtained during growth in BYE broth at different optical densities at 660 nm and incubated with the indicated lipids for 2.5 h at 37 °C. Then the release of FFA was quantified. The results represent the means and standard deviations of duplicate samples (n=2) and are representative of two independent experiments.

Since the LPLA activity in the culture supernatant originates mainly from the already characterized LPLA PlaA, it was of special interest to characterize the protein(s) responsible for the PLA activity which predominantly cleaves the diacylphospholipids DPPC and DPPG. Towards this end, 1.2 l of BYE broth was inoculated with *L. pneumophila* 130b and the bacteria were grown to an optical density at 660 nm of 2.0, which corresponded to late logarithmic growth phase. Figure 4.30 gives an overview of subsequent purification steps which were employed in order to isolate the protein(s) causing the PLA activity in the culture supernatant.

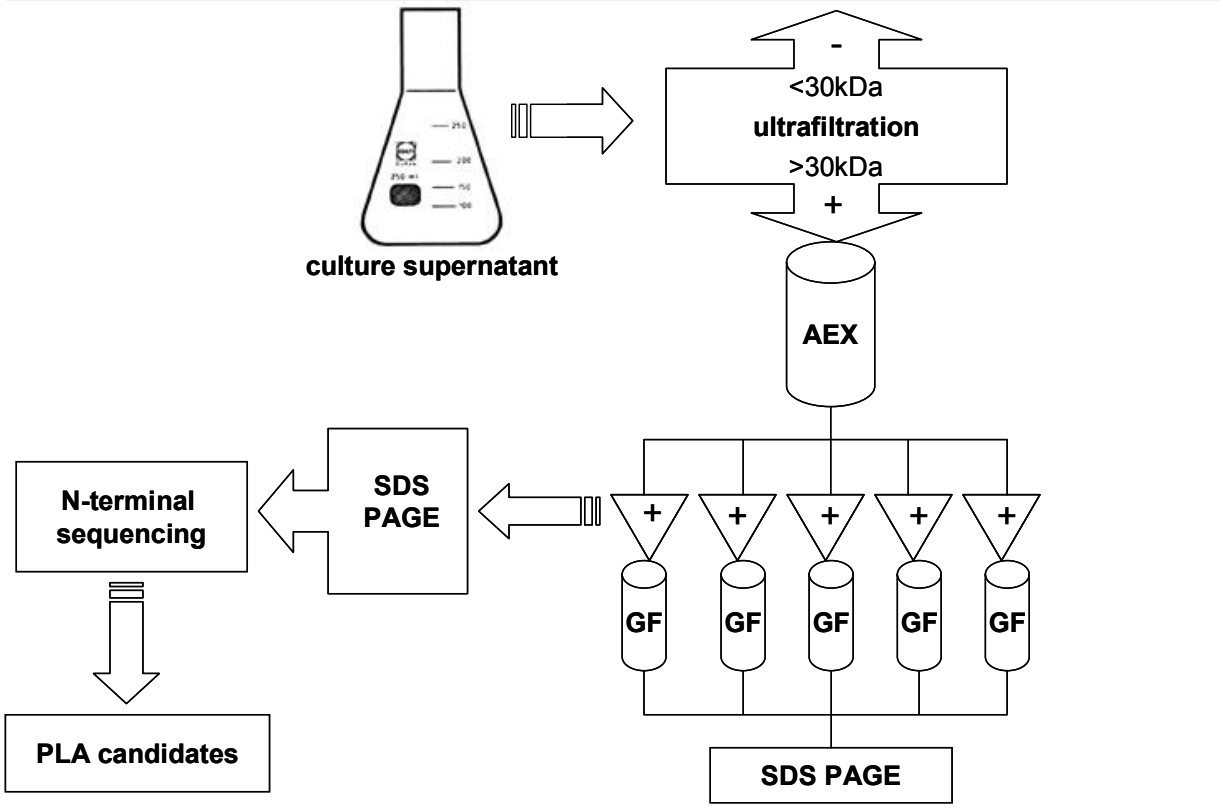

FIG. 4.30. Schematic overview of the purification steps used for the identification of PLA and LPLA candidate proteins. 1.2 l of *L. pneumophila* culture supernatant was ultrafiltrated with an exclusion size of 30 kDa and the PLA and LPLA activities (+) were found in the retentate (>30 kDa). The retentate was then subjected to anion exchange chromatography (AEX). The proteins present in the chromatographic fractions with PLA and/or LPLA activity (+) were separated by SDS PAGE, transferred to a PVDF membrane, and subjected to N-terminal protein sequencing which yielded PLA candidate proteins. In addition, the remaining fractions with PLA and/or LPLA activities (+) were further subjected to gel filtration (GF) and the proteins were separated by SDS PAGE. The protein concentrations after the gel filtration were not sufficient for N-terminal sequencing and were therefore only analyzed by reducing SDS PAGE. + marks PLA and/or LPLA activities, - marks no or low PLA and/or LPLA activities.

The culture supernatant was obtained by centrifugation and sterile filtered. Since a lower volume was necessary for the subsequent anion exchange chromatography, the culture supernatant was concentrated tenfold by ultrafiltration (exclusion size 30 kDa). As shown in figure 4.31, the phospholipase A and lysophospholipase A activities were mainly obtained in the retentate (i.e. did not pass the filter) showing that the respective proteins were greater than 30 kDa or formed aggregates which were larger than 30 kDa. The permeate (approximately 1 l) containing proteins which were smaller than 30 kDa showed some PLA activity which was inhibited by 5 mM EDTA, suggesting that *L. pneumophila* might possess a ion-cofactor dependent PLA. As most of the PLA and LPLA activities were found in the retentate and were not inhibited by EDTA, it was continued with the purification of the corresponding proteins in the retentate (Fig. 4.31). Since the *L. pneumophila* culture supernatant contains a high amount of the zinc metalloprotease ProA, EDTA was added to the retentate and the permeate in order to inhibit protease activity. The addition of EDTA did not inhibit PLA or LPLA activities in the retentate (Fig. 4.31).

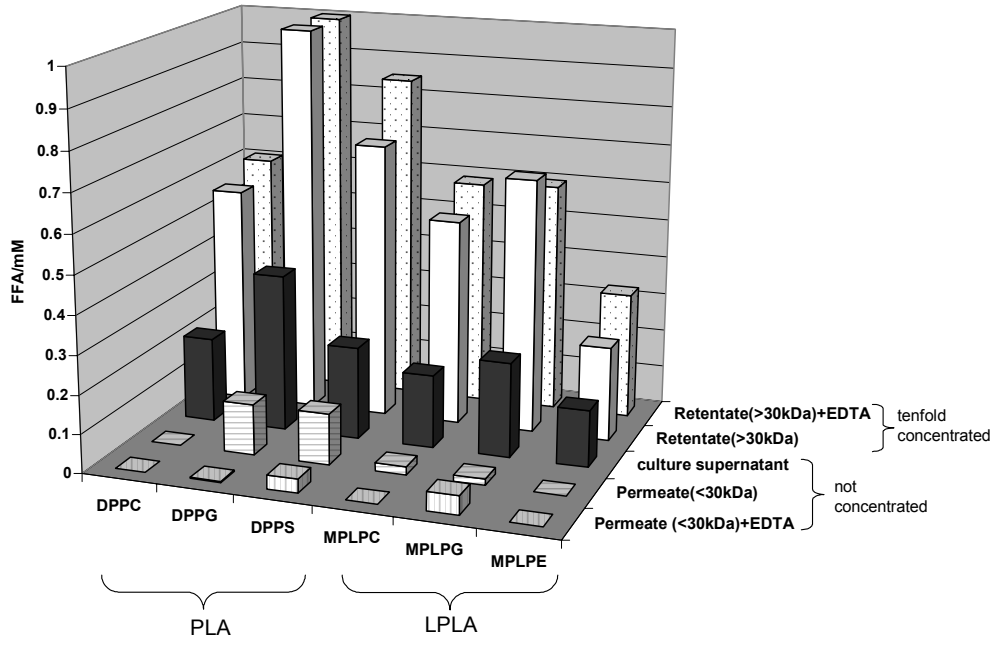

FIG.4.31. PLA and LPLA activities of *L. pneumophila* 130b culture supernatant after ultrafiltration. 1.2 l of *L. pneumophila* culture supernatant was concentrated tenfold by ultrafiltration with an exclusion size of 30 kDa. The different fractions were incubated for 5h with the indicated lipids with and without the addition of 5 mM (final concentration) EDTA. Number of experiments: 2.

Subsequently, the concentrated culture supernatant (100 ml) (=retentate) was subjected to an anion exchange chromatography (AEX) (start buffer: 20 mM Tris-HCl+5mM Na_2EDTA, pH 7.5). The resulting fractions were assayed for phospholipase A, lysophospholipase A, and lipase activities (Fig. 4.32). PLA, LPLA, and lipase activities were measured by the release of fatty acids from diacylphospholipids, monoacylphospholipids, or 1-MPG. Figure 4.32 shows at least five peaks of phospholipase A activity present in the AEX fractions 2, 12, 22, 42/44, and 72. The highest lysophospholipase A activity was found in the AEX fractions 22 and 24 indicating that these fractions contained one or more proteins with LPLA activity (Fig. 4.32 and Table 4.4). These fractions also showed the highest lipase activity. The AEX fractions were also analyzed by SDS PAGE under reducing conditions. Notably, AEX fraction 12 which shows a peak of PLA activity only contained one protein band of approximately 20 kDa after silver staining (sensitivity ≥ 50 ng) which was identified as LvrE, a protein recently reported to be a substrate of the *L. pneumophila* Tat translocation system (Fig. 4.32, Fig. 4.33) (54). AEX fraction 22 which showed the highest PLA and LPLA activities contained several protein bands ranging from approximately 20 kDa -37 kDa. It was suspected that the 37 kDa band which was present from fractions 21 to 45 might represent the zinc metalloprotease ProA. Therefore, a qualitative protease assay was performed on casein agar plates and protease activity was indicated by the development of a milky precipitation (caused by para-caseinate). Indeed, AEX fractions 22, 26-37, and 42 showed protease activity suggesting the presence of ProA and/or other proteases in these fractions. The AEX fractions 2, 12, 21, and 22 which showed a peak of PLA and/or LPLA activity were separated on a 12.5 % SDS gel under reducing conditions and then transferred onto a PVDF membrane. The blot was stained with Ponceau-S and visible bands were marked and N-terminally sequenced by the group of Stefan Stevanovic (Universität Tübingen). The N-terminal sequences which were thus obtained were used in a BLAST search against the *L. pneumophila* Philadelphia-1 genomic database (38). This search yielded six different proteins which are listed in Table 4.5.: ProA, (sequenced from fraction 22), LvrE (sequenced from fraction 12), Unk1 (sequenced from fractions 21, 22), Unk2 (sequenced from fractions 21, 22), HbpB (sequenced from fraction 2), and Aas (sequenced from fraction 21). The fact that the 37 kDa protein in fraction 22 (which showed protease activity) was identified as ProA indicates that the protease activity in this fraction is caused by ProA. ProA was also sequenced from the protease active fraction 32 (which did not contain any other band) suggesting that the protease activity of the other fractions might also result from ProA (Fig. 4.30 and data not shown). The newly identified proteins are further described in chapters 4.5-4.9.

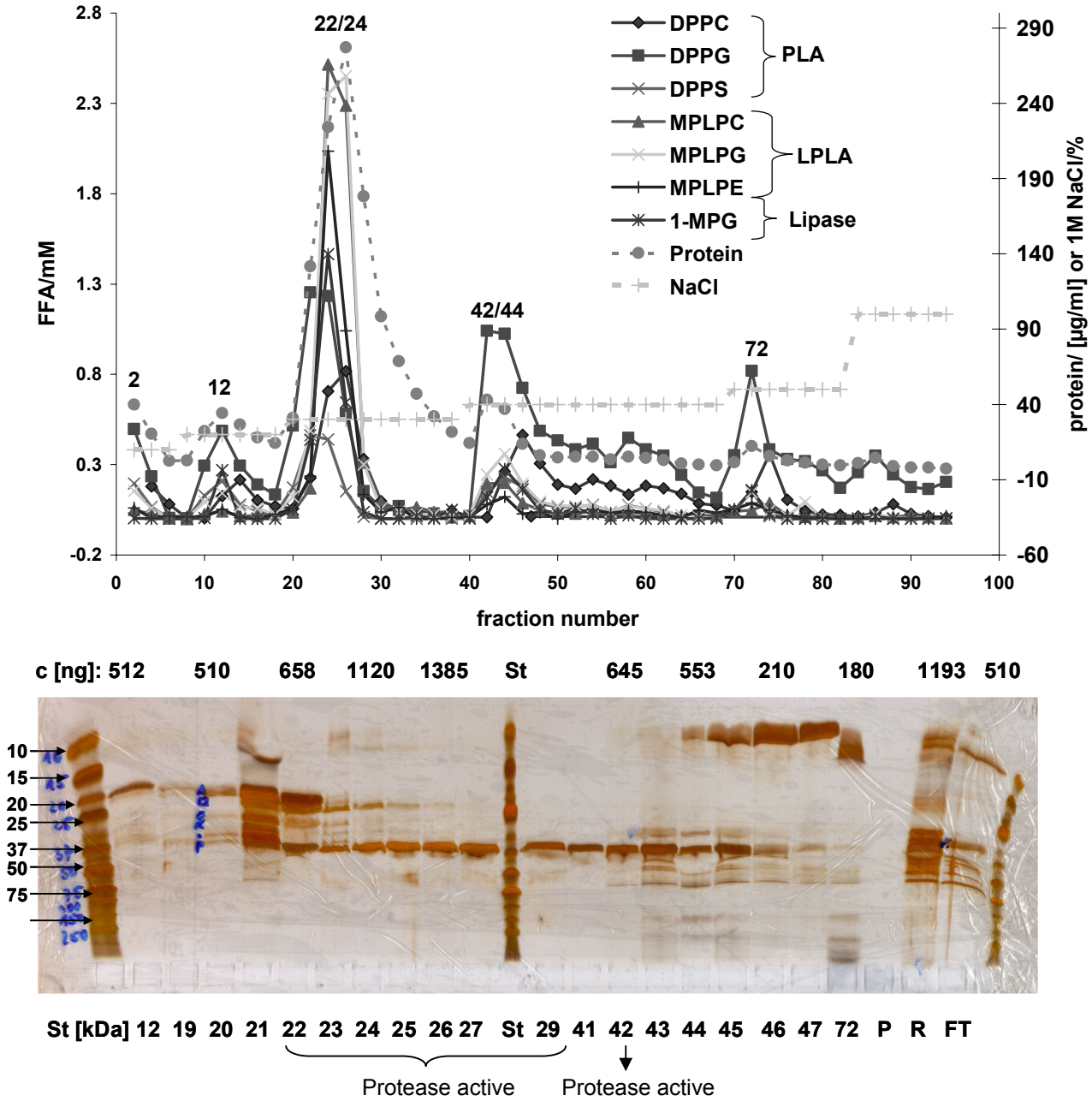

FIG.4.32. PLA, LPLA, and lipase activities of AEX fractions and SDS PAGE. 1.2 l of *L. pneumophila* 130b culture supernatant was concentrated tenfold by ultrafiltration and subjected to AEX (1 ml Resource Q column, flow rate: 0.5 ml/min, fraction size: 1.3 ml). Every second fraction was incubated with DPPC, DDPG, DPPS, MPLPC, MPLG, MPLPE, and 1-MPG for 1 h at 37 °C and the release of fatty acids was quantified. The amount of protein in every second fraction was quantified as well. Fractions showing lipolytic activity were loaded on a 12.5% SDS gel (amount of protein per gel pocket 180-1385 ng), separated by electrophoresis and stained with silver stain. The amount of protein per gel pocket (in ng) is indicated above and the fraction number is indicated below the gel. St: protein standard, P: permeate (<30 kDa), R: retentate (>30 kDa), FT: AEX flow through. Shown is a representative result from 3 independent experiments.

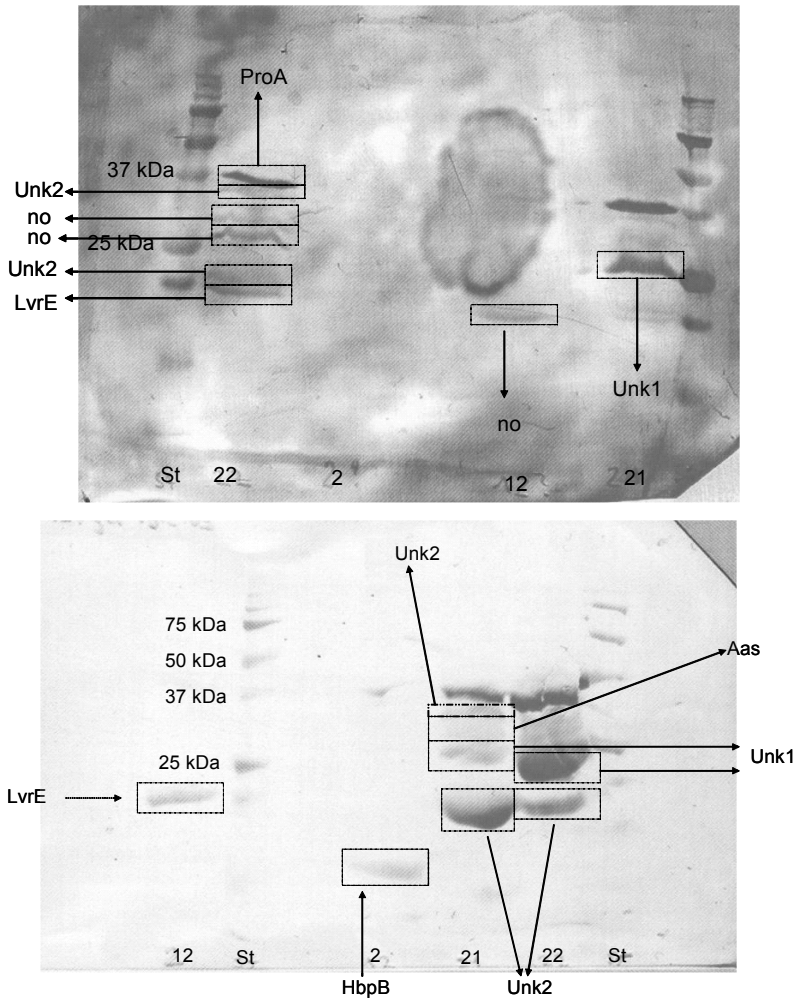

FIG.4.33. Western Blot of AEX fractions. AEX fractions 2, 12, 21, and 22 were concentrated twentyfold, subjected to SDS PAGE (12% and 15% gel, respectively), and transferred onto a PVDF membrane. Staining was performed with the reversible dye Ponceau S. Visible bands were cut-out and subjected to Edman degradation (by the group of Stefan Stevanovic, Universität Tübingen). The proteins which were identified in this way are indicated at the respective protein band and further described in table 4.4. 'no' means no sequence obtained.

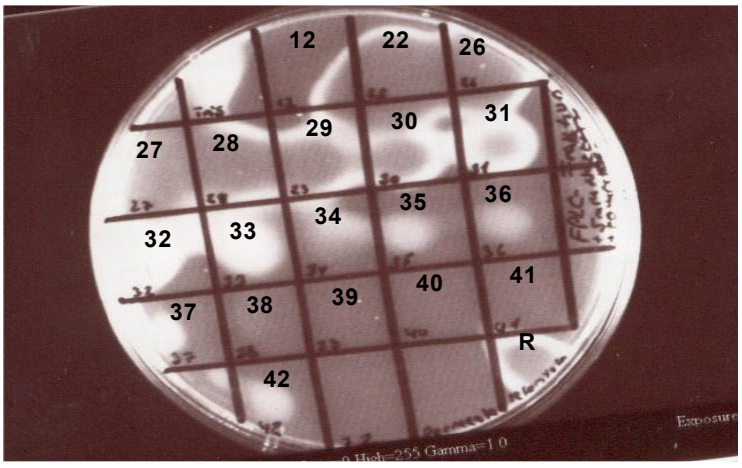

FIG.4.34. Protease activity of selected AEX fractions. 9 µl of AEX fractions + 1 µl 20 mM $ZnCl_2$ per fraction were incubated over night at 37 °C on agar plates containing 10 g/l casein. A milky precipitation indicated protease activity. Due to high protease activity the precipitation spread also over to negative fractions (e.g. Tris-HCl). Abbreviations: R: retentate.

In order to further purify the potential PLA and LPLA enzymes, the remaining AEX fractions (which were not used for blotting) with PLA and LPLA activities were pooled when appropriate (AEX fractions 1+3+5, 10+11+13, 23-26, 42-46, and 70+71+73+74) and first concentrated four- to fivefold by means of centrifugal filter devices (exclusion size 10 kDa) and further purified by gel filtration (GF). The fractions from gel filtration were again assayed for lipolytic activities (Fig. 4.36-4.40, data not shown for 1+3+5). Notably, the lipolytic activities of the GF fractions of the five different AEX peaks showed a similar pattern and they were found to contain a similar protein pattern as well. With respect to their activities, they either contained a single peak of predominant PLA activity (GF of fractions 1+3+5, 10+11+13, 70+71+73+74) or additionally contained a second peak of LPLA and lipase activity (GF of fractions 23-26, 42-46). The PLA activity eluted very early and was close to the void volume ($V_0 \approx 115$ ml determined with blue Dextrane), whereas the peak of LPLA and lipase activity appeared late (199 or 207 ml). Gel filtration allows the determination of the molecular mass of the substances by estimating their elution volume and comparing it with the elution volume of commercially available protein standards. By this method the molecular mass of the proteins in the PLA and LPLA active fractions was estimated. The GF fractions from all five AEX fractions contained a peak of PLA activity corresponding to a molecular mass of 248 or 275 kDa (mass determination by means of mass standard, Fig. 4.35). Two of the five AEX fractions (AEX 23-26, AEX 42-46) contained an additional peak of LPLA activity in their GF fractions corresponding to a molecular mass of approximately 43-50 kDa. The SDS PAGE of the GF fractions shows that GF fractions 49/50 of AEX23-26, GF fraction 3 of AEX 42-46, and GF fractions 43/44 of AEX (70, 71, 73, 74) possessing PLA activity contain the same two protein bands, one of approximately 34 kDa and a second of approximately 70 kDa (figures 4.38, 4.39, 4.41). However, a dimer of these two proteins would only amount to 104 kDa which is only 1/3 of the molecular mass estimated by GF. Interestingly, a molecular mass of 70 kDa correlates well with the predicted molecular mass of PatA (see chapter 4.3). Notably, the SDS PAGE of GF fraction 62-63 of AEX 23-26 which showed a peak of LPLA activity contains a protein band of about 28 kDa which corresponds to the processed form of PlaA, the major secreted LPLA (figures 4.36 and 4.40). This band is not visible in the GF fractions 17/18 of AEX 42-46 which also possess LPLA activity which might be due to a lower protein concentration in these fractions (Fig. 4.40).

Since the molecular mass of the protein responsible for the LPLA activity as determined by GF amounted to 50 kDa, PlaA possibly forms dimers. It has already been reported that the experimentally found molecular mass of PlaA is greater than that of the monomer (73). The PLA, LPLA and lipase activities of the different purification steps are summarized in Table 4.3. Table 4.3 shows that the PLA activity per µg protein increased after each purification step. Again, the fractions from the different gel filtrations containing high PLA and/or LPLA activities [GF AEX (23-26) fraction 49, 62, 63 and GF AEX (42-46) fraction 3, 17] were blotted and stained with Ponceau S (Fig. 4.41). This time, however, the protein concentration was too low for N-terminal sequencing and only one N-terminal protein sequence (that of ProA) was obtained.

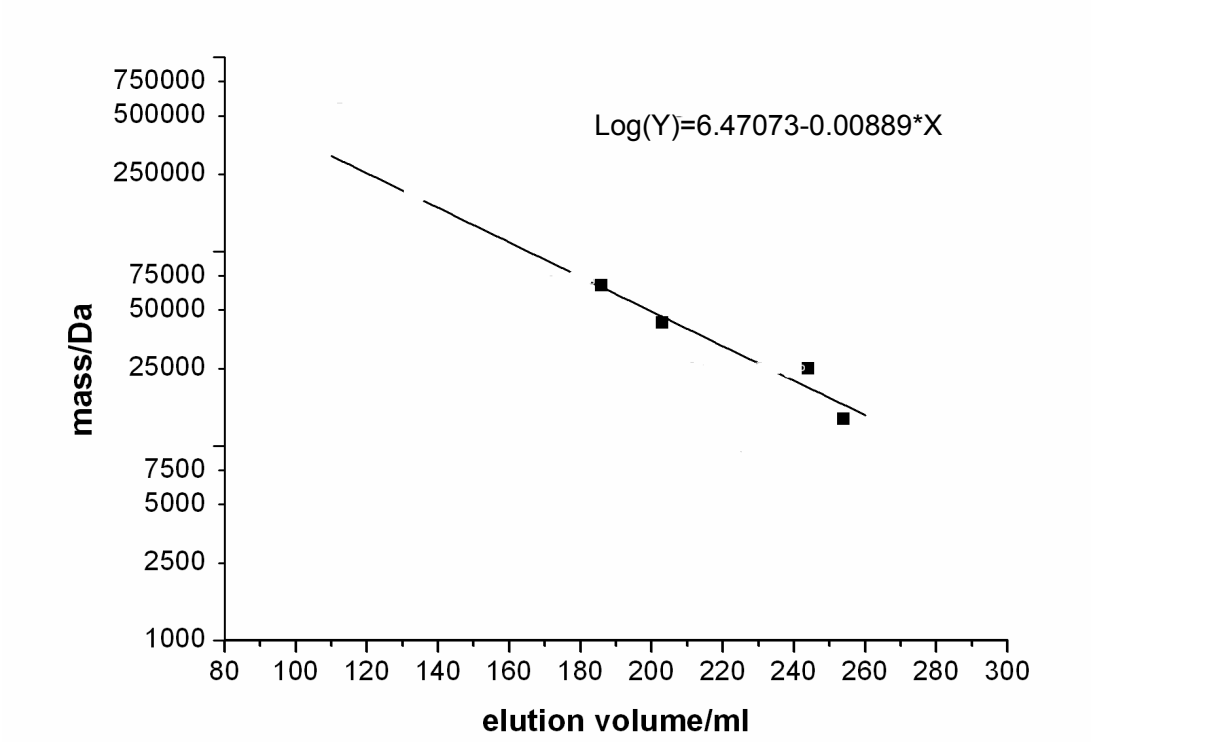

FIG.4.35. Mass determination of proteins by gel filtration. In order to estimate the molecular mass of proteins by gel filtration the low molecular weight calibration kit from Amersham was used. Protein standards (Ribonuclease A=13.7 kDa, Chymotrypsinogen A=25 kDa, Ovalbumin=43 kDa, Albumin=67 kDa) were subjected to gel filtration (HiLoad 26/60 Superdex 200 prep grade column, flow rate: 1 ml/min) under the same conditions which were subsequently used for the gel filtration of the samples. The elution volume of the mass standards was then used to estimate the molecular mass of unknown proteins by means of their elution volume.

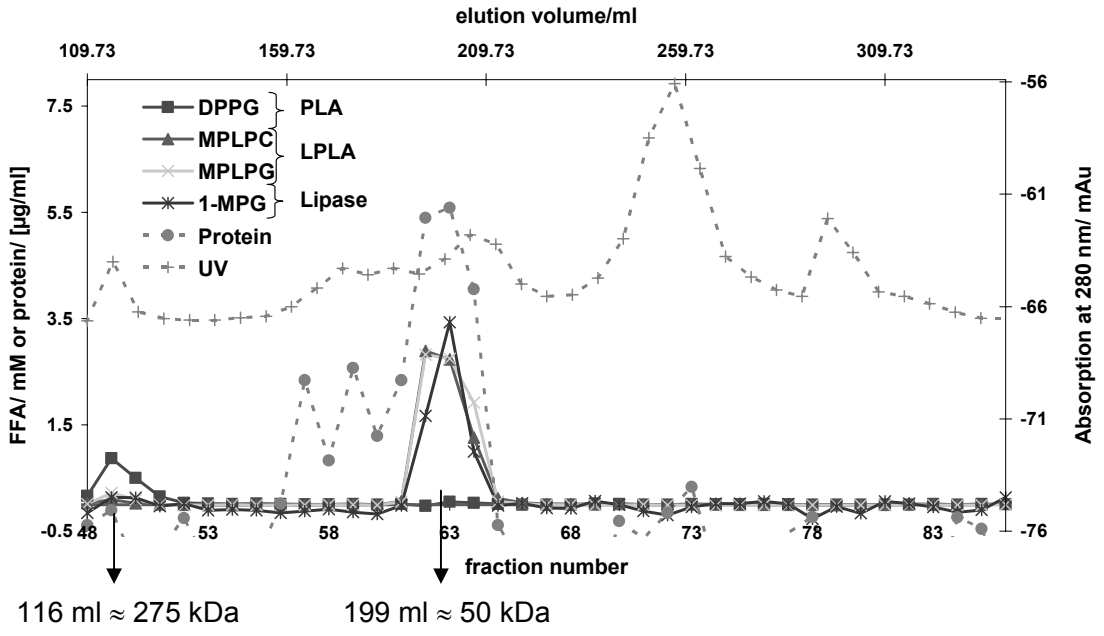

FIG.4.36. PLA, LPLA, and lipase activities of GF fractions from the pooled AEX fractions 23-26. PLA-active AEX fractions 23-26 were pooled, concentrated fourfold and subjected to gel filtration (HiLoad 26/60 Superdex 200 column, flow rate: 1 ml/min, fraction size: 6 ml). Resulting fractions were incubated with DPPG, MPLPC, MPLPG, and 1-MPG for 20 h at 37 °C and the release of fatty acids was quantified.

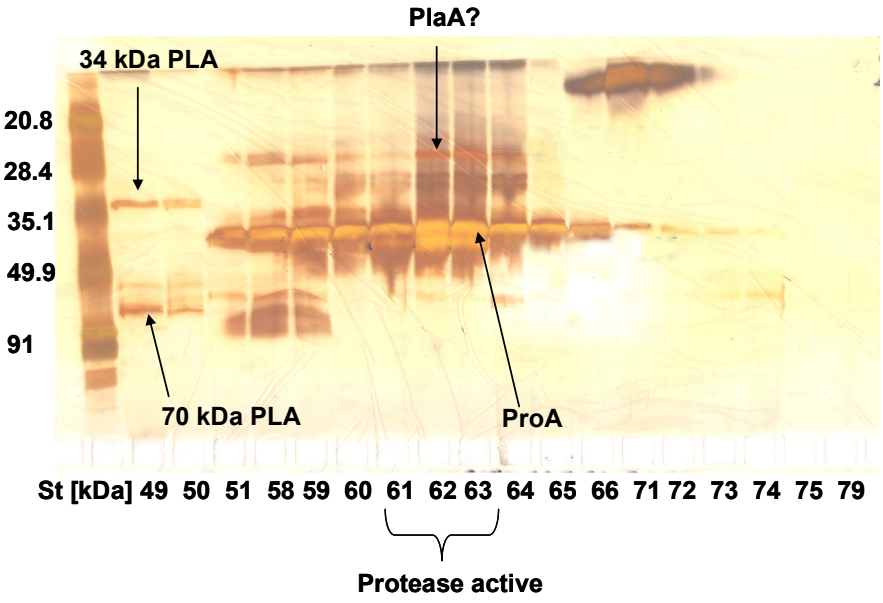

FIG.4.37. Proteins present in PLA-active GF fractions from the pooled AEX fractions 23-26. PLA-active AEX fractions 23-26 were pooled, concentrated fourfold and subjected to gel filtration (HiLoad 26/60 Superdex 200 column, flow rate: 1 ml/min, fraction size: 6 ml). The fractions from GF showing PLA/LPLA activity were concentrated thirtyfold (exclusion size: 3 kDa) and subjected to SDS PAGE under reducing conditions. Fractions 61-64 were qualitatively assayed for protease activity and were found to be positive. St: protein standard.

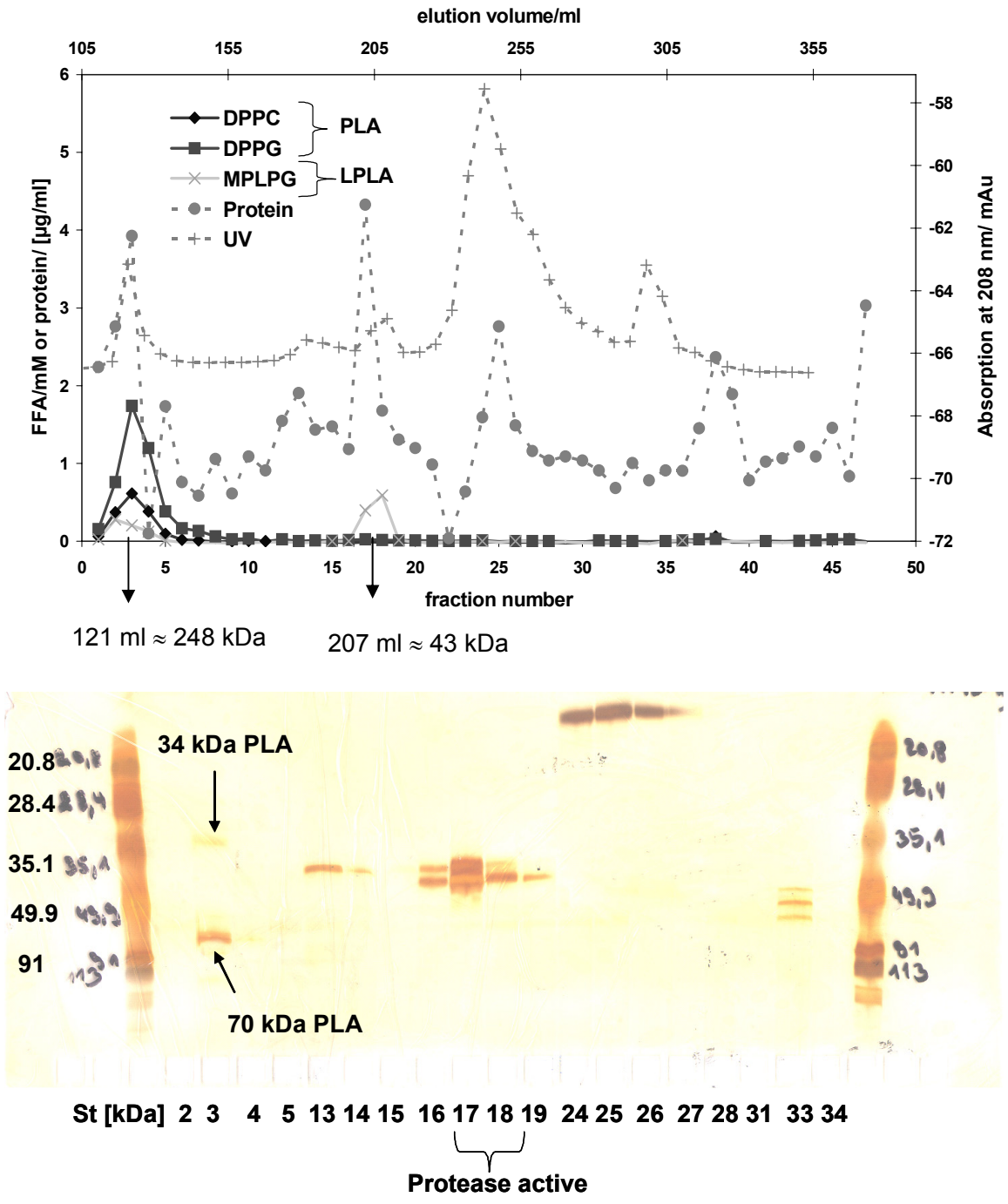

FIG.4.38. PLA and LPLA activities of GF fractions from the pooled AEX fractions 42-46. PLA-active AEX fractions 42-46 were pooled, concentrated fivefold and subjected to gel filtration (HiLoad 26/60 Superdex 200 column, flow rate: 1 ml/min, fraction size: 6 ml). Resulting fractions were incubated with DPPC, DPPG, and MPLPG for 24 h at 37 °C and the release of fatty acids was quantified. The fractions from GF showing PLA/LPLA activity were concentrated 5-8-fold (exclusion size: 3 kDa) and subjected to SDS PAGE under reducing conditions. Fractions 17, 18 were qualitatively assayed for protease activity and were found to be positive. St = protein standard.

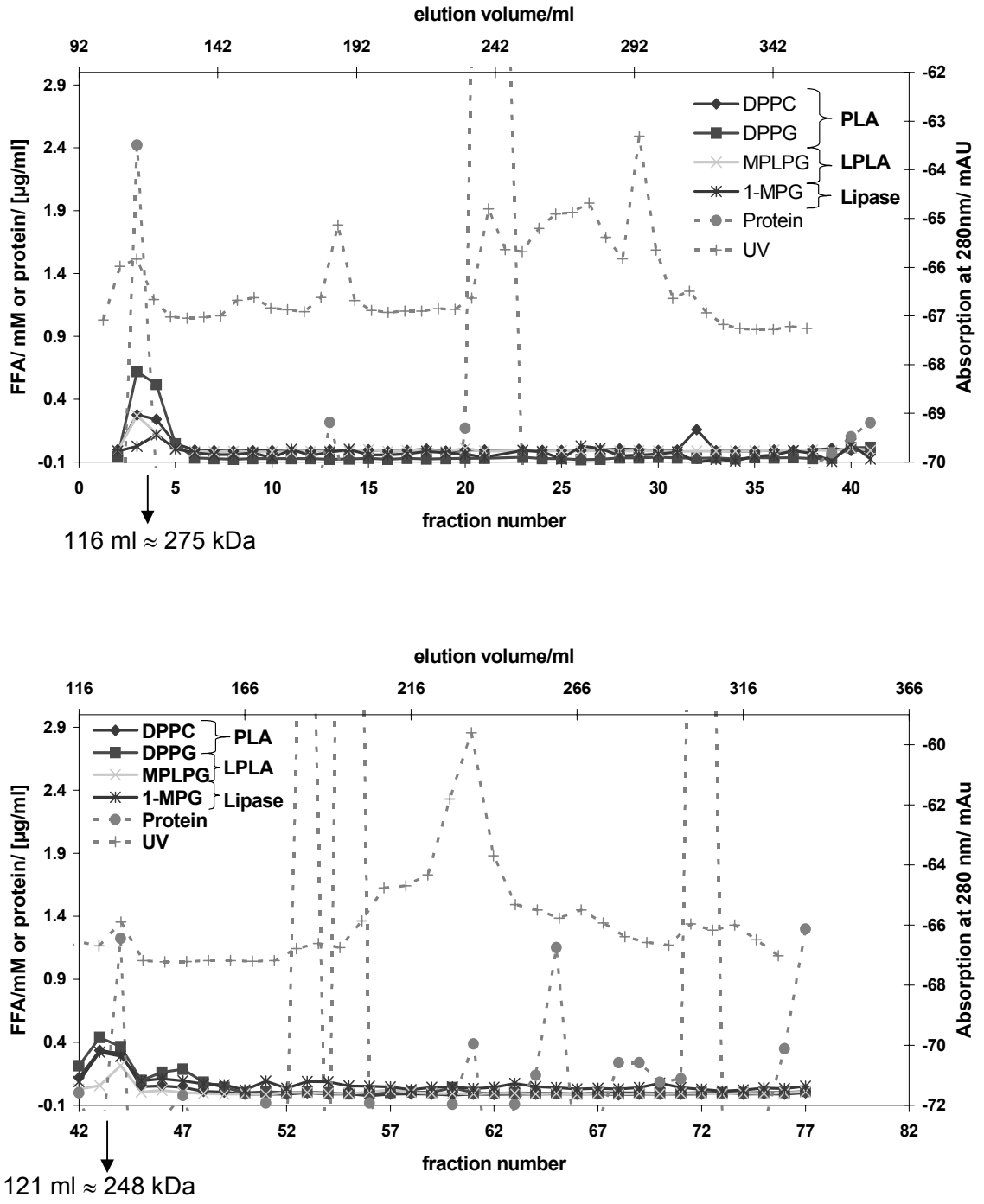

FIG.4.39. PLA, LPLA, and lipase activities of GF fractions from the pooled AEX fractions 10, 11, 13 as well as 70, 71, 73, 74. PLA-active AEX fractions 10, 11, 13 (upper panel) as well as 70, 71, 73, 74 (lower panel) were pooled, concentrated fourfold and subjected to gel filtration (HiLoad 26/60 Superdex 200 column, flow rate: 1 ml/min, fraction size: 6 ml). Resulting fractions were incubated with DPPC, DPPG, MPLPG, and 1-MPG for 19 h and 22 h, respectively at 37 °C and the release of fatty acids was quantified.

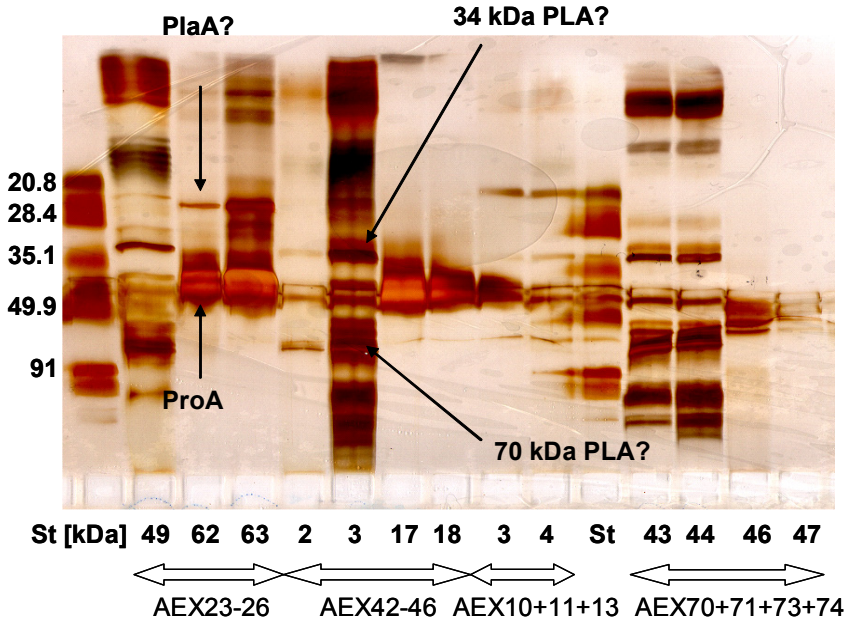

FIG.4.40. SDS PAGE of selected GF fractions. The fractions from GF showing PLA/LPLA activity were concentrated 35-40-fold (exclusion size: 3 kDa) and subjected to SDS PAGE under reducing conditions. Fractions 49 of AEX (23-26), fraction 3 of AEX (42-46), and fraction 43/44 of AEX (70+71+73+74) all contained a protein band of approximately 34 kDa and a second band of approximately 70 kDa (possibly PatA) which might represent PLAs.

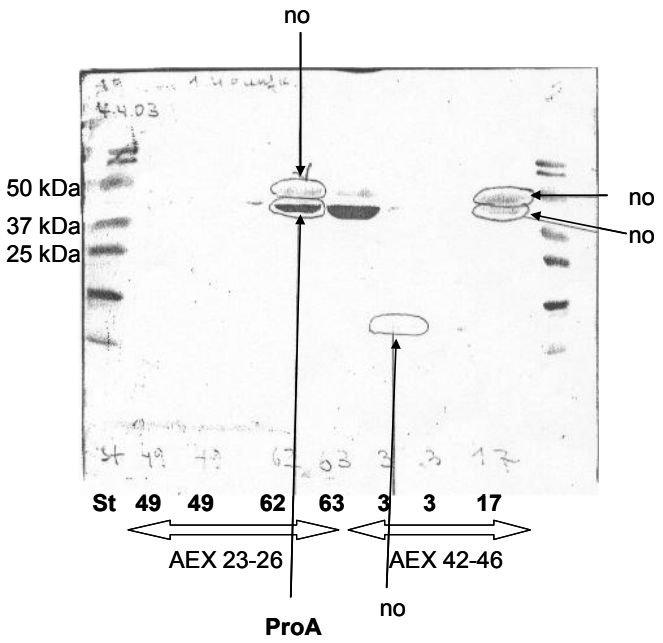

FIG.4.41. Western Blot of selected GF fractions. GF fractions 49, 62, and 63 of AEX fraction 23-26 and GF fractions 3 and 17 of AEX fractions 42-46 were concentrated fiftyfold, subjected to SDS PAGE (12 or 15 % gel), and transferred onto a PVDF membrane. Staining was performed with the reversible dye Ponceau-S. Visible bands were cut-out and subjected to Edman degradation (by the Group of Stefan Stevanovic, Universität Tübingen). The amount of protein on the membrane was too low for N-terminal sequencing and thus only one sequence (ProA) could be obtained. 'no' means that no sequence was obtained.

Table 4.3. Protein concentration as well as PLA, LPLA, and lipase activities (in the presence of 5 mM EDTA) of *L. pneumophila* 130b culture supernatant after each concentration/ purification step

	Protein/ [µg/ml]	PLA DPPG [nmol× ml^{-1}× h^{-1}]	PLA/µg Protein [nmol× μg^{-1}×h^{-1}]	LPLA MPLPG [nmol× ml^{-1}×h^{-1}]	LPLA/ µg Protein [nmol× μg^{-1}× h^{-1}]	Lipase 1-MPG [nmol× ml^{-1}× h^{-1}]	Lipase/ mg Protein [nmol× μg^{-1}×h^{-1}]
Culture sup	51	36	0.7	22	0.4	nd*	-
Retentate	79	91	1.2	60	0.8	nd	-
Permeate	33	0.3	0.01	3	0.1	nd	-
			AEX				
AEX **2**	40	497	12.4	154	3.9	3	0.1
AEX **1+3+4+5**	70	744	11	140	2	0	0
AEX **12**	34	486	14.3	142	4.2	270	7.9
AEX **10+11+13**	106	1100	10	296	2.8	306	2.9
AEX **22**	132	1253	9.5	486	3.7	437	3.3
AEX **23-26**	929	3508	3.8	7487	8.1	5038	5.4
AEX **42-46**	159	3900	24.5	1100	6.9	960	6
AEX **72**	12	819	68.3	147	12.3	353	29.4
AEX **70+71+73+74**	23	1600	69.6	295	12.8	250	10.9
			GF				
GF AEX [10, 11, 13] **3+4**	2	60	30	21	10.5	7	3.5
GF AEX[23-26] **49**	0	44	>44	11	>11	7	>7
GF AEX[23-26] **62+63+64**	14	4	0.3	370	26	305	21.8
GF AEX [42-46] **3+4**	4	122	30.5	14	3.5	nd	-
GF AEX [42-46] **18**	2	0.7	0.4	25	12.5	nd	-
GF AEX [70, 71, 73, 74] **43+44**	1	36.6	36.6	12.5	12.5	28	28

*nd= not determined

Since the first attempt of purifying PLA protein yielded a too low amount of protein after the gel filtration, a second purification cycle was started. This time a larger initial volume of culture supernatant was utilized for the purification (3 l). Again, the culture supernatant (OD_{660}= 1.8) was concentrated by ultrafiltration (thirtyfold) and subjected to an anion exchange chromatography. The resulting fractions were assayed for phospholipase A, lysophospholipase A, and lipase activities and additionally for GCAT activity (Fig. 4.42 and 4.43). GCAT activity was determined by the capability of generating cholesterol ester from DPPG and cholesterol. Again, several peaks of PLA and LPLA activities were obtained. Figure 4.42 shows at least four peaks of PLA activity present in the fractions 2, 4, 7, and 10. The highest LPLA activity was found in the fractions 9, 10, and 11 indicating that these fractions contained one or more LPLA (Fig. 4.42).

The GCAT activity did not show any distinct peak but was rather found throughout the fractions 4-14 (Fig. 4.43). The AEX fractions were also analyzed by SDS Page (Fig. 4.44). Notably, the fractions 10 and 11 contained a protein band of approximately 28 kDa which corresponded to the size of processed PlaA (Fig. 4.44) (73). Since these fractions also contained high LPLA activity (Fig. 4.42), this activity could be due to PlaA. As all of the secreted GCAT activity of *L. pneumophila* is caused by PlaC (see chapter 4.1), it is very likely that the GCAT activity of the AEX fractions were caused by PlaC. Indeed, the SDS PAGE of the AEX fractions displayed a protein of approximately 50 kDa in the fractions with GCAT activity which correlates in size with the processed form of PlaC of approximately 47 kDa (figures 4.43 and 4.44). The fractions 9-12 showed a thick band of approximately 37 kDa which corresponds to the size of the processed form of the major secreted zinc metalloprotease ProA. Earlier experiments had indeed shown that protease activity was present in fractions which eluted at 1 mM NaCl concentration from 20%-40% (figures 4.28 and 4.30) and N-terminal sequencing had shown that ProA was present in those fractions.

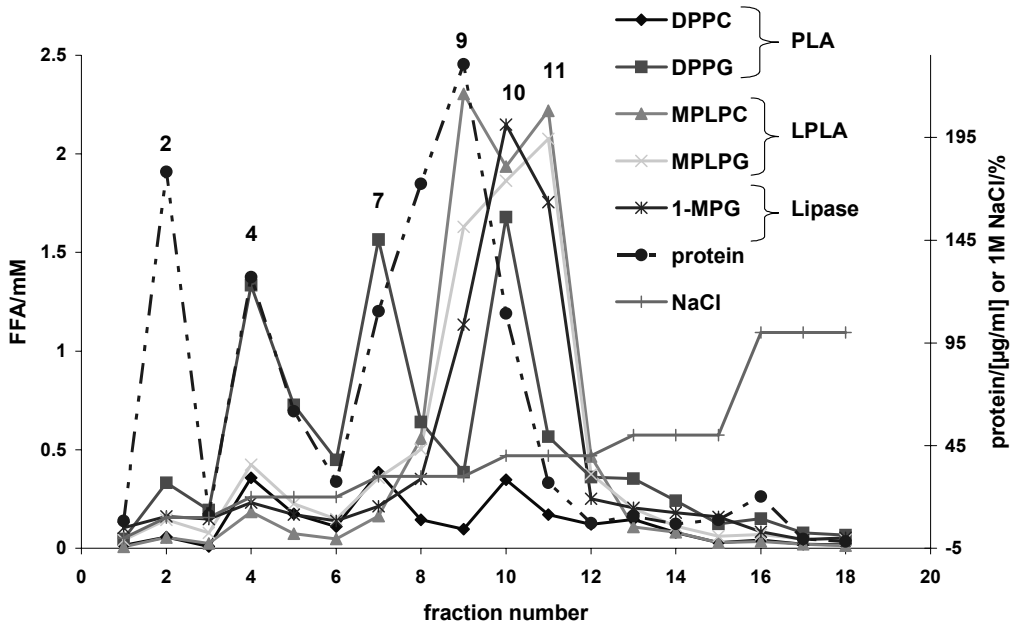

FIG.4.42. PLA, LPLA, and lipase activities of anion exchange chromatography fractions. 3 l of *L. pneumophila* 130b culture supernatant was concentrated thirtyfold by ultrafiltration and subjected to anion exchange chromatography (6 ml Resource Q column, flow rate: 0.5 ml/min, fraction size: 10 ml). Resulting fractions were incubated with DPPC, DDPG, MPLPC, and 1-MPG for 1h at 37 °C and the release of fatty acids was quantified (n=1). The amount of protein in each fraction was quantified as well. The peaks of PLA, LPLA and/or lipase activities are marked with the corresponding fraction number.

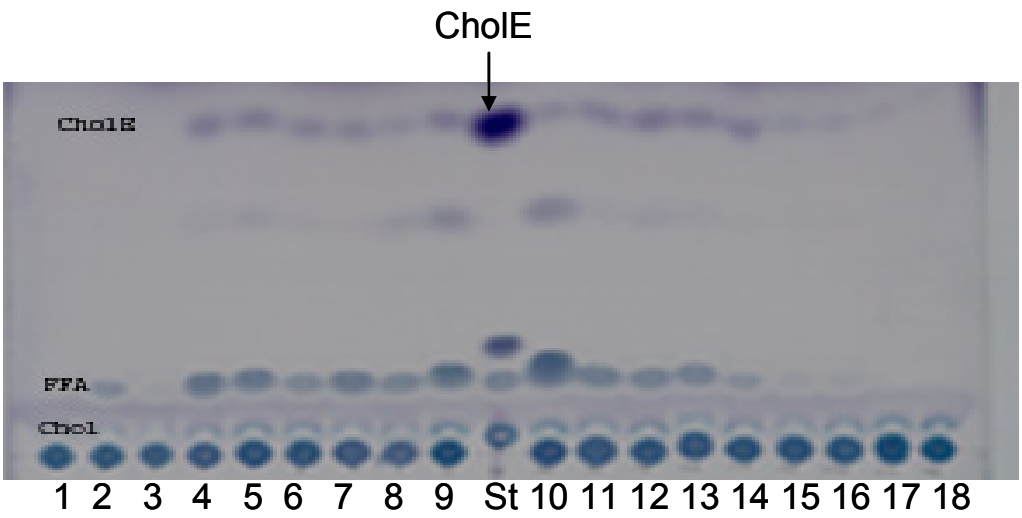

FIG.4.43. GCAT activity of anion exchange chromatography fractions. 3 l of *L. pneumophila* 130b culture supernatant was concentrated thirtyfold by ultrafiltration and subjected to anion exchange chromatography (6 ml Resource Q column, flow rate: 0.5 ml/min, fraction size: 10 ml). Resulting fractions were incubated with DPPG and cholesterol for 10 h at 37 °C, lipids were extracted and analyzed by TLC for the formation of cholesterol ester.

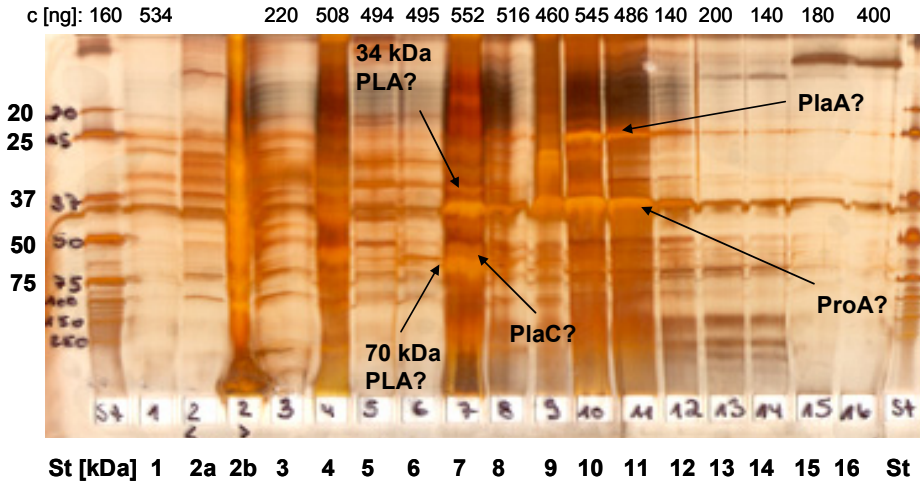

FIG.4.44. SDS PAGE of anion exchange chromatography fractions. 3 l of *L. pneumophila* 130b culture supernatant was concentrated thirtyfold by ultrafiltration and subjected to anion exchange chromatography (6 ml Resource Q column, flow rate: 0.5 ml/min, fraction size: 10 ml). Resulting fractions were loaded on a 12.5% SDS gel (amount of protein per gel pocket 140 ng to 550 ng), separated by electrophoresis and stained with silver stain. Fraction 2 was concentrated 40-fold using a filter with an exclusion size of 100 kDa and both fractions 2a (< 100 kDa) and 2b (>100 kDa) are shown. The amount of protein per gel pocket (in ng) is indicated above and the fraction number is indicated below the gel. The protein bands probably representing PlaA, ProA, PlaC and the 34 kDa PLA and 70 kDa PLA (possibly PatA) are marked.

9 ml of the AEX fractions with high PLA and LPLA activities (AEX fractions 4, 7, 9, 10, and 11) were first concentrated ten to twentyfold by means of centrifugal filter devices (exclusion size 10 kDa) and were further purified by gel filtration (GF). The fractions from gel filtration were again assayed for lipolytic activities (Fig. 4.45-4.48). After GF, the PLA and LPLA activities were again visible as two distinct activity peaks. The PLA peaks also showed LPLA and lipase activity while the dominant LPLA peaks had additional lipase activity (Fig. 4.45-4.48).

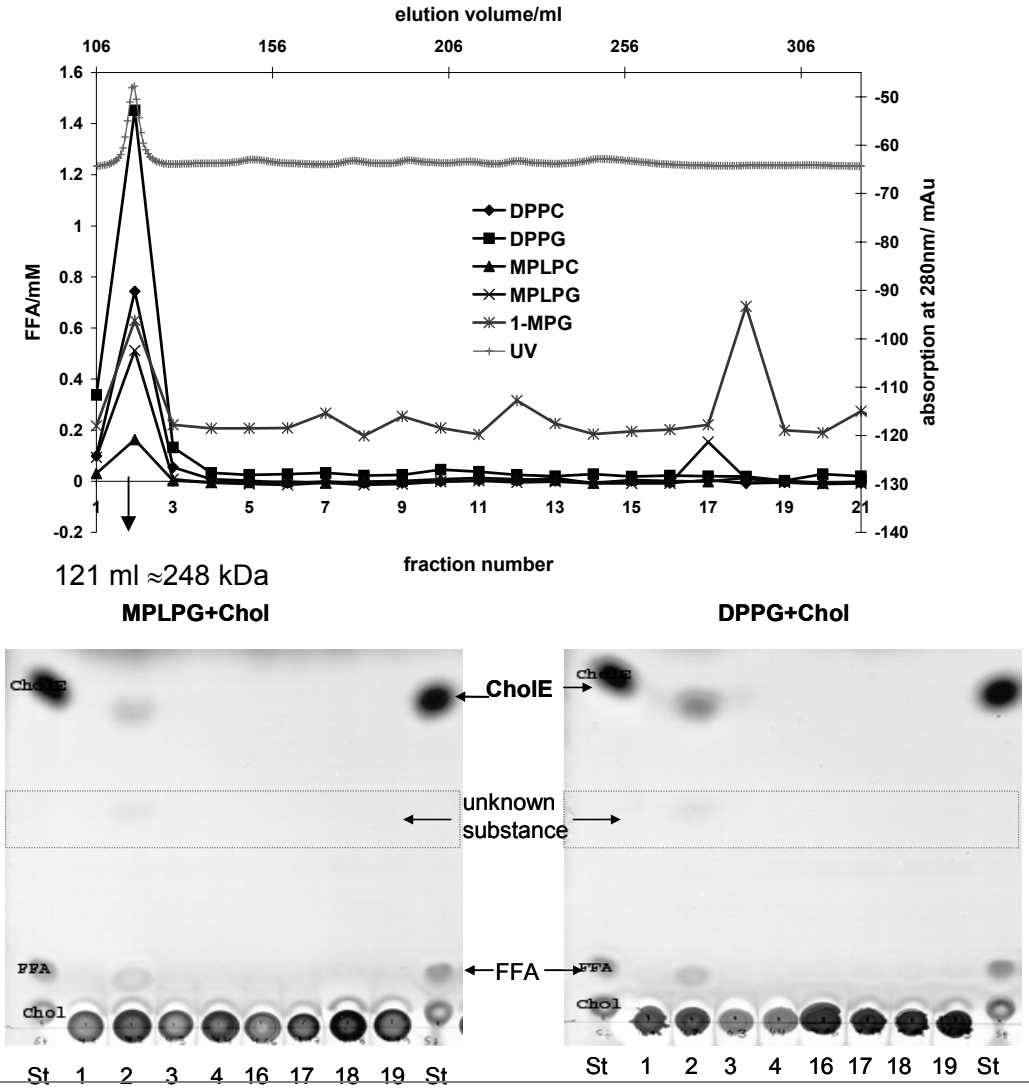

FIG.4.45. PLA, LPLA, lipase, and GCAT activities of GF fractions from AEX fraction 4. 9 ml of fraction 4 from AEX with high PLA activity was concentrated tenfold and subjected to gel filtration. Resulting fractions were incubated with DPPC, DDPG, MPLPC, and 1-MPG for 10 h at 37 °C and the release of fatty acids was quantified (upper panel). The GF fractions were also tested for GCAT activity by incubation with DPPG or MPLPG and cholesterol for 20 h at 37 °C and subsequent TLC analysis for the formation of cholesterol ester (lower panel). Comparable results were obtained on one more occasion.

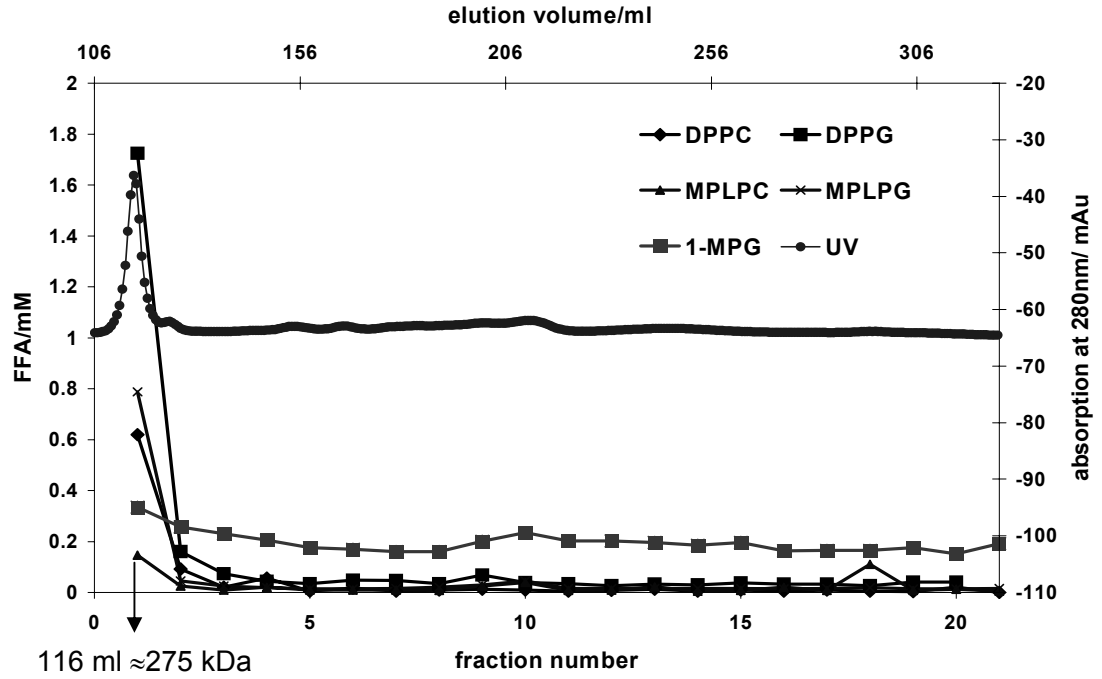

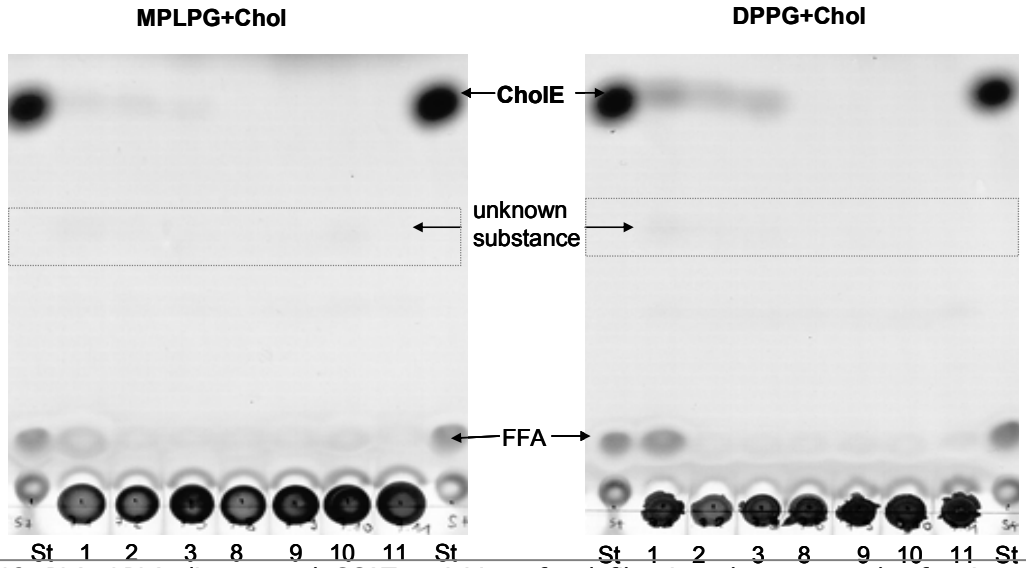

FIG.4.46. PLA, LPLA, lipase, and GCAT activities of gel filtration chromatography fractions from AEX fraction 7. 9 ml of fraction 7 from anion exchange chromatography with high PLA activity was concentrated fifteenfold and subjected to gel filtration. Resulting fractions were incubated with DPPC, DDPG, MPLPC, and 1-MPG for 10 h at 37 °C and the release of fatty acids was quantified (upper panel). The GF fractions were also tested for GCAT activity by incubation with DPPG or MPLPG and cholesterol for 20 h at 37 °C and subsequent TLC analysis for the formation of cholesterol ester (lower panel). Comparable results were obtained on one more occasion.

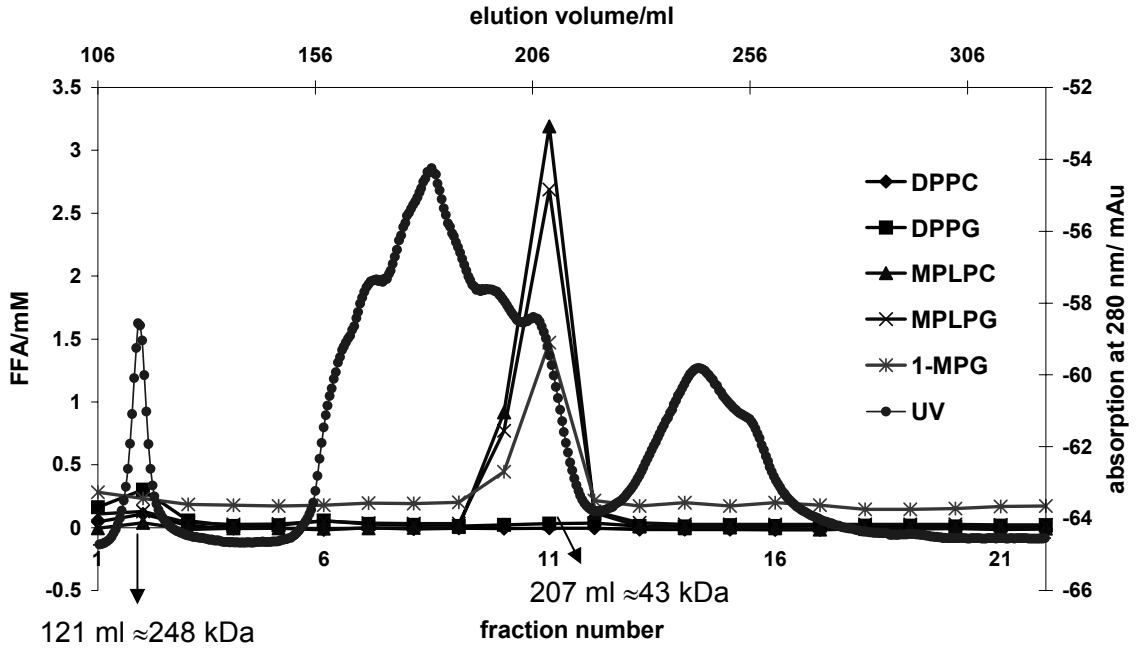

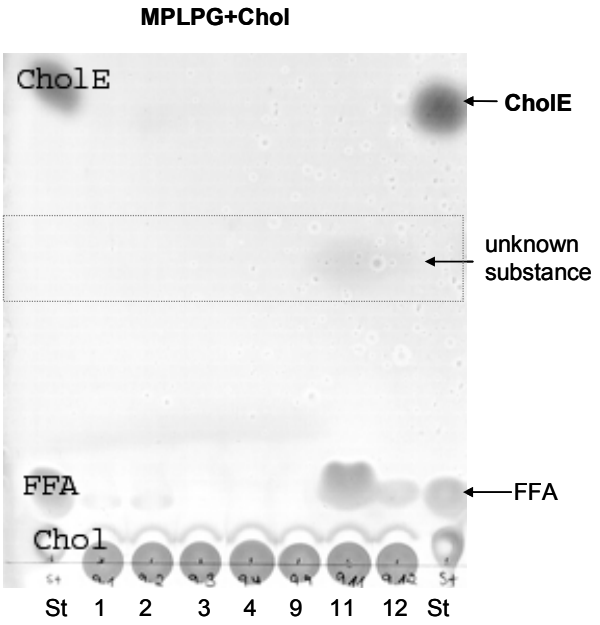

FIG.4.47. PLA, LPLA, lipase, and GCAT activities of gel filtration chromatography fractions from AEX fraction 9. 9 ml of fraction 9 from anion exchange chromatography with high LPLA activity was concentrated tenfold and subjected to gel filtration. Resulting fractions were incubated with DPPC, DDPG, MPLPC, and 1-MPG for 10 h at 37 °C and the release of fatty acids was quantified (upper panel). The GF fractions were also tested for GCAT activity by incubation with MPLPG and cholesterol for 20 h at 37 °C and subsequent TLC analysis for the formation of cholesterol ester (lower panel). Comparable results were obtained on one more occasion.

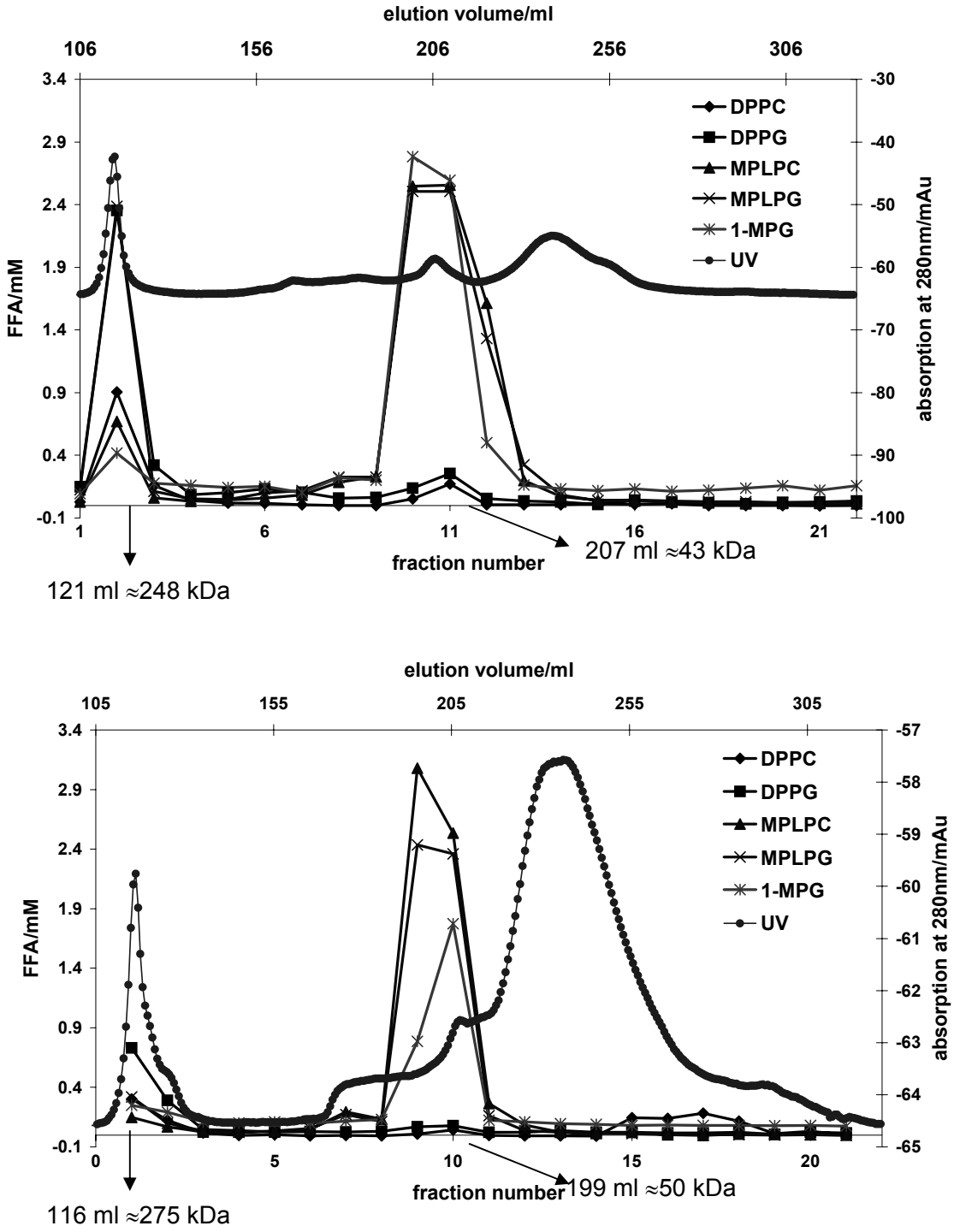

FIG.4.48. PLA, LPLA, lipase activities of gel filtration chromatography fractions from AEX fraction 10 and 11. 9 ml of fraction 10 (upper panel) and 11 (lower panel) from anion exchange chromatography with high PLA and LPLA activities was concentrated fifteen- and twentyfold and subjected to gel filtration. Resulting fractions were incubated with DPPC, DDPG, MPLPC, MPLPG, and 1-MPG for 24 h at 37 °C and the release of fatty acids was quantified. The elution volume and the absorption at 280 nm have been correlated with the fraction number and lipolytic activities.

The GF fraction 2 of AEX fraction 4 (AEX4 GF2) and GF fraction 1 of AEX fraction 7 (AEX7 GF1) showing high PLA activity also showed high GCAT activity (Fig. 4.45-4.46). The GCAT activity was able to transfer fatty acids from either DPPG or MPLPG to cholesterol (Fig. 4.45-4.46). Since PlaC, has PLA and LPLA activities in addition to its GCAT activity (see chapter 4.3), the observed PLA and GCAT activities in the same fractions could be caused by PlaC alone. However, as the proteins in the PLA and GCAT active fractions display a high molecular mass (figures 4.45-4.46), it might also be possible that two different enzymes possessing the two different activities might be present as a complex, e.g. PlaC and PatA. The TLC pictures revealed the generation of another unidentified compound apart from cholesterol ester in the fractions with GCAT activity when these were incubated with DPPG or MPLPG and cholesterol (figures 4.45-4.46). This compound which was also generated in dependence of PlaC (figures 4.5 and 4.9) was only observed in the presence of cholesterol and might therefore represent a cholesterol derivative (data not shown). SDS PAGE analysis of the proteins present in the PLA-active GF fractions revealed protein bands which corresponded in size to PlaA (28 kDa), PlaC (50 kDa), and PatA (70 kDa) (Fig. 4.49). A 34 kDa protein which was found to be present in the same fractions as the 70 kDa protein was also detected (Fig 4.49).

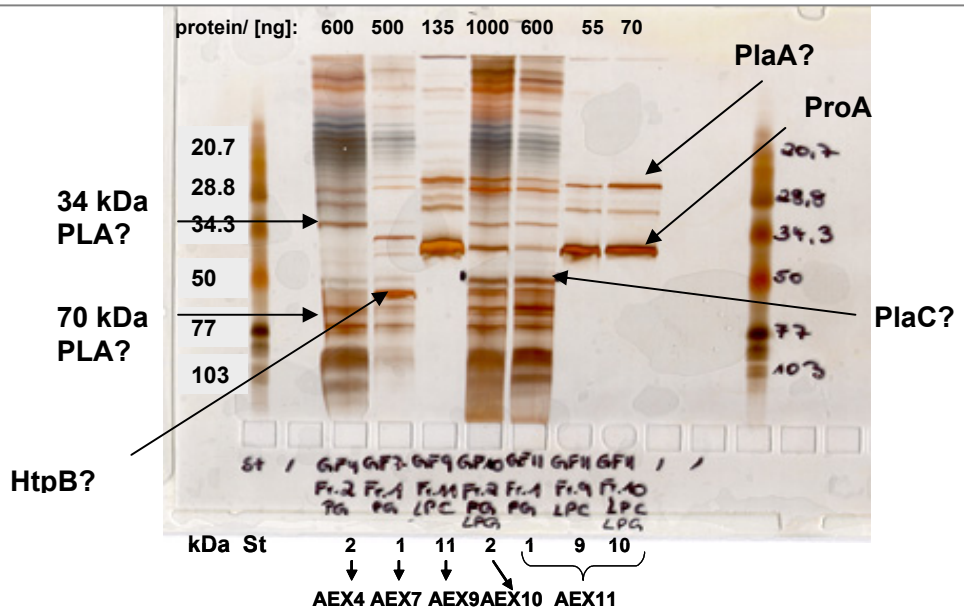

FIG.4.49. SDS PAGE of GF fractions. Concentrated culture supernatant of strain 130b was subjected to AEX and fractions 4, 7, 9, 10, and 11 with high PLA/LPLA activity were further purified by GF. Resulting fractions which contained high PLA/LPLA activity were separated by SDS PAGE and stained with silver stain. Fractions AEX10 GF2 and AEX11 GF1 were concentrated 5- and 10-fold with centrifugal filter devices (molecular weight cut-off: 10 kDa). St: protein standard.

500 µl of the AEX fractions 2 (> 100 kDa), 4, 7, and 9 were concentrated 10-20-fold, blotted and sent for sequencing. In addition to ProA (sequenced from fraction 9), the only sequence which could be assigned to a *Legionella* protein was HtpB, the heat shock protein, which was sequenced from fraction 7 (Table 4.4). This time, many short fragments (5-7 amino acids) were obtained which were not sufficient for protein identification (data not shown). Many of the sequenced protein bands contained additionally the sequence of ProA (data not shown). The fractions from gel filtration with high PLA activity (GF2 of AEX4, GF1 of AEX7, GF11 of AEX9, and the pooled fractions GF10+11 of AEX11, and GF2 of AEX10 + GF1 of AEX11) were concentrated 50-fold and blotted. Again only a protein band corresponding to the size of ProA was visibly stained by Ponceau S indicating that in spite of high enzymatic activity the protein(s) with PLA activity might be present only in low amounts (data not shown).

4.4.2 Identification of *L. pneumophila* PLA candidates by N-terminal protein sequencing

In order to identify the enzyme or enzymes responsible for the secreted *L. pneumophila* PLA activity, concentrated culture supernatant (exclusion size: 30 kDa) was subjected to anion exchange chromatography. The resulting fractions which contained high PLA activity were concentrated fortyfold and the contained proteins were separated by electrophoresis (figures 4.32 and 4.33). Afterwards the proteins were transferred to a PVDF membrane and single bands were cut-out and sequenced by our collaborating group under the supervision of Prof. Stefan Stevanovic (Universität Tübingen). The obtained amino acid sequences which could be assigned to specific *L. pneumophila* Philadelphia-1 proteins are shown in Table 4.4. Three of the seven identified proteins were viewed as possible PLA candidates: 1. Unk1, because it possessed considerable sequence similarity to the triacylglycerol lipase Lip3 of *Mycoplasma pneumoniae*, 2. LvrE, because it was the only detectable protein in the fraction (Fig. 4.32 and 4.33), 3. Aas, because it contains conserved regions of amino acid homology to a group of acyltransferases which are involved in phospholipid metabolism and its best characterized homolog is the Aas protein of *E. coli*, which is an inner-membrane protein with 2-acylglycerophosphoethanolamine acyltransferase activity (105). The four other identified proteins were not considered likely to possess PLA activity and were therefore not or only initially (in case of HbpB and Unk2) characterized further. ProA is the already well characterized major type II secreted zinc metalloprotease, while HtpB is a paralog of Htp, a chaperonin also known as Hsp60 (116).

HbpB is the paralog of Hbp which has been described as a heme binding protein (144). Unk2 does not possess homology to any known protein. Since an initial investigation of Unk2 and Hbp2 expressed in *E. coli* did not show any PLA, LPLA or lipase activities, the proteins were not investigated further in this study (data not shown).

Table 4.4. Overview of proteins sequenced from *L. pneumophila* 130b PLA active anion exchange chromatography fractions. Concentrated *L. pneumophila* 130b culture supernatant was subjected to AEX. Proteins from AEX fractions with high PLA activity were separated by SDS PAGE and transferred onto a PVDF membrane and cut-out and sequenced by Edman degradation. The obtained N-terminal sequences were used for a BLAST search against the *L. pneumophila* Philadelphia-1 genome database (38) and the *Legionella* proteins which were found are listed. Possible homologous proteins in other organisms are listed as well (Expect Value≤1)

Experimentally found sequence	Name	Gi Number	Signal-peptide (Signal-P prediction)	Homology (expect value)
ETIDFPTQIVRVSGN (sequenced from position 59) found in AEX fractions 21 and 22	UNK1 (novel)	52840444	Yes , cleavage between position 19/20	Hypothetical protein (gi23488575) from *Plasmodium yoelii yoelii* (0.01); triacylglycerol lipase, esterase (gi1674078) from *Mycoplasma pneumoniae* (0.094)
EVLPSSKDAQLXTNA (sequenced from position 2) found in AEX fractions 21+22	UNK2 (novel)	52840256	No	No homology
XDKELXAHIEALYSK (sequenced from position 24) found in AEX fraction 12 and 22	LvrE	52841476	Yes, cleavage between position 21/22	LvrE from *Legionella pneumophila*; Hypothetical protein (gi68550846) from *Pelodictyon phaeoclathratiforme* (10^{-16})
GSDT(F)LN(G)QN (sequenced from position 385) found in AEX fraction 21	Aas (novel)	52840834	No	AMP-dependent synthetase and ligase:Phospholipid/ glycerol acyltransferase (gi71548720) from *Nitrosomonas eutropha* (10^{-179})
SEEGACPDINVIKAEGLPMA (sequenced from position 35) found in AEX fraction 2	HbpB (novel)	52842426	Yes, cleavage between position 34/35	Heme binding protein from *Legionella pneumophila*
AKELRFGDDARLQML (sequenced from position 4) found in AEX fraction 7 (2. purification)	HtpB	52840925	No	Heat shock protein Hsp60 from *Legionella pneumophila*
GKVQAKGMGFGGNRK (sequenced from position 208) various AEX fractions, e.g. 22 and 32	ProA	52840256	Yes, cleavage between position 24/25	Zink metalloprotease from *Legionella pneumophila* (156)

4.4.3 Characterization of Unk1

4.4.3.1 Genetic locus of *L. pneumophila unk1*

One protein which was sequenced from the PLA active anion exchange fractions 22 and 23 (Fig. 4.33), was coded by an ORF of 867 bp, representing a protein of 288 amino acids with a molecular mass of 33.3 kDa and an isoelectric point of 4.9. Furthermore, the newly found protein possessed a predicted signal sequence with a probable cleavage site between positions 19 and 20. Therefore, it is a likely substrate of the *L. pneumophila* type II secretion system. However, the predicted cleavage site does not correspond with the experimentally found N-terminus which started at position 59 of the putative protein (Table 4.4). The Unk1 protein sequence of strain 130b differs in four amino acids from the sequence of strain Philadelphia-1 which is within the range observed for other proteins (data not shown). The protein (gi52840444) displayed partial homologies to a hypothetical protein (gi23488575) and to an erythrocyte binding protein (gi82539865) of *Plasmodium yoelii yoelii* with expect values of 0.011 and 0.12, respectively. Erythrocyte binding proteins are secreted by malaria parasites and bind to specific receptors of erythrocytes via conserved cysteine-rich regions (2). The homologous regions between the *Legionella* protein and the erythrocyte binding protein did, however, not include these cysteine-rich regions. But most interestingly, the newly found protein displayed partial homology to a triacylglycerol lipase/ esterase (gi1674078) of *Mycoplasma pneumoniae* (expect value=1, 25 % identities, 37 % similarities). However, an alignment of the two proteins showed that in spite of considerable sequence similarity of the *L. pneumophila* protein with Lip3 of *M. pneumoniae*, the *L. pneumophila* protein lacked the lipase motif GXSXG which encloses the catalytic active serine of lipolytic enzymes (Fig. 4.50). Since there was no significant homology to indicate a putative function, the newly identified *L. pneumophila* protein was designated Unk1, for unknown protein 1. Interestingly, all three sequenced *L. pneumophila* genomes encode a paralog of Unk1 with an expect value of 2×10^{-71} (50 % identities, 67 % similarities), a hypothetical protein (gi52841107) with no significant homology to proteins of other organisms.

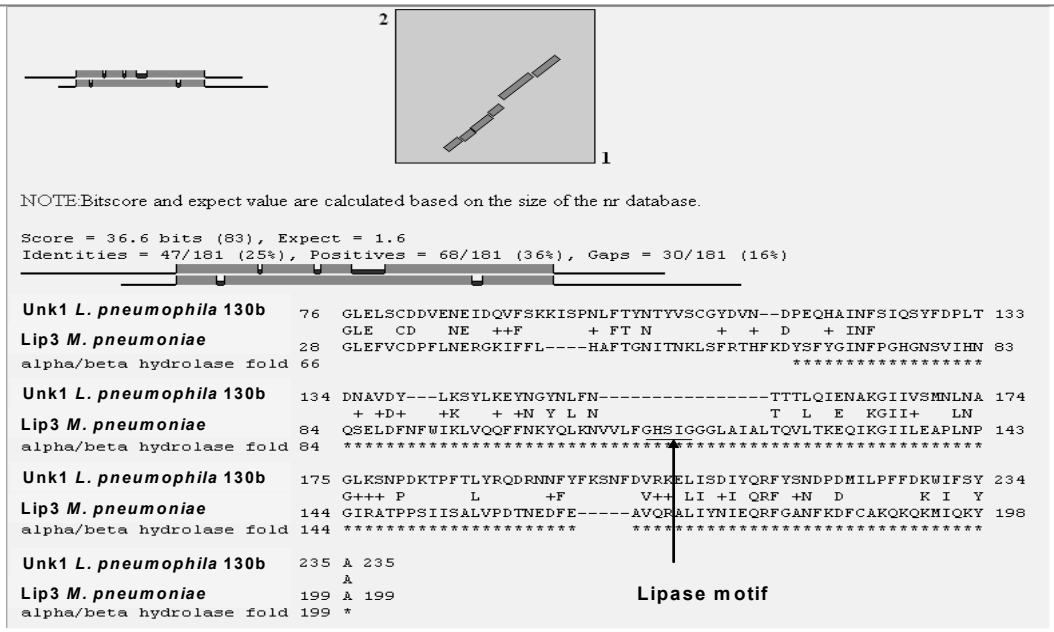

FIG. 4.50. Pairwise BLAST alignment of *L. pneumophila* 130b Unk1 and *M. pneumoniae* Lip3. The protein sequences of *L. pneumophila* Unk1 and *M. pneumoniae* Lip3 were aligned with the blastp program provided by the ncbi server (http://www.ncbi.nlm.nih.gov/blast/bl2seq/wblast2.cgi).

Two ORFs flank the *unk1* gene in strain Philadelphia-1. The oppositely oriented downstream ORF2 contains a PFAM domain of CoA transferases family III and is homologous to a CAIB/BAIF (=domain of CoA transferases which are involved in carnitine metabolism) family protein (gi83814994) of *Salinibacter ruber*. The upstream ORF3 which has the same direction as *unk1* possesses homology to NADH dehydrogenase subunit 2 (gi31126992) of the insect *Lepidopsocid*. Interestingly, a gene encoding a zinc metalloprotease (gi52840442) which is not ProA is located next to ORF2 (Fig. 4.51). It is impossible that *unk1* and ORF2 form an operon as they are oppositely oriented. Moreover, it is unlikely that ORF3 and *unk1* represent an operon as a -10 and a -35 box is located in the 105 bp intergenic region. The Unk1 locus in strains Paris and Lens differs from that in strain Philadelphia-1 in respect to the absence of ORF3 and two other upstream ORFs in strains Paris and Lens, respectively (not shown).

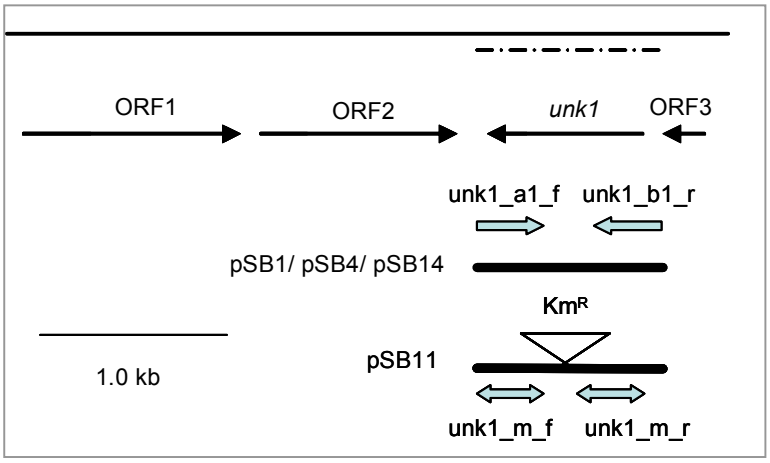

FIG. 4.51. The *unk1* locus in *L. pneumophila* and recombinant *E. coli*. The upper line represents the *L. pneumophila* Philadelphia-1 chromosome region that contains the *unk1* gene. The dotted line below illustrates the region which was sequenced from 130b. The arrows below this line depict the relative location, size, and orientation of *unk1* and neighboring ORFs. The lines at the bottom of the figure represent the segments of *Legionella* DNA that were cloned into plasmid vectors. The thick arrows represent the primers which were used for the amplification of the *unk1* gene from the 130b genome (these are not drawn to scale). Plasmid pSB11 contained a Km^R gene cassette. Constructs: pSB1=pGEMTez+*unk1*, pSB4=pBCKS+*unk1*, pSB14=pMMB2002+*unk1*, pSB11=pBCKS+*unk1*::Km^R.

4.4.3.2 Isolation of *L. pneumophila* 130b *unk1* mutants

In order to investigate the role of Unk1 in the lipolytic activities of *L. pneumophila*, knockout mutants of this gene were constructed. First, an approximately 1000 bp fragment containing the *unk1* ORF with its putative promoter region was amplified from the 130b genome and cloned into the vector pGEMTez, yielding pSB1. The *unk1* gene from pSB1 was subcloned into the vector pBCKS thereby generating pSB4 (Table 3.21). pSB4 then served as a template for the insertion of a Km^R cassette into *unk1* (after base position 231 of the gene and the corresponding amino acid position 77, respectively) by site-directed mutagenesis using primers unk1_m_f and unk1_m_r, yielding plasmid pSB11 (see chapter 3.2.2.6). Then pSB11 was used to introduce the disrupted *unk1* gene into the *L. pneumophila* 130b genome by taking advantage of the natural competence of the bacteria when grown at 30 °C. The kanamycin resistent *L. pneumophila* 130b *unk1* mutants were analysed by PCR and Southern blot (appendix).

Three independent *L. pneumophila* 130b *unk1* mutants (unk1- cl1, unk1- cl2, and unk1- cl.3) were obtained. Southern blot analysis, however, indicated that only one of the mutants (unk1- cl1) was a true *unk1* mutant while the other two appeared to be merodiploids, i.e. contained both the wild type gene and the mutant gene. To further investigate this possibility, the mutants unk1- cl1 and unk1- cl2 were analyzed for an *unk1* transcript by RT-PCR. Indeed, only unk1- cl1 was found to lack *unk1* mRNA showing that it was a true mutant. unk1- cl2 on the other hand still showed *unk1* expression confirming that it was a merodiploid.

4.4.3.3 Lipolytic activities of *L. pneumophila* 130b *unk1* mutants

Since Unk1 was viewed as a potential secreted PLA, the corresponding *L. pneumophila* mutants were assessed for lipolytic activities. To this purpose, *L. pneumophila* 130b and *unk1* mutants were grown to late logarithmic growth phase (OD_{660}=1.8) in BYE broth and the culture supernatants were obtained. The culture supernatants were then assayed for hydrolysis of diacylphospholipids (DPPC, DPPG), monoacylphospholipids (MPLPG, MPLPC), and 1-MPG. As shown in figure 4.52, compared to the wild type, the culture supernatants of unk1- cl1 released reduced amounts of fatty acids from the all the employed substrates, indicating that Unk1 might contribute to the secreted PLA, LPLA and lipase activities of *L. pneumophila* 130b. The reduction in PLA activity in this mutant was complemented by the introduction of pSB14 containing an intact *unk1* gene while the reduction of LPLA and lipase activities were not complemented in this way. Notably, clone 2 which was previously found to still express *unk1* displayed a significant decrease in the hydrolysis of PLA and LPLA substrates which was complemented by the introduction of *unk1* in *trans* (Fig. 4.52). In summary, these data suggest that *L. pneumophila unk1* mutants possess marginally reduced lipolytic activities in their culture supernatant.

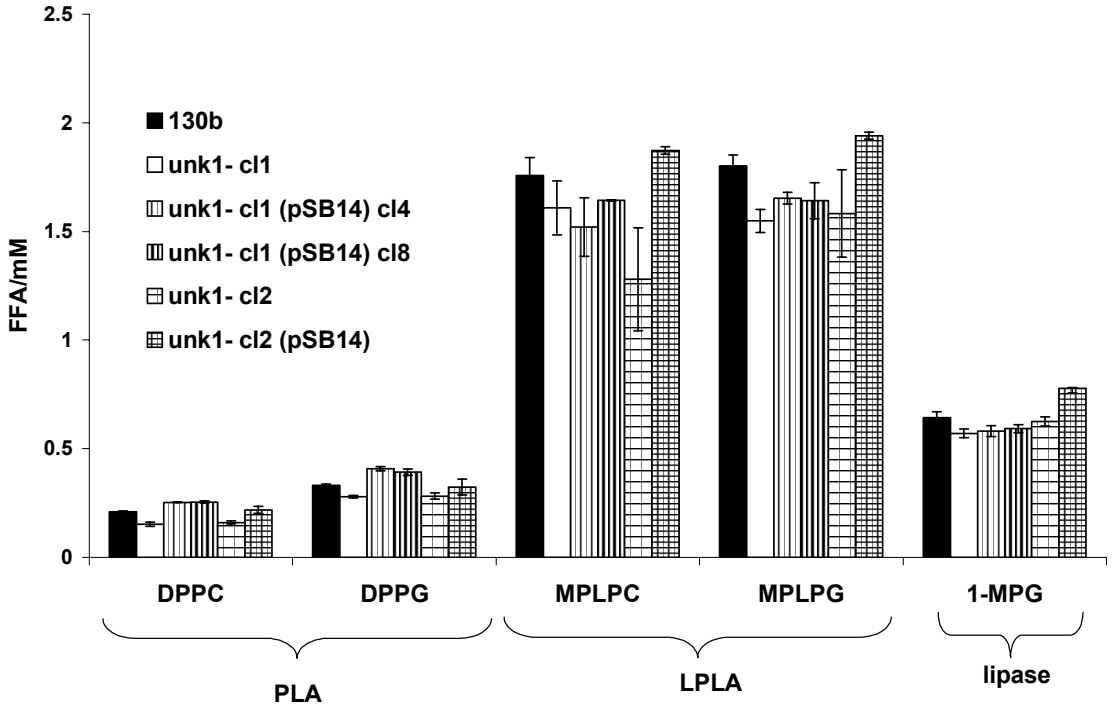

FIG. 4.52. Lipolytic activities of *L. pneumophila* wild type, *unk1* mutants, and complemented strains. Culture supernatants (obtained at OD_{660}=1.8) of wild type, *unk1* mutant clones 1 and 2 and *unk1* mutant clones 1 and 2 harbouring pSB16 were incubated with DPPC, DPPG, MPLP, and MPLPG or 1-MPG for 10 h at 37°C. The release of FFA was quantified. Data are expressed as differences between the amount of FFA released by culture supernatants and the amount released by BYE broth. The results represent the means and standard deviations of triplicate samples and are representative of three (only mutants) and two (complementation clones) independent experiments. pSB14=pMMB2002+*unk1*.

The wild type and the mutant culture supernatants were also analyzed for their capacity to cleave the artificial substrate p-nitrophenyl butyrate which is cleaved by a variety of esterases. The culture supernatants of the wild type and of the *L. pneumophila unk1* mutant and *trans* complemented clones showed a similar level of p-nitrophenol hydrolysis (Fig. 4.53). This observation suggests that Unk1 does not possess esterase activity. In summary, it was found that Unk1 does not contribute to the secreted esterase activity of *L. pneumophila* but might contribute to the secreted PLA, LPLA, and lipase activities in a minor degree.

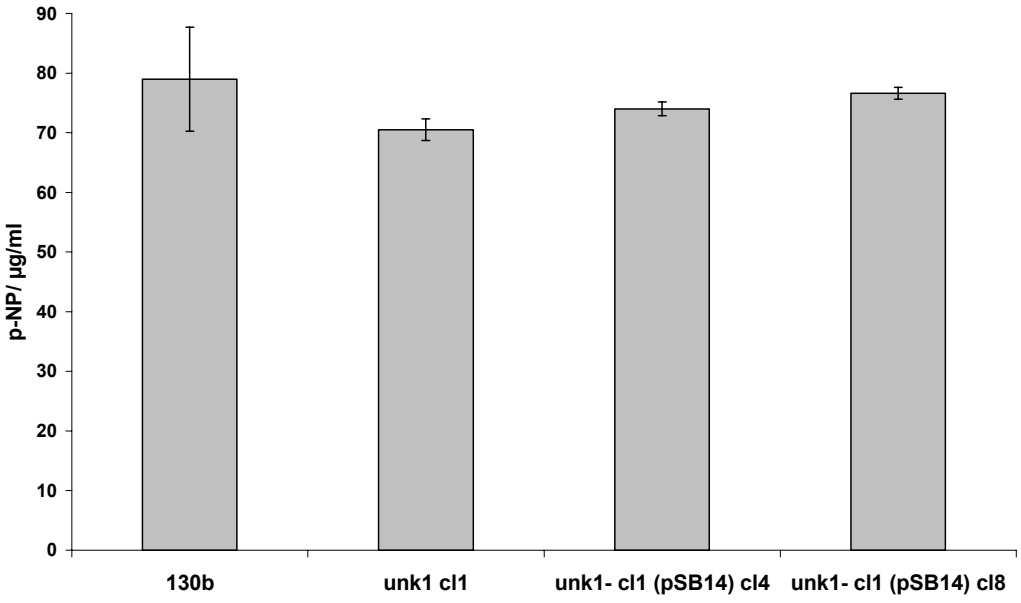

FIG. 4.53. Secreted esterase activity of *L. pneumophila* 130b wild type, *unk1* mutant, and complemented strain. Culture supernatants of wild type, *unk1* mutant clone 1 and *unk1* mutant clone 1 harbouring pSB14 were obtained at OD660=2.0 (late logarithmic growth phase) and incubated with p-nitrophenylbutyrate for 30 min at 37°C. The release of p-nitrophenol (p-NP) was quantified. Data are expressed as differences between the amount of FFA released by culture supernatants and the amount released by BYE broth. The results represent the means and standard deviations of quadruplicate samples and are representative of two independent experiments. pSB14=pMMB2002+*unk1*.

4.4.3.4 Enzymatic activities of *E. coli* clones expressing *L. pneumophila* 130b *unk1*

Since *L. pneumophila unk1* mutants (Fig. 4.54) showed a tendency of reduced PLA and LPLA activities, the lipolytic activities of *E. coli* clones harbouring *unk1* in *trans* were assessed in the following. For this purpose, the *L. pneumophila unk1* gene including its putative promoter region was amplified from the 130b genome using primers unk1_a1_f and unk1_b1_r and cloned into the vector pGEMTeasy, yielding pSB1 and then subcloned into the vector pBCKS, yielding pSB4. Further subcloning into the vector pMMB2002 generated pSB14 (Table 3.22). An expression analysis by means of RT-PCR of *E. coli* clones harbouring pSB14 showed that expression of *unk1* in *E. coli* only occurred in the presence of 1 mM IPTG (data not shown). Culture supernatants and cell lysates of *E. coli* clones harbouring pSB4 or the pBCKS vector were analysed for hydrolysis of DPPC and DPPG, representing PLA substrates, for hydrolysis of the triacylglycerol TPG, representing a lipase substrate, and for the hydrolysis of MPLPG, which is a LPLA substrate.

As shown in figure 4.54, there was no difference in the capacity of the *E. coli* clones harbouring *unk1 in trans* to cleave the substrates to that of the clones carrying the vector only. Since it might be possible that Unk1 requires a *Legionella* factor for its activity, culture supernatants and cell lysates of the clones harbouring *unk1* or the vector control were preincubated with culture supernatant of *L. pneumophila* 130b wild type. Again there was no enhanced lipolytic activity in the clones carrying *unk1* in *trans* indicating that no secreted *Legionella* factor could activate any lipolytic properties of Unk1 (Fig. 4.55). The analysis of the secreted and cell-associated lipolytic activities of *E. coli* clones carrying *unk1* in the low copy vector pMMB2002 (=pSB14) yielded similar results. In conclusion, these data show that Unk1 does not confer lipolytic activities to *E. coli* clones.

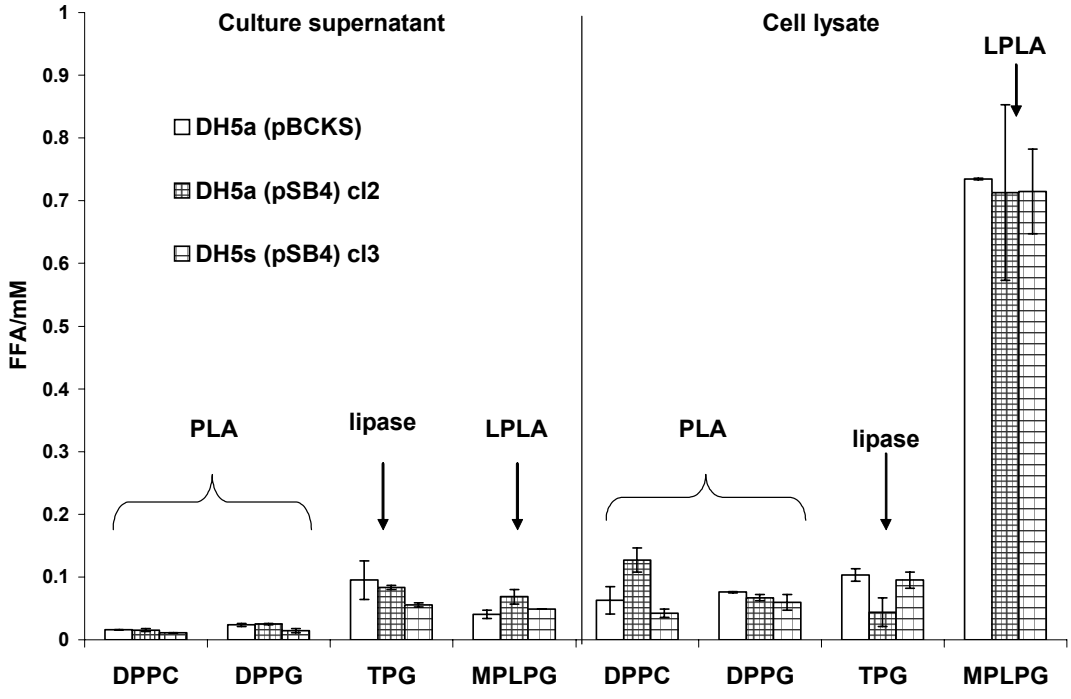

FIG.4.54. Secreted and cell-associated lipolytic activities of recombinant *E. coli* DH5α containing *L. pneumophila* 130b *unk1*. *E. coli* containing pBCKS or its derivative pBSB4 were grown in the presence of 1 mM IPTG and obtained at OD_{660}=2.0. Culture supernatants or cell lysates were mixed with DPPC, DPPG, TPG, or MPLPG. The results represent the means and standard deviations of duplicate samples and are representative of three independent experiments. pSB4=pBCKS+*unk1*.

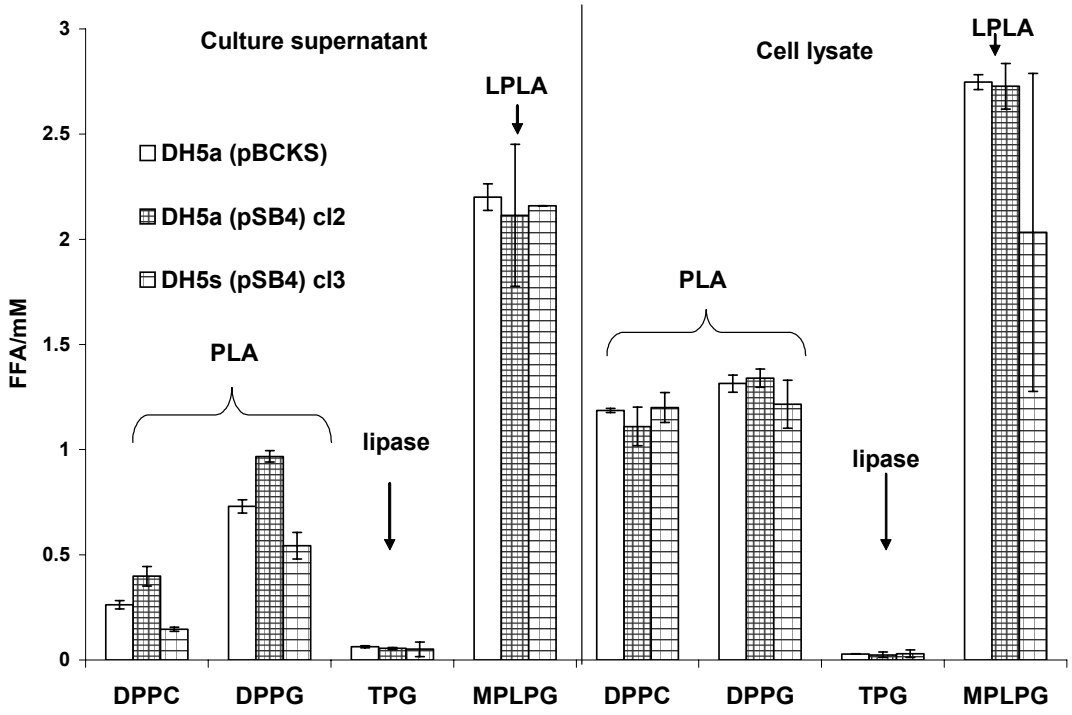

FIG.4.55. Secreted and cell-associated lipolytic activities of *E. coli* DH5α containing *L. pneumophila unk1* after preincubation with *Legionella* culture supernatant. *E. coli* containing pBCKS or its derivative pBSB4 were grown in the presence of 1 mM IPTG and obtained at OD_{660}=2.0. 25 µl of culture supernatants or cell lysates were incubated with 25 µl of *L. pneumophila* 130b culture supernatant (OD_{660}=2.0) for 15 min at 25 °C, and 25 µl of this mixture was subsequently mixed with the lipids. After 20 h incubation at 37°C, the release of FFA was quantified. The results represent the means and standard deviations of duplicate samples and are representative of two independent experiments. pSB4=pBCKS+*unk1*.

4.4.3.5 The role of Unk1 during intracellular infection

Although the enzymatic function of *L. pneumophila* Unk1 still remains to be elucidated, its role during intracellular infection was investigated in the following. To this purpose, *A. castellanii* amoebae and U937 macrophages were infected with *L. pneumophila* 130b wild type or *unk1* mutants. The CFU of the *L. pneumophila* wild type increased by three and four logarithmic units during 48 h and 72 h of infection, respectively (Fig. 4.56). In comparison, the CFU of the *unk1* mutant remained one logarithmic unit behind from 48 h after infection on. Notably, the mutant unk1- cl2 showed an even greater intracellular growth defect (tenfold reduced compared to mutant clone 1, data not shown). In summary, these data indicate an essential role for Unk1 in infections of amoebae and macrophages by *L. pneumophila*. The intracellular growth of the

mutant unk1- cl1 could not be restored to wild type level by introducing the *unk1* gene *in trans* (Fig. 4.39, upper part). Therefore, the possibility that the observed defect of the mutant was caused by a second site mutation cannot be excluded.

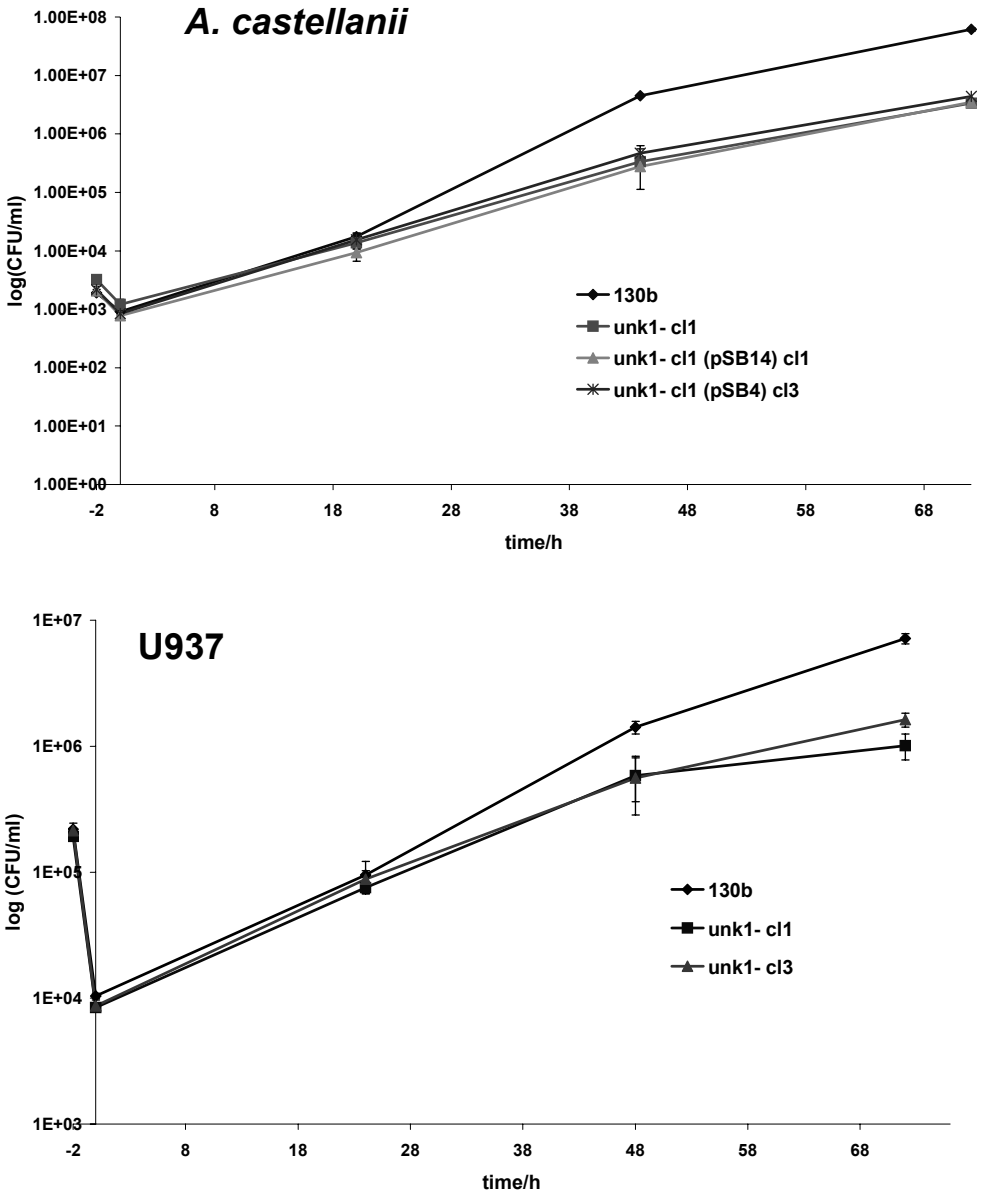

FIG.4.56. Intracellular infection of host cells by wild type 130b and *unk1* mutant *L. pneumophila*. *A. castellanii* amoebae and U937 macrophages (upper and lower figure, respectively) were inoculated with *L. pneumophila unk1* knockout mutants or *L. pneumophila* wild type (MOI of 0.01 and 1, respectively). At various time points post inoculation, the number of bacteria was quantified by plating aliquots on BCYE agar. Results represent the means and standard deviations of triplicate samples and are representative of three independent experiments. Constructs: pSB4=pBCKS+*unk1*, pSB14=pMMB2002+*unk1*.

4.4.4 Characterization of LvrE

4.4.4.1 Genetic locus of *L. pneumophila lvrE* in strain Philadelphia-1

The major protein found in the PLA active anion exchange chromatography fraction 12 and additionally sequenced from fraction 22 (Fig. 4.33) was represented by an ORF of 810 bp and encoded a protein of 269 amino acids with an isoelecric point of 6.2. This ORF has already been reported to be located within a region holding components of the *L. pneumophila* Lvh type IVA secretion system and therefore has been named *lvrE* (gi52841476) for *Legionella vir* region gene E (180). It is located in a region which shows high variation between different *L. pneumophila* strains (28, 172). A probable ortholog of LvrE as evaluated by the expect value is a vir region protein-like protein (gi86133053) from *Tenacibaculum* sp. which are pathogenic marine bacteria (E-value= 2×10^{-20}, Identity: 36 %, Similarity: 55 %). Furthermore, part of the LvrE sequence (starting from amino acid position 95) displayed 44 % sequence similarity to a protein phosphatase 2C-like protein (gi68550832) of the green sulphur bacterium *Pelodictyon phaeoclathratiforme* (E-value=2×10^{-11}, Identity: 30 %, Similarity: 44 %) and 48 % sequence similarity (amino acids 102-184) to the Omp36 porin (gi13384123) of *Enterobacter aerogenes* (E-value=0.14, Identity: 34 %, Similarity: 48 %) (204). Next, the *lvrE* locus in strain Philadelphia-1 was analyzed (Fig. 4.57). Both surrounding ORFs have the same orientation as *lvrE*. The downstream ORF1 is a putative protein with homology to a hypothetical protein (gi41817894) of *Treponema denticola*. The next ORF upstream to *lvrE* is *lvhD4* (gi52841477), a component of the *L. pneumophila* type IVA translocation system and a member of the TraG/TraG gene family (180). ORF1, further upstream of *lvrE* is an ISSod13 transposase (gi52841474) with a PFAM integrase core domain. It is unlikely that *lvHD4* forms an operon with *lvrE*, because they are separated by 85 bp which includes a -10 and -35 box region. ORF2 and *lvrE* might form an operon as there is no predicted promoter in the 87 bp intergenic region.

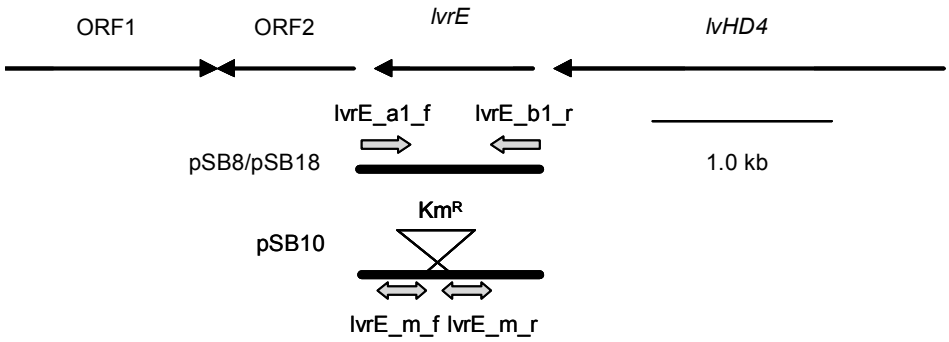

FIG. 4.57. The *lvrE* locus in *L. pneumophila* Philadelphia-1 and recombinant *E. coli*. The arrows depict the relative location, size, and orientation of *lvrE* and neighboring ORFs. The lines at the bottom of the figure represent the segments of *Legionella* DNA that were cloned into plasmid vectors. Plasmid pSB10 contains the *lvrE* gene where 25 amino acids were deleted and replaced by a Km^R gene cassette by site-directed mutagenesis. The thick arrows (not drawn to scale) represent the primers which were used for the amplification of the *lvrE* gene. Constructs: pSB8=pGEMTez+*lvrE*, pSB18=pMMB2002+*lvrE*, pSB10=pGEMTez+Δ*lvrE*::Km^R.

4.4.4.2 Isolation of *L. pneumophila* Philadelphia-1 and 130b *lvrE* mutants

With the aim of elucidating the enzymatic function of LvrE and its importance for the infection of host cells, *L. pneumophila lvrE* mutants were constructed in the strains 130b and Philadelphia-1. For this purpose, the *lvrE* gene was amplified from the *L. pneumophila* Philadelphia-1 genome and cloned into the plasmid pGEMTeasy, yielding pSB8. Then pSB8 was used as a template for the in-frame introduction of a Km^R cassette (at base position 387 of the gene and the corresponding amino acid position 129, respectively) by site-directed mutagenesis by means of the primers lvrE_mu_a1f and lvrE_mu_b1r which generated pSB10 (see chapter 3.2.2.6). The genomic *lvrE* gene of *L. pneumophila* 130b and Philadelphia-1 was replaced by the disrupted *lvrE* gene of pSB10 by allelic exchange. Four *lvrE* mutants in *L. pneumophila* strain Philadelphia-1 (lvrE- cl16, lvrE- cl19, lvrE- cl22, and lvrE- cl23), and four independent mutants in strain 130b (lvrE- cl1.1, lvrE- cl2.1, lvrE- cl2A, and lvrE- 4c) were obtained. All mutants were analyzed by Southern blot and found to have inserted the Km^R cassette into the *lvrE* gene. Southern blot analysis also indicated the presence of an additional *lvrE* copy in strain 130b which has already been suggested by an earlier study (172). An RT-PCR analysis of the Philadelphia-1 *lvrE* mutant clones confirmed the absence of an *lvrE* transcript in the mutants while it was present in the Philadelphia-1 wild type (data not shown). The expression analysis of the 130b mutants lvrE- cl1.1 and 2.1 showed that clone 2.1 still expressed *lvrE* which might

result from the second *lvrE* copy. The mutant lvrE- cl1.1 did not show the presence of wild type *lvrE* mRNA but possessed an approximately 900 bp larger transcript which probably represented an *lvrE*+Km^R transcript (data not shown). Thus, in spite of identical hydridization patterns of the *lvrE* and Km^R probes between the two 130b *lvrE* mutants the two clones differed in their expression of the *lvrE* gene.

4.4.4.3 Enzymatic activities of *L. pneumophila* Philadelphia-1 and 130b *lvrE* mutants

Since *L. pneumophila* secretes a number of lipolytic enzymes into the culture supernatant, the loss of one might be compensated by others and might therefore not be obvious. Therefore, the culture supernatants of the Philadelphia wild type and of *lvrE* mutants were obtained at two different bacterial optical densities (OD_{660} 1.0 and 1.8) corresponding to early and mid to late logarithmic growth phases (Fig. 4.25) to ensure the detection of a transient difference in the PLA, LPLA, or lipase activities between wild type and mutants. The culture supernatants of the wild type and the Philadelphia-1 *lvrE* mutants were then tested for hydrolysis of the diacylphospholipids DPPC and DPPG, the monoacylphospholipids MPLPC and MPLPG, and the lipid 1-MPG. As shown in figure 4.58, three of the four *L. pneumophila* Philadelphia-1 *lvrE* mutants displayed a reduced hydrolysis of DPPG, MPLPG, and MPLPC in the early logarithmic growth phase compared to wild type, suggesting that LvrE might possess PLA and LPLA activities. However, the mutant clone 23 behaved differently and displayed an increased hydrolysis of all used substrates with the exception of DPPC and 1-MPG. Notably, there was no reduction of secreted PLA, LPLA or lipase activities in the mutants detectable at mid logarithmic growth phase (Fig. 4.58, lower part). The mutant clone 16 even showed an increased release of fatty acids from the lysophospholipids MPLPC and MPLPG and the lipid 1-MPG at mid logarithmic growth phase.

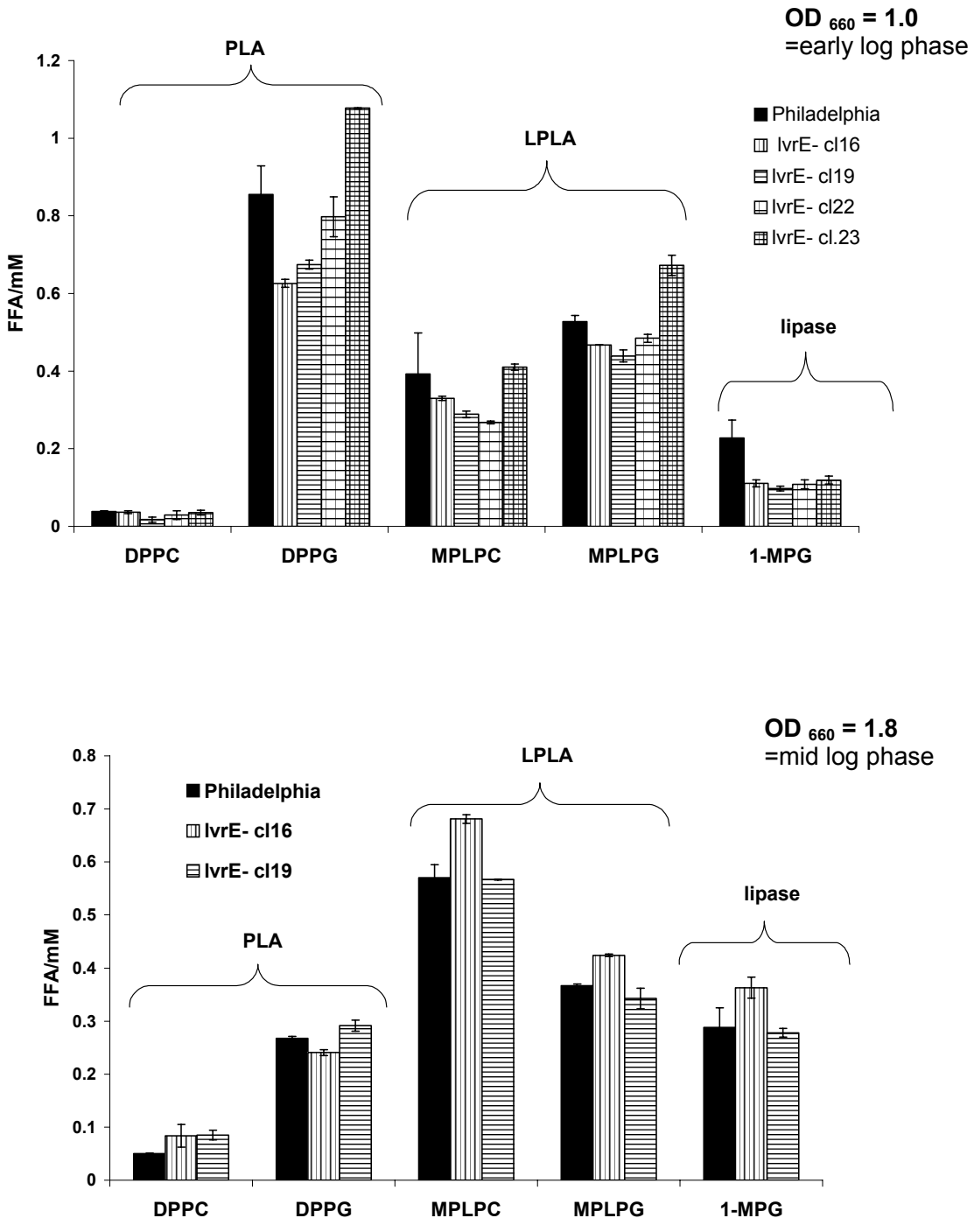

FIG. 4.58. Secreted lipolytic activities of *L. pneumophila* Philadelphia-1 wild type and *lvrE* mutants. Culture supernatants of wild type and *lvrE* mutants were incubated with DPPC, DPPG, MPLPC, MPLPG, or 1-MPG for 5 h at 37°C. The release of FFA was quantified. Data are expressed as differences between the amount of FFA released by culture supernatants and the amount released by BYE broth. The results represent the means and standard deviations of duplicate cultures and are representative of three independent experiments.

Next the 130b *lvrE* mutants were analyzed with respect to their secreted PLA and LPLA activities. Compared to wild type, the culture supernatant of the 130b *lvrE* mutant clone 1.1 displayed a slight reduction in DPPC and DPPG hydrolysis during early and late logarithmic growth phases (Fig. 4.59). The mutant lvrE- cl1.1 also displayed an increase in the hydrolysis of MPLPC during early logarithmic growth phase which was not so distinct but still detectable during late logarithmic growth phase (Fig. 4.59). The reduced secreted PLA and LPLA activities of lvrE-cl1.1 were complemented by the introduction of the *lvrE* gene in *trans* during late logarithmic growth phase (Fig. 4.59. lower part). The secreted lipolytic properties of the *lvrE* mutant clone 2.1 were comparable to wild type activities at early logarithmic growth phase which matches the fact that there is still *lvrE* expression detectable in the mutant (Fig. 4.42, upper part). However, additional independent experiments showed an increase in the secreted lysophospholipid hydrolysis at late logarithmic growth phases which indicates that the mutant did not retain wild type properties (data not shown). No difference in the PLA and LPLA activities of the cell lysates between *L. pneumophila* Philadelphia-1 or 130b wild types and the respective *lvrE* mutants could be detected (data not shown). Since LvrE seemed to influence both PLA and LPLA activities, it was of interest to know whether glycerophospholipid:cholesterol acyltransferase (GCAT) activity was influenced, too. Therefore, the culture supernatants of *L. pneumophila* Philadelphia-1 *lvrE* mutants were assessed at early and mid logarithmic growth phases for their GCAT activity and it was found to be comparable to wild type activity (data not shown). In summary, it was shown that the culture supernatants of Philadelphia-1 and 130b *lvrE* mutants display reduced PLA activity and Philadelphia-1 mutants additionally display reduced LPLA activity during early logarithmic growth phase. During mid to late logarithmic growth phases, compared to the respective wild type strains, the secreted LPLA activity is increased in the 130b and Philadelphia *lvrE* mutants. Thus it was concluded that LvrE directly or indirectly contributes to the secreted PLA and LPLA activities of *L. pneumophila*.

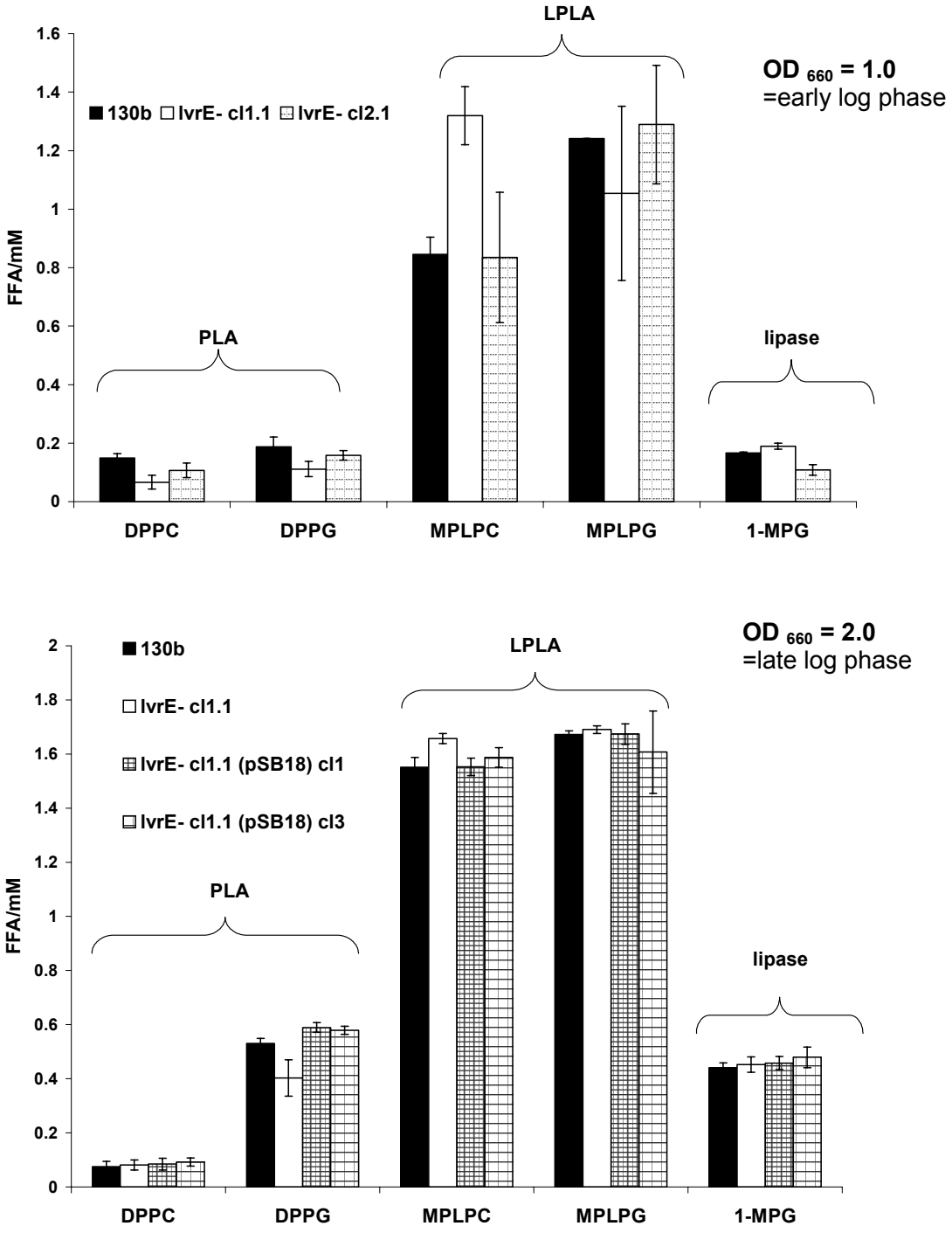

FIG.4.59. Secreted lipolytic activities of *L. pneumophila* 130b wild type and *lvrE* mutants. Culture supernatants of 130b wild type and *lvrE* mutants and complemented strains were incubated with DPPC, DPPG, MPLPC, MPLPG, or 1-MPG for 5.5 h (upper picture) and 7h (lower picture) at 37°C. The release of FFA was quantified. Data are expressed as differences between the amount of FFA released by culture supernatants and the amount released by BYE broth. The results represent the means and standard deviations of triplicate samples and are representative of three independent experiments (complementation experiment only performed once).

Since the LvrE sequence shared homologous regions with phosphatases and kinases, the Philadelphia-1 and 130b *lvrE* mutants were also assessed for their secreted phosphatase activity at mid logarithmic growth phase with the artificial substrate p-nitrophenyl phosphate (p-NPP). Since most of the secreted phosphatase activity in *L. pneumophila* 130b is caused by the major acid phosphatase Map, which can be inhibited by tartrate, incubations were also performed in the presence of 10 mM tartrate (8). As can be inferred from figure 4.60, the culture supernatant of the *L. pneumophila* 130b *lvrE* mutant clone 1.1 did not show a significant difference of p-NPP hydrolysis to the culture supernatant of the 130b wild type. Moreover, the addition of 10 mM tartrate led to an approximately 50 % reduced phosphatase activity in the culture supernatants of the 130b wild type and the *lvrE* mutant. The culture supernatant of the Philadelphia-1 wild type showed a much lesser hydrolysis of p-NPP than the 130b wild type which was also inhibited by tartrate. Moreover, there was no difference between the phosphatase activity of the Philadelphia-1 wild type and the *lvrE* mutant clone 19. Thus, these data show that LvrE does not contribute to the secreted phosphatase activity in *L. pneumophila* strains 130b and Philadelphia-1.

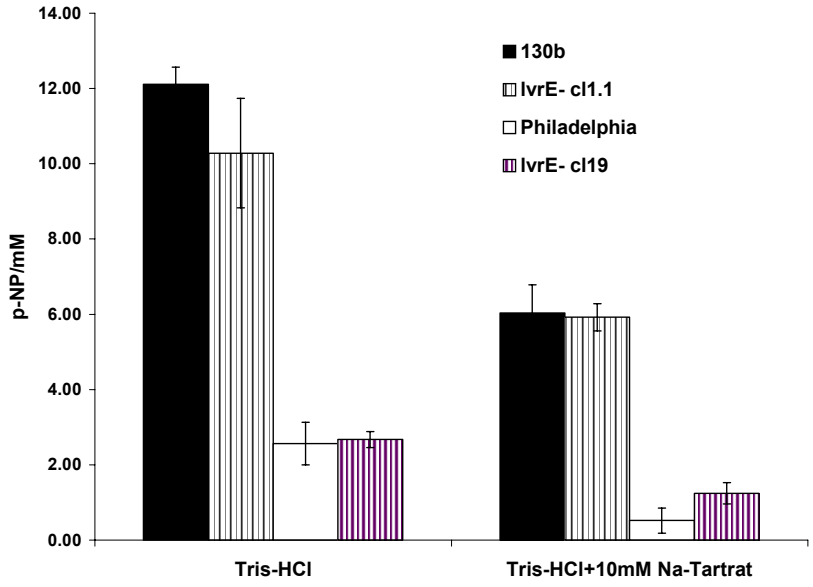

FIG.4.60. Secreted phosphatase activity of *L. pneumophila* 130b and Philadelphia-1 wild type and corresponding *lvrE* mutants. Culture supernatants (obtained at OD_{660}=1.5) of 130b and Philadelphia-1 wild type and the corresponding *lvrE* mutants were incubated for 40 min with p-nitrophenylphosphat (p-NPP) at 37°C. The release of p-nitrophenol (p-NP) was quantified. Data are expressed as differences between the amount of p-nitrophenol released by culture supernatants and the amount released by BYE broth. The results represent the means and standard deviations of quadruplicate samples and are representative of two independent experiments.

4.4.4.4 Enzymatic activities of *E. coli* clones expressing *L. pneumophila lvrE*

The differences in the enzymatic activities between the *L. pneumophila* wild type and the *lvrE* mutants suggest an influence of LvrE on the secreted *L. pneumophila* PLA and LPLA activities. To further address this issue, the enzymatic activities of *L. pneumophila* LvrE were studied in *E. coli*. To that end, the Philadelphia-1 *lvrE* gene from plasmid pSB8 including its putative promoter region was subcloned into the vector pMMB2002, yielding pSB18 (Table 3.21). An expression analysis confirmed the expression of *lvrE* in *E. coli* clones harbouring pSB18, in the presence as well as in the absence of IPTG (data not shown). Culture supernatants and cell lysates from *E. coli* DH5α clones carrying either pSB18 or the empty pMMB2002 vector were assayed for the release of fatty acids from DPPC, DPPG, MPLPC, MPLPG, and 1-MPG to test for PLA, LPLA, and lipase activities, respectively (Fig. 4.61 and 4.62).

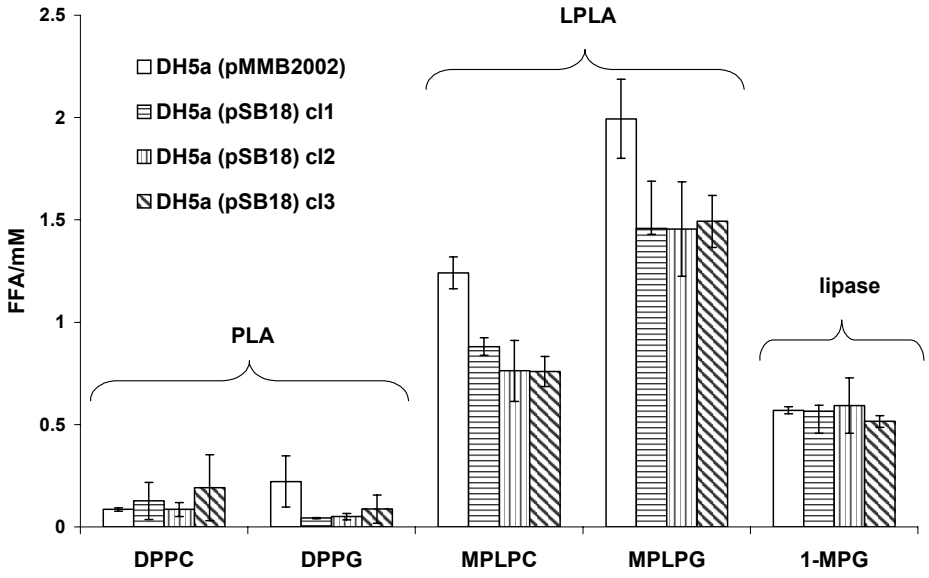

FIG.4.61. Cell-associated lipolytic activities of recombinant *E. coli* DH5α containing *L. pneumophila* Philadelphia-1 *lvrE*. *E. coli* clones containing pBMMB2002 or its derivative pSB18 were grown to an OD_{660}=2.0 and the corresponding cell lysates were concentrated threefold and mixed with DPPG, DPPC, MPLPC, MPLPG, and 1-MPG. After 48 h incubation at 37°C, the release of FFA was quantified. Data are expressed as differences between the amount of FFA released by cell lysate and the amount released by Tris-HCl buffer. The results represent the means and standard deviations of triplicate samples and are representative of three independent experiments.

There was, however, no increase in the hydrolysis of any of the used substrates by the clones harbouring *lvrE* in comparison to the one carrying the vector only (Fig. 4.61 and 4.62). Instead, a distinct decrease in the cell-associated MPLPC and MPLPG hydrolysis was observed in the clones harbouring pSB18 suggesting that LvrE might inhibit the *E. coli* cell-associated LPLA activity (Fig. 4.61). The addition of *L. pneumophila* Philadelphia lvrE- cl19 mutant culture supernatant to the reaction in order to supply with possibly missing *Legionella* cofactors did not lead to enhanced PLA or LPLA activity in the respective *E. coli* clones (data not shown) showing that LvrE does not have lipolytic properties itself.

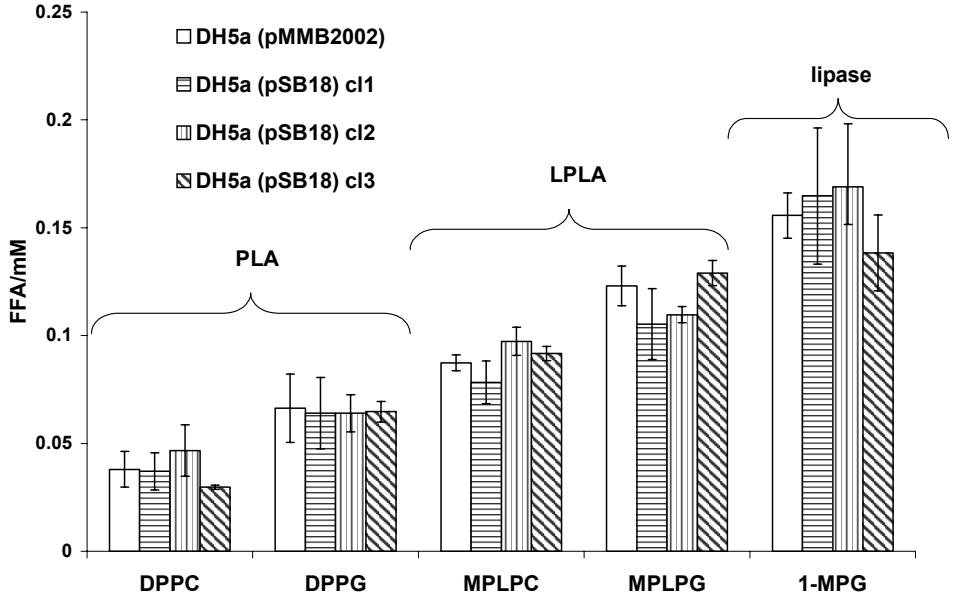

FIG.4.62. Secreted lipolytic activities of recombinant *E. coli* DH5α containing *L. pneumophila* Philadelphia-1 *lvrE*. *E. coli* clones containing pBMMB2002 or its derivative pSB18 were grown to an OD_{660}=2.0 and the culture supernatants were mixed with DPPG, DPPC, MPLPC, MPLPG, and 1-MPG. After 48 h incubation at 37°C, the release of FFA was quantified. Data are expressed as differences between the amount of FFA released by cell lysate and the amount released by Tris-HCl buffer. The results represent the means and standard deviations of triplicate samples and are representative of two independent experiments.

4.4.4.5 The role of LvrE during intracellular infection

Since LvrE seems to influence the secreted PLA and LPLA activities of *L. pneumophila*, it was of interest to investigate whether it might also influence the bacterial intracellular infection of host cells. Therefore, *A. castellanii* were infected with Philadelphia-1 wild type or the mutants lvrE- cl16, cl19, cl22, and cl23. As shown in figure 4.63, the *lvrE* mutant clone 16 showed an even better growth than the wild type, while the mutant clone 19 showed a tenfold reduced growth at 72 h post infection compared to the wild type. The CFU of the mutant clones 22 and 23 even displayed a decrease in the CFU indicating that they were completely impaired in intracellular growth. When the mutants were assayed for the infection of U937 macrophages the clone lvrE- cl16 again displayed a slightly higher increase in CFU than the Philadelphia wild type. Interestingly, the *L. pneumophila* Philadelphia *lvrE* mutant clone 19 did not show any growth defect in the macrophage host. Here, the CFU of both mutants and the wild type increased by three and five logarithmic units after 48 h and 72 h of infection, respectively. However, the clones 22 and 23 were also defective for the infection of U937 macrophages (Fig. 4.63, lower part). Since it was not possible to restore the growth defect of the Philadelphia lvrE- mutant clone 19 in the amoebal model by the introduction of pSB18 (pMMB2002+*lvrE*) and since clone 16 does not show a growth defect in both infection models, it seems likely that all clones except lvrE- cl16 have a second-site mutation which leads to the observed growth defects (data not shown).

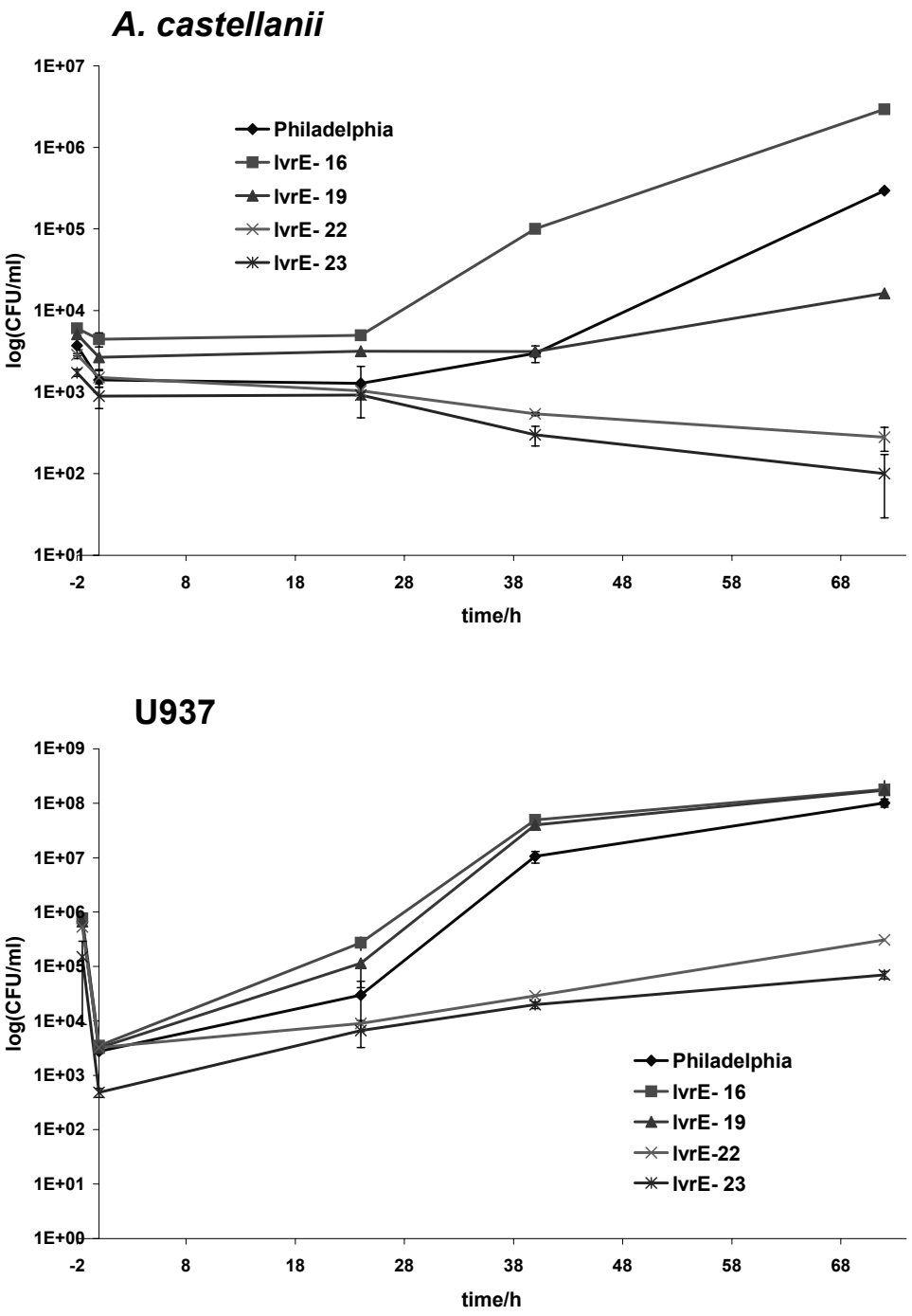

FIG.4.63. Intracellular infection of host cells by wild type Philadelphia-1 and *lvrE* mutant *L. pneumophila*. *Acanthamoeba castellanii* amoebae and U937 macrophages (upper and lower figures, respectively) were inoculated with *L. pneumophila lvrE* knockout mutants as well as *L. pneumophila* wild type (MOI of 0.1 and 1, respectively). At various time points post inoculation, the number of bacteria was quantified by plating aliquots on BCYE agar. Results represent the means and standard deviations of triplicate samples and are representative of three independent experiments.

In case of the strain 130b mutants, the clone lvrE- cl.1.1 showed an approximately three log growth defect in the amoebal model compared to the 130b wild type after 72 h of infection which could not be complemented by the introduction of pSB18 (pMMB2002+*lvrE*) (Fig. 4.64). Therefore, new mutants were generated (lvrE- cl2A and 4C) and assayed for intracellular infection of macrophages. The two new mutant clones were found to have similar intracellular growth rates in the amoebal and macrophage hosts as the 130b wild type (Fig. 4.65). Thus it appears that the growth defect of lvrE- cl1.1 in the amoebal model might have been caused by a second-site mutation (intracellular growth of clone 1.1 was not determined in the macrophage model). In summary it was concluded that LvrE is dispensable for the intracellular growth in amoebal and macrophage host cells in the *L. pneumophila* strains 130b and Philadelphia-1. However, it was observed that when *L. pneumophila* was plated-out together with *A. castellanii* on BCYE agar plates the presence of LvrE led to a faster consumption of *L. pneumophila* colonies by the amoebae. It is known that *A. castellanii* amoebae feed on bacteria, e.g. *Legionella* and this phenomenon has been used for the screening of *L. pneumophila* virulence factors, because less virulent bacteria are more rapidly consumed (personal communication by Philipp Auraß) (3). This is also demonstrated by the phenomenon that colonies of *L. pneumophila* strain Philadelphia-1, a less virulent strain, are more rapidly consumed after being plated-out together with *A. castellanii* than colonies of the more virulent strain 130b (data not shown). It was now found that Philadelphia *lvrE* mutants, e.g. lvrE- clones 16 and 19, were less rapidly consumed by amoebae than the Philadelphia-1 wild type after being plated-out with *A. castellanii* on BCYE agar plates indicating that the absence of LvrE protected the bacteria from being devoured by the amoebae in spite of the fact that the same clone possibly displayed a growth defect in the infection model (4.66 A and B). Since the 130b wild type was not visibly consumed at all by the amoebae at the chosen conditions, it was not possible to determine any difference between the wild type and 130b *lvrE* mutants. It was however found that *trans* complemented 130b *lvrE* mutants were more rapidly consumed by *A. castellanii* after they had been plated out together with the amoebae than the corresponding mutant or the wild type, indicating that over expression of *lvrE* renders *L. pneumophila* more susceptible to being eaten by *A. castellanii* on agar plates (Fig. 4.66 C, D, E). How LvrE might render *L. pneumophila* more susceptible to being consumed by amoeba is currently not known. This phenomenon is, however, reminiscent of the characteristics of porins which enable the entry of specific

molecules through the bacterial membrane and which therefore might also provide a gateway for amoebal toxins.

In conclusion, LvrE was identified as a factor which influences the secreted PLA and LPLA activities of *L. pneumophila* in a growth phase dependent manner and which renders *L. pneumophila* more susceptible to consumption by amoebae on agar plates.

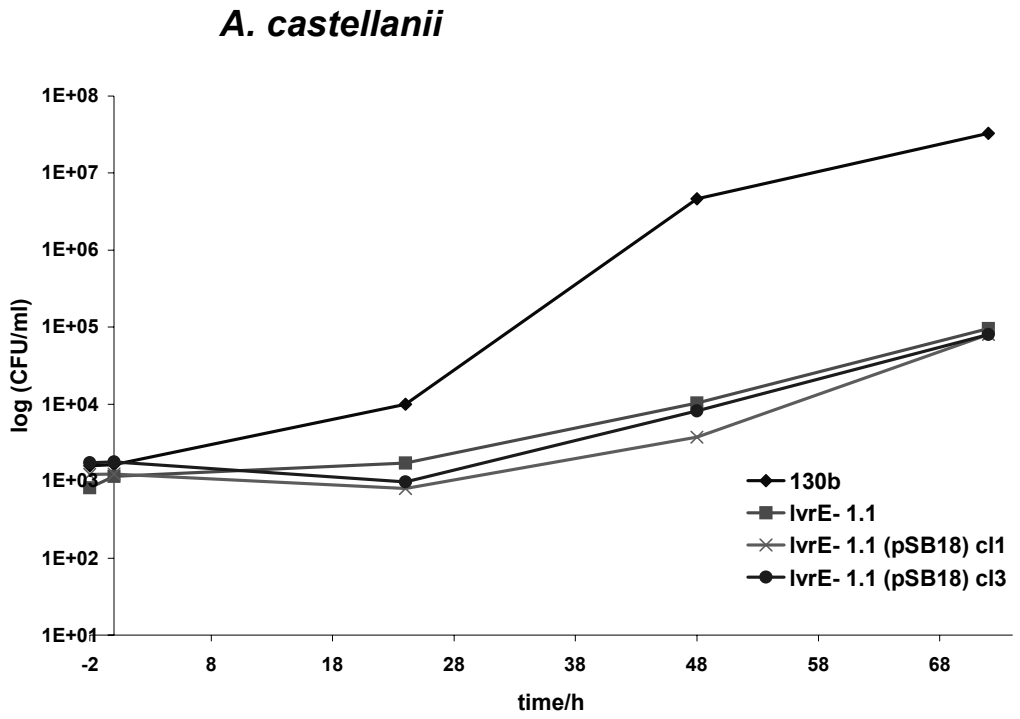

FIG.4.64. Intracellular infection of *A. castellanii* by wild type 130b and *lvrE* mutant *L. pneumophila*. *Acanthamoeba castellanii* amoebae were inoculated with an *L. pneumophila lvrE* knockout mutant or *trans* complemented strains well as *L. pneumophila* 130b wild type (MOI of 0.01). At various time points post inoculation, the number of bacteria was quantified by plating aliquots on BCYE agar. Results represent the means and standard deviations of triplicate samples and are representative of three (mutant only) and two (*trans* complemented strains) independent experiments.

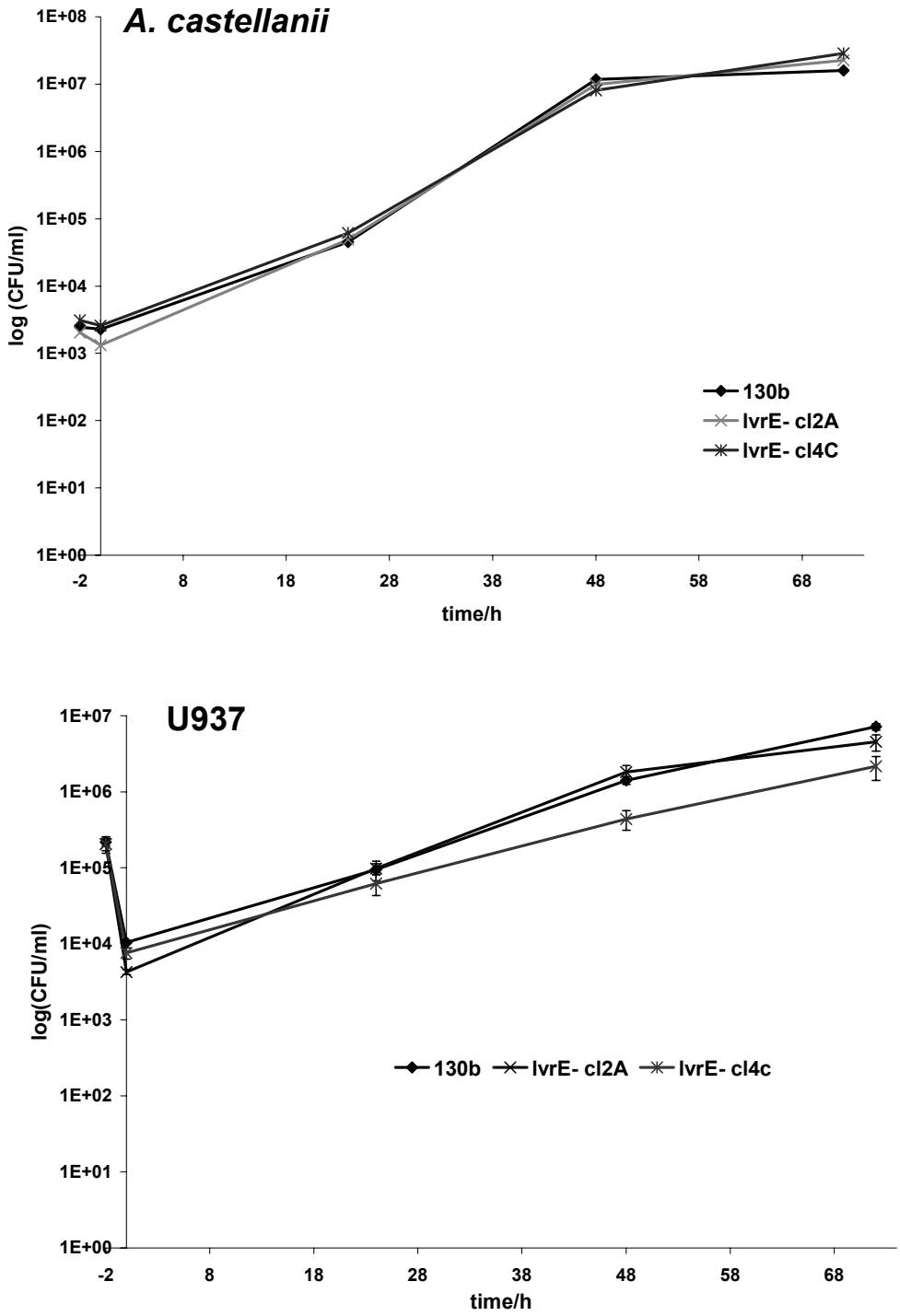

FIG.4.65. Intracellular infection of host cells by wild type 130b and *lvrE* mutant *L. pneumophila*. *Acanthamoeba castellanii* amoebae and U937 macrophages (upper and lower figures, respectively) were inoculated with *L. pneumophila lvrE* knockout mutants as well as *L. pneumophila* 130b wild type (MOI of 0.01 and 1, respectively). At various time points post inoculation, the number of bacteria was quantified by plating aliquots on BCYE agar. Results represent the means and standard deviations of triplicate samples and are representative of three independent experiments.

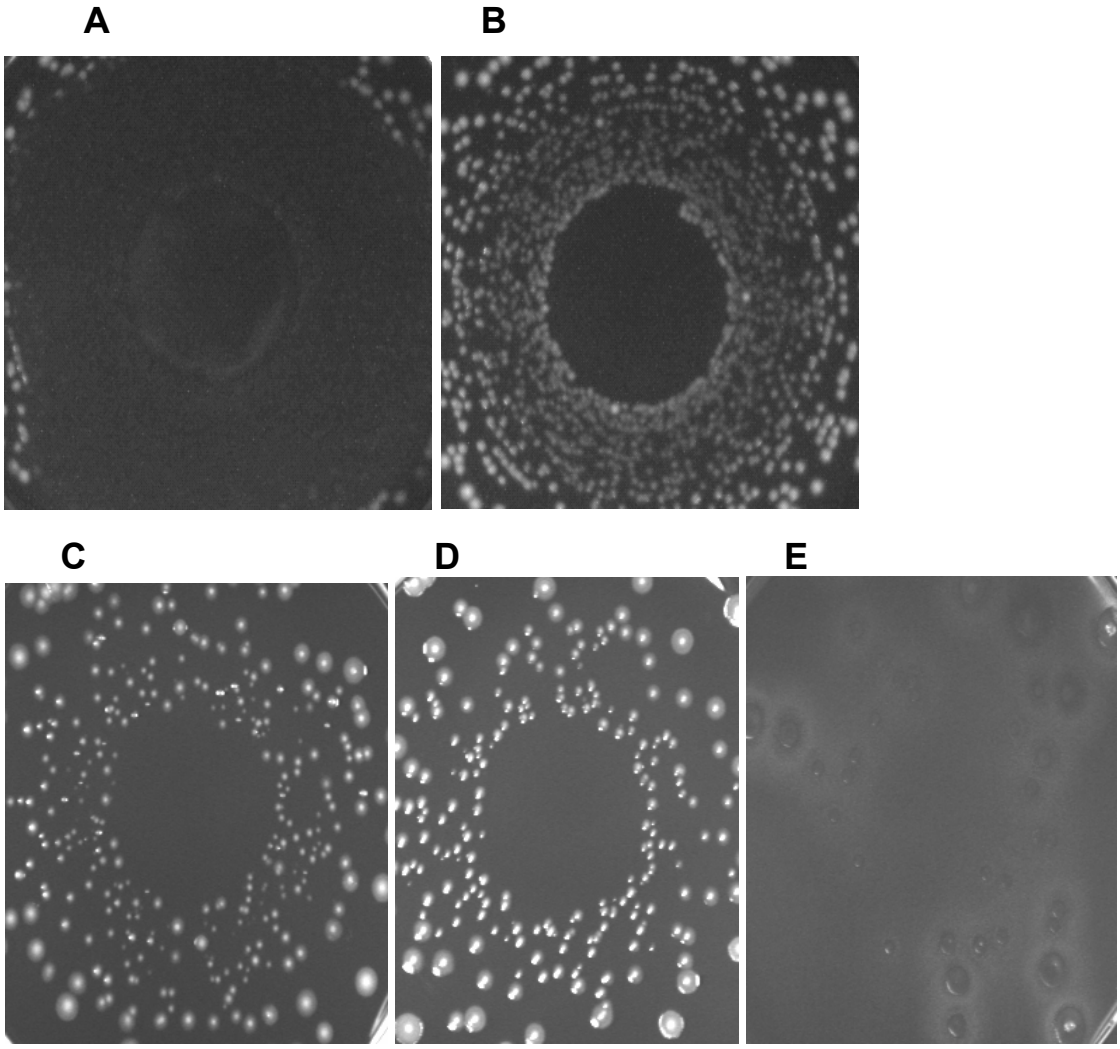

FIG.4.66. Growth of Philadelphia-1 and 130b wild type and corresponding *lvrE* mutants on BCYE agar in the presence of *A. castellanii*. A standard infection was conducted. *A. castellanii* were inoculated with *L. pneumophila* wild type Philadelphia-1 (A) and the corresponding mutant lvrE- cl. 19 (B) with an MOI of 0.1. Additionally, *A. castellanii* were inoculated with the 130b wild type (C), the corresponding mutant lvrE- cl.4C (D), and the *trans* complemented mutant lvrE- 4C (pMMNlvrE) (E) with an MOI of 0.01, all with the addition of 1 mM IPTG. After 24 h, aliquots of the bacteria were plated out on BCYE agar and after an initial incubation for 72 h at 37 °C to provide growth of the *Legionella* the plates were further incubated at 25 °C for 21 (A and B) or 10 (C, D, E) days. Results are representative of three (A and B) and two (C, D, E) independent experiments.

4.4.5 Characterization of Aas

4.4.5.1 Genetic locus of *L. pneumophila aas* in strain Philadelphia-1

The third PLA-candidate protein which was sequenced from 130b PLA-active AEX fraction number 21 (Fig. 4.39) was a protein encoded by the *L. pneumophila aas* gene (gi52840834) consisting of 733 amino acids and a molecular mass of 81.95 kDa and an isoelectric point of 8.1. The experimentally found N-terminus corresponded to position 385 of the whole protein sequence. Furthermore, the protein did not contain a predicted signal peptide and therefore is probably not secreted by the type II secretion system. Notably, the newly identified protein contained two PFAM domains: an acyltransferase domain (amino acids 33-154) and an AMP-binding domain (amino acids 248-657), indicating that the enzyme most probably has acyltransferase activity which requires activation by AMP. The protein with the highest sequence identity was found to be the AMP-dependent synthetase and ligase:phospholipid/glycerol acyltransferase (gi71548729) of *Nitrosomonas eutropha* (e-value: 2×10^{-179}, Identity: 44 %, Similarity: 64 %). The best characterized ortholog of *L. pneumophila* Aas is the Aas protein of *E. coli* (e-value: 1×10^{-145}, Identity: 40 %, Similarity: 58 %) which is also a bifunctional protein with the same two domains. The *aas* locus in strain Philadelphia-1 was examined in the following (Fig. 4.67). The upstream ORF2 is oppositely oriented to *aas* and encodes a putative protein with homology to the DedA:Rhodanese-like protein (gi62955819) of *Magnetococcus* sp. (expect value: 3×10^{-29}, identity: 46%, similarity: 63%). DedA family proteins have multiple predicted transmembrane regions, but have not been functionally characterized so far. The downstream ORF3 has the same orientation as *aas* and encodes a hypothetical protein with homology to conserved hypothetical proteins of different other bacteria, in particular to the hypothetical protein MED92_12074 (gi89095399) of *Oceanospirillum* sp (expect value: 4×10^{-4}, identity: 31%, similarity: 50%). The farther upstream ORF1 has a PFAM domain of aminotransferase class IV with homology to a putative 4-amino-4-deoxychorismate lyase (gi29541027) of *Coxiella burnetii* (expect value: 7×10^{-29}, identity: 34%, similarity: 57%). Since there are no -10 and -30 promotor regions between *aas* and ORF3, they might be transcribed by the same promoter.

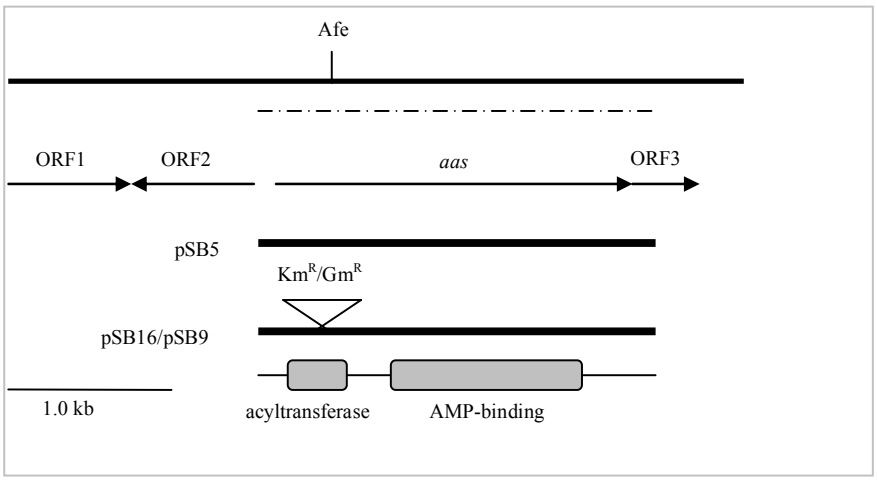

FIG. 4.67. The *aas* locus in *L. pneumophila* Philadelphia-1 and recombinant *E. coli*. The upper line represents the *L. pneumophila* Philadelphia-1 chromosome region that contains the *aas* gene, along with the location of the relevant AfeI restriction site which was utilized for introduction of Km^R and Gm^R cassettes. The dotted line below illustrates the region which was sequenced from 130b. The arrows below this line depict the relative location, size, and orientation of *aas* and neighboring ORFs. The lines at the middle of the figure represent the segments of *Legionella* DNA that were cloned into plasmid vectors and the corresponding protein with its catalytic domains. Plasmid pSB16 and pSB9 contained a Km^R/Gm^R gene cassette, respectively. Constructs: pSB5=pGEMTez+*aas*, pSB16=pGEMTez+*aas*::Km^R, pSB9=pGEMTez+*aas*::Gm^R.

4.4.5.2 Isolation of *L. pneumophila* 130b *aas* mutants

For the purpose of studying the enzymatic function of the *L. pneumophila aas* gene, mutants were constructed. First, an approximately 2.5 kb fragment including *aas* with its putative promoter region was amplified from the *L. pneumophila* 130b genome with means of the primers aas_a1_f and aas_b1_r and cloned into the vector pGEMTeasy, resulting in pSB5. Then, a Km^R or a Gm^R cassette was inserted into the AfeI restriction site of *aas*, yielding pSB16 and pSB9, respectively (Table 3.21). The interrupted aas gene of pSB16 was subsequently used to replace *L. pneumophila* 130b genomic *aas* by allelic exchange. Three mutants were obtained (aas- cl9a, aas- cl13a, and aas- cl16b) and confirmed by PCR and Southern blot (Appendix). In order to generate double knockout mutants, genomic *aas* of an *L. pneumophila* 130b *plaB* mutant (the 130b *plaB* mutant was constructed by Kerstin Rydzewski, Robert Koch-Institut) was replaced by the interrupted *aas* of pSB9 which contained a Gm^R cassette in the aas gene. Two independent kanamycin and gentamycin resistant mutants were obtained (aas/plaB cl2D and aas/plaB cl7B) and likewise confirmed by PCR and Southern blot analysis.

4.4.5.3 Lipolytic activities of *L. pneumophila* 130b *aas* mutants

The *L. pneumophila* wild type and two independent *aas* mutants were analyzed for lipolytic activities in their culture supernatant and cell lysates. It was found that the culture supernatants of the 130b wild type and the *aas* mutants released comparable amounts of fatty acids from all the tested substrates (DPPC,DPPG, MPLPC, MPLPG, 1-MPG) (data not shown). Compared to the wild type, the cell lysates of the *L. pneumophila aas* mutants showed a slight reduction in the hydrolysis of the phospholipids DPPC and DPPG and the lysophospholipids MPLPC and MPLPG (Fig. 4.68). The hydrolysis of 1-MPG was comparable to the wild type level. These results indicate that Aas is associated with the bacterial membrane and contributes to the cell associated-PLA and LPLA activity either directly or indirectly by influencing the activity of the cell-associated PLA/LPLA PlaB.

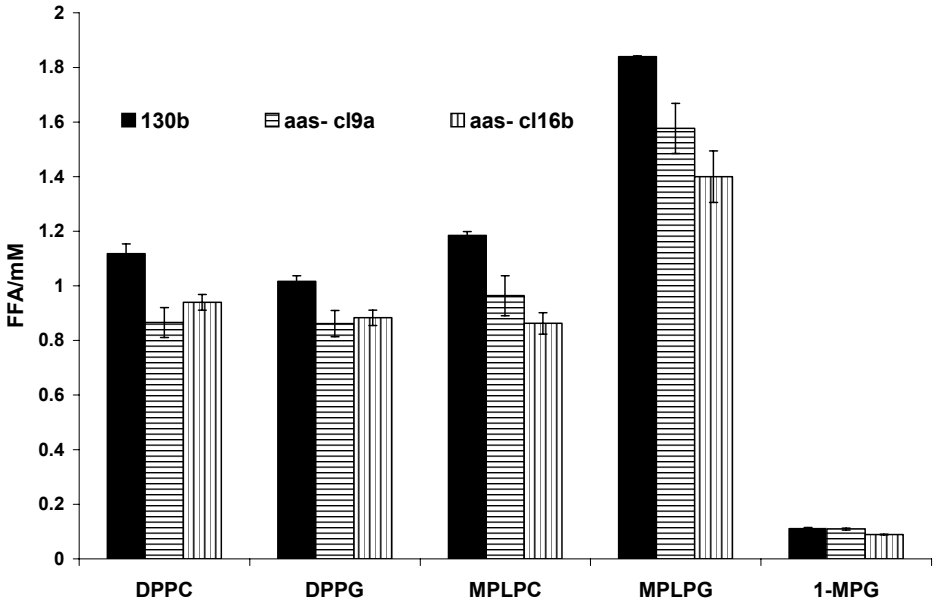

FIG. 4.68. Cell-associated lipolytic activities of *L. pneumophila* 130b wild type and *aas* mutants. *L. pneumophila* 130b wild type and *aas* mutants were grown to an OD660=2.0. The corresponding culture supernatants were tenfold diluted and incubated with DPPC, DPPG, MPLPC, MPLPG, or 1-MPG for 2 h at 37°C. The release of FFA was quantified. Data are expressed as differences between the amount of FFA released by culture supernatants and the amount released by Tris-HCl. The results represent the means and standard deviations of duplicate samples and are representative of three independent experiments.

L. pneumophila Aas contains the characteristic protein domain of a group of acyltransferases which transfer fatty acids to an acceptor molecule, e.g. lysophospholipids. It is homologous to *E. coli* Aas which is located in the bacterial inner membrane and functions as a salvage pathway for the incorporation of fatty acids and lysophospholipids into the bacterial membrane (102). Although the physiological substrate of E. coli Aas is probably lysophosphatidylethanolamine the enzyme was also found to acylate the non-physiological substrate lysophosphatidylcholine to diacylphosphatidylcholine (103). It was analyzed in the following whether *L. pneumophila* 130b possessed a similar cell-associated acyltransferase activity and whether this activity was dependent on Aas. To this purpose, *L. pneumophila* 130b wild type and two independent *aas* mutants were grown in liquid culture until mid logarithmic phase (OD_{660}=2.0) and the pelleted cells were fractionated into an osmotic shockate fraction and a lysate fraction (chapter 3.2.3). First the osmotic lysate fraction was incubated with palmitic acid and the lysophospholipid MPLPG in the presence of ATP and Mg^{2+} or as a control with Tris-HCl buffer and analyzed for the formation of the corresponding diacylphospholipid (DPPG) by TLC. After the incubation with Tris-HCl, the wild type cell lysate only contained fatty acids but no phospholipids (Fig. 4.69). Since the cell lysate of *L. pneumophila* already contains phospholipids, the absence of these after incubation at 37 °C can only be attributed to their hydrolysis by a cell associated PLA/LPLA, most probably PlaB (chapter 4.2). In the *aas* mutants, however, some remaining DPPC of the cell membrane was still detectable after incubation at 37 °C with Tris-HCl, suggesting that a minor part of the cell-associated lipid hydrolysis was due to Aas (Fig. 4.69). When the osmotic shock lysates of the wild type and *aas* mutants were incubated with MPLPG and FFA and analyzed for polar lipids, it was found that the added MPLPG had been almost completely transformed in the wild type and the mutants and that it was therefore barely detectable, but no DPPG could be detected instead which was to serve as a marker for acyltransferase activity (Fig. 4.69). It was thus concluded that the cell-associated PLA/LPLA activity of *L. pneumophila* was responsible for the hydrolysis of the MPLPG. Since the activity of PlaB seemed to hinder the detection of any acyltransferase activity, the same reactions were also carried out with the osmotic shock lysates of an *L. pneumophila plaB* mutant and two independent *L. pneumophila plaB/aas* double mutants (Fig. 4.69). Again the cell lysates of mid logarithmic bacteria were analyzed after incubation with MPLPG and palmitic acid or Tris-HCl buffer only. This time, the major phospholipids of the cell membrane, in particular DPPE, DPPG, and DPPC were still detectable in the *plaB* mutant and the *plaB*/*aas* double mutants following incubation with Tris-HCl, confirming that PlaB had indeed been responsible for the hydrolysis of the cell membrane phospholipids in the earlier incubations (Fig. 4.69). When the cell lysate of the *plaB*

mutant was incubated with MPLPG and palmitic acid in the presence of ATP and Mg^{2+}, three additional spots appeared which, however, did not match with any of the used lipid standards and which therefore could not be identified (Fig. 4.69). The lowest spot was slightly less polar than MPLPG, the middle spot was less polar than DPPG, but more polar than DPPE and the upper spot was less polar than DPPE. Since these two spots were also generated by the cell lysates of the *plaB/aas* double mutants, they do not seem to be dependent on Aas. Moreover, no increased formation of DPPG was observed which might have been indicative for acyltransferase activity. Thus, there was no difference in any generated compound between the *plaB* mutant and the *plaB/aas* double mutants detectable, except that less of the added MPLPG was hydrolyzed by the cell lysates of the double mutants. Taken together, our data confirm that Aas contributes to a very minor extent to the cell associated phospholipid hydrolysis of *L. pneumophila*. Under the chosen conditions, no acyltransferase activity of Aas was detectable in the osmotic shock lysate of the 130b wild type or the mutants.

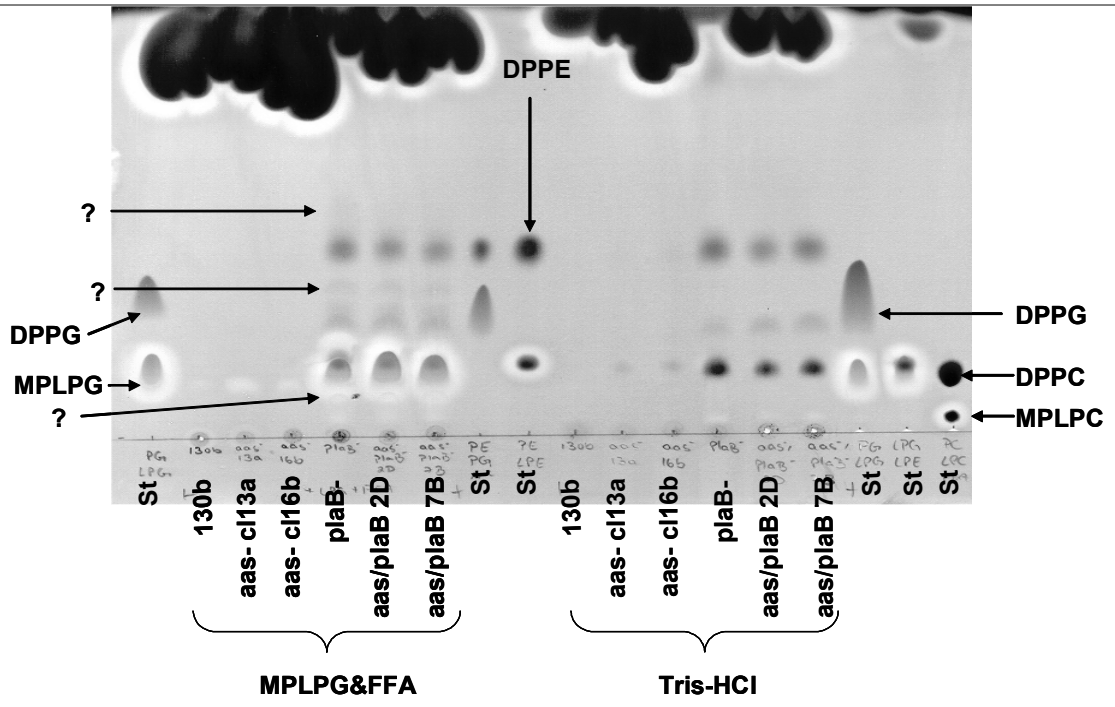

FIG.4.69. TLC analysis of acyltransferase activity and lipid hydrolysis. The osmotic shock lysates of 130b wild type, two independent *aas* mutants, a *plaB* mutant and two independent *plaB/aas* double knockout mutants (all obtained at OD_{660}=2.0) were incubated with MPLPG in the presence of ATP and Mg^{2+}, or as a background control with buffer, only for 24 h at 37 °C, and then lipids were extracted and subjected to TLC. A polar solvent mixture was employed for the sparation of the polar lipids, in particular phospholipids and lysophospholipids. For qualitative identification of the lipid spots, lanes containing lipid standards (St) were included. The observations depicted here were made on one more occasion.

Next, the osmotic shockate fraction was analyzed for acyltransferase activity. For this purpose, the osmotic shockates of the 130b wild type, two independent *aas* mutants, a *plaB* mutant, and two independent *plaB*/*aas* double mutants were incubated with palmitic acid and MPLPG in the presence of ATP and Mg^{2+}, or as a control with Tris-HCl buffer and analyzed for the formation of DPPG by TLC. In the Tris-HCl control reactions, almost no membrane phospholipids were detectable in any of the clones (except for trace amounts of DPPC) showing that most of the membrane lipids had remained in the lysate fraction (Fig. 4.70). When the osmotic shockate of the 130b wild type and *aas* mutants were incubated with MPLPG and FFA and analyzed for polar lipids, it was found that apart from the previously added MPLPG three additional lipids had been generated, which corresponded to DPPE, DPPG, and MPLPC of the lipid standards. Since the formation of DPPG from MPLPG can arise from 2-glycerophospholipid acyltransferase activity, it was concluded that the wild type indeed possessed such an activity. As the *aas* mutants also showed the formation of DPPG (and the other two lipids) in the presence of MPLPG and FFA, the observed acyltransferase activity was obviously not caused by *L. pneumophila* Aas (Fig. 4.70). How phosphatidylethanolamine (DPPE) was formed from lysophosphatidylglycerol (MPLPG) and fatty acids is not clear. Notably, it was found that the 130b *plaB* mutant and the *aas*/*plaB* double mutants were not able to generate DPPG and DPPE from the MPLPG precursor. This initial observation implies an important role of PlaB in the formation of membrane lipids, e.g. by providing lipid precursors for other enzymes involved in lipid biogenesis. It should, however, be noted that the major part of the enzymatic activity of PlaB was found in the osmotic lysate fraction.

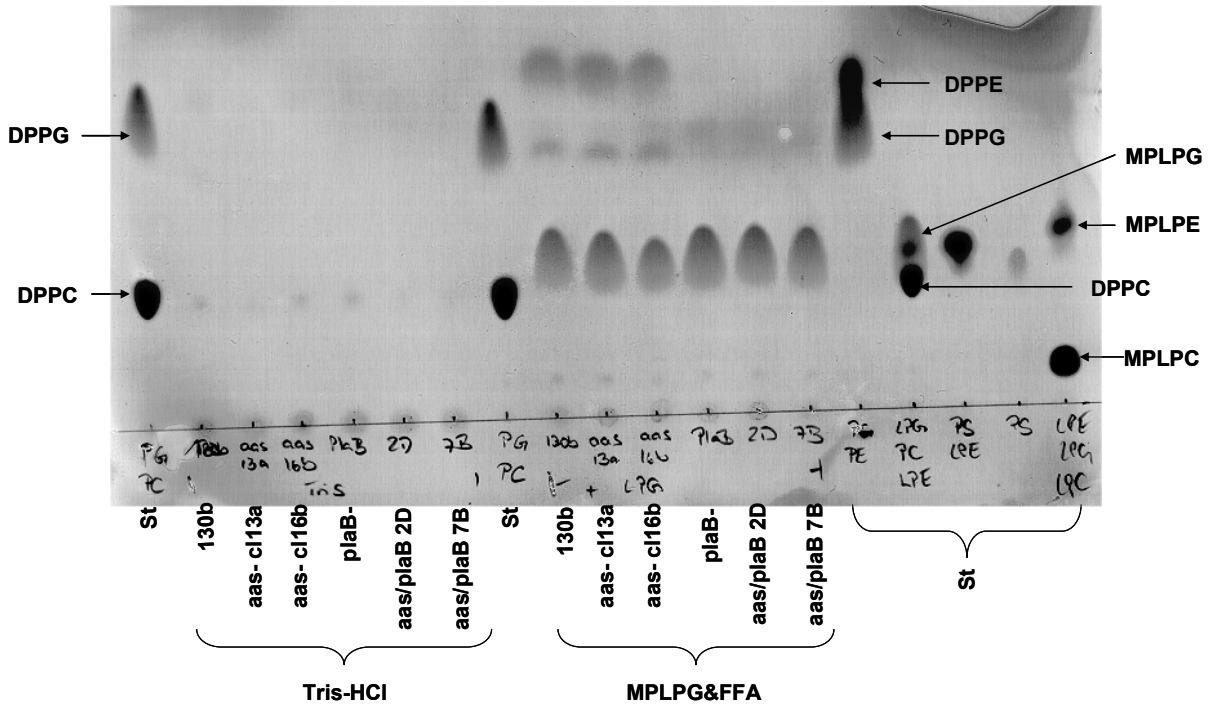

FIG.4.70. TLC analysis of acyltransferase activity and lipid hydrolysis. The osmotic shockate of 130b wild type, two independent *aas* mutants, a *plaB* mutant and two independent *plaB*/*aas* double knockout mutants (all obtained at OD_{660}=2.0) were incubated with MPLPG and FFA in the presence of ATP and Mg^{2+}, or as a background control with buffer, only for 24 h at 37 °C, and then lipids were extracted and subjected to TLC. A polar solvent mixture was employed for the sparation of the polar lipids, in particular phospholipids and lysophospholipids. For qualitative identification of the lipid spots, lanes containing lipid standards (St) were included. The observations depicted here were only made once.

4.4.5.4 Membrane lipid composition of *L. pneumophila* 130b *aas* mutants

The best characterized ortholog of *L. pneumophila* Aas is the Aas protein of *E. coli*. *E. coli* Aas is an inner-membrane protein with acyltransferase activity, shown to be involved in the acylation of endogenous and exogenous lysophosphatidylethanolamine, and in the incorporation of the resulting diacylphosphathidylethanolamine into the bacterial membrane (105). Accordingly, *E. coli aas* mutants accumulate lysophosphatidylethanolamine in their membrane (102). Although *L. pneumophila* Aas was sequenced from the bacterial culture supernatant, the corresponding 130b *aas* mutants possessed slightly reduced PLA and LPLA activities in their cell lysates but not in the culture supernatant (Fig. 4.68), indicating that the sequenced Aas protein might have been a fragmented form which was accidentally shed into the culture supernatant. It seems likely that Aas might be actually present in association with the cell and might fulfil a function comparable to *E. coli* Aas. Therefore, it was of interest to analyze the bacterial

membrane lipid composition of the *L. pneumophila aas* mutants and the 130b wild type by TLC. Towards this end, *L. pneumophila aas* mutants and the wild type were grown in liquid culture until late logarithmic growth phase (OD_{660}=2.0), cells were pelleted and lysed by means of lysozyme and Triton X-100, and an 100 µl aliquot was immediately used for chloroform/methanol extraction. As can be seen in figure 4.71, which shows a TLC of the isolated bacterial membrane lipids, the membrane of the wild type mainly consists of the phospholipids DPPE, DPPC, and to a lesser extent DPPG and MPLPC. The *L. pneumophila aas* mutants possessed the same phospholipids, but have an increased amount of the lysophospholipid MPLPC and decreased amounts of the diacylphospholipids DPPE, DPPC, and DPPG compared to the wild type. This observation therefore indicates that Aas might be involved in the transfer of fatty acids to lysophospholipids and incorporation of diacylphospholipids into the bacterial membrane.

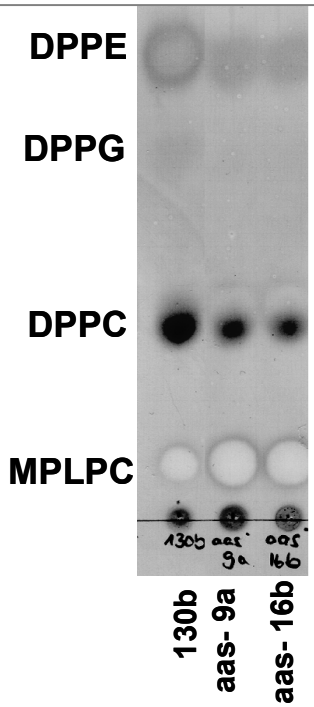

FIG.4.71. Comparative TLC analysis of cell lipids from *L. pneumophila* 130b wild type and *aas* mutants. To analyze the cell lipids, bacteria were grown to late logarithmic phase (obtained at OD_{660}=2.0) and lipids were immediately extracted from fresh cell lysates and separated by TLC. A polar solvent mixture was employed for the sparation of the polar lipids, in particular phospholipids and lysophospholipids. The observations depicted here were made on one more occasion.

4.4.5.5 Cytolytic effects of MPLPC on *L. pneumophila aas* mutants

Since *L. pneumophila* Aas might transfer fatty acids to lysophospholipids, it could also serve to neutralize cytolytic lysophospholipids by converting them to diacylphospholipids. Therefore the susceptibility of *L. pneumophila* 130b *aas* mutants towards lysophosphatidylcholine was assayed. To this purpose, *L. pneumophila* wild type and two *L. pneumophila aas* mutants were grown to an OD_{660} of 1.5 (mid logarithmic growth phase) and then incubated for 16h with or without 0.2mM MPLPC at 37 °C. Subsequently, the bacteria were plated on BCYE plates to determine the CFU. As shown in figure 4.72, the CFU of the wild type when grown with the addition of MPLPC is comparable to its CFU when grown without MPLPC, indicating that *L. pneumophila* is able to neutralize this cytolytic agent. The CFU of the *L. pneumophila aas* mutants when grown without MPLPC is similar to that of the wild type. However, when MPLPC is added to the mutants, they show a growth defect of approximately two logarithmic units, suggesting that Aas might be necessary to counteract the cytolytic effect of MPLPC (Fig. 4.72). Furthermore, the membrane lipid composition of the 130b wild type and the *aas* mutants were compared under normal growth in BYE broth to growth in the presence of 0.2 mM MPLPC. Compared to standard growth in BYE, the amount of membrane phospholipids and lysophospholipids of each clone did not significantly change when MPLPC was added during the growth (data not shown). The amount of the less polar lipids of the 130b wild type did also not change by the addition of MPLPC (Fig. 4.73). However, this was found to be different for the *L. pneumophila aas* mutants. Under normal growth conditions the aas mutants showed similar to the wild type only trace amounts of fatty acids in their membrane (Fig. 4.73). When MPLPC was added during growth, the mutants unlike the 130b wild type displayed a distict increase in the amount of fatty acids (Fig. 4.73). This finding indicates that Aas might be required for processing exogenous fatty acids which were generated by the hydrolysis of MPLPC.

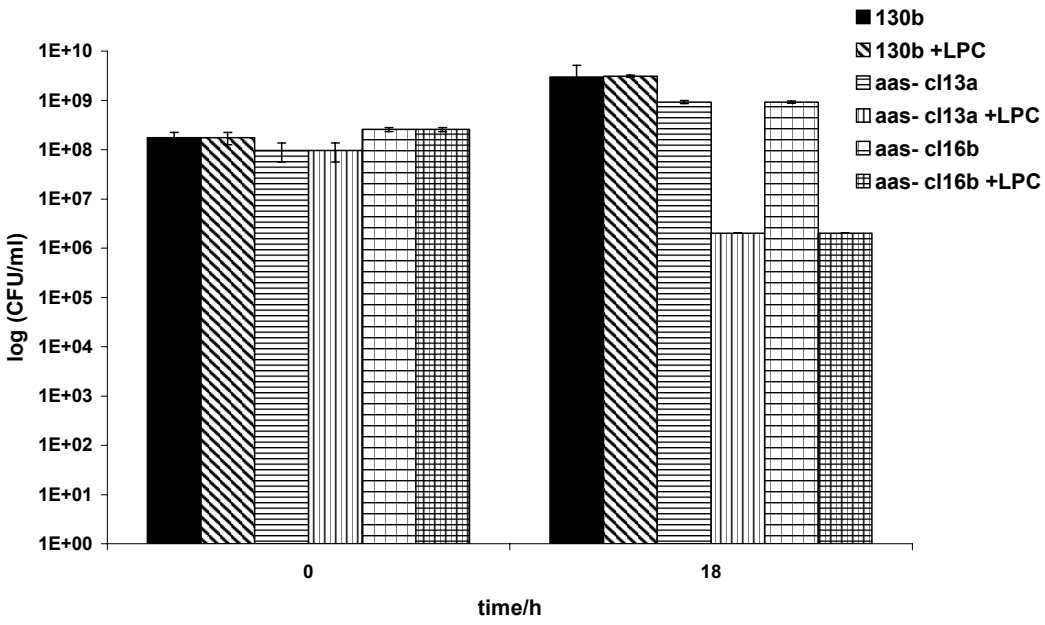

FIG.4.72. Effect of cytolytic MPLPC on the bacterial viability. To assess the effect of cytolytic MPLPC on the viability of *L. pneumophila*, the 130b wild type and two independent *aas* mutants were grown to mid logarithmic phase (OD_{660}=1.5), 0.2 mM MPLPC was added, cultures were grown for further 16 h, and the CFU were determined. The results represent the means and standard deviations of duplicate samples and are representative of three independent experiments

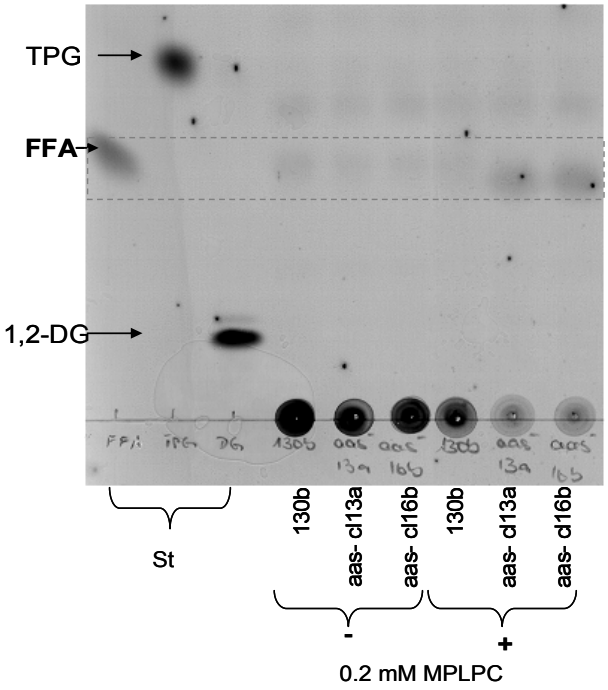

FIG.4.73. Effect of MPLPC on the cell lipids of *L. pneumophila* 130b wild type and *aas* mutants. To analyze the effect of MPLPC on the bacterial cell lipids, the 130b wild type and two independent *aas* mutants were grown to mid logarithmic phase, then 0.2 mM MPLPC (or Tris-HCl as a control) was added. Cultures were grown for further 16 h. An aliquot of 400 µl was pelleted and lipids were directly extracted and separated by TLC. The observations depicted here were made on one more occasion. St=lipid standard.

4.4.5.6 The role of Aas during intracellular infection

Since *L. pneumophila* Aas is important for the neutralization of lysophospholipids and the incorporation of phospholipids into the bacterial membrane, it might be an essential enzyme during the bacterial infection of host cells. To address this point, *L. pneumophila* 130b *aas* mutants were used to infect *A. castellanii* amoebae, the natural host of *Legionellae*. Figure 4.74 shows that the mutants displayed the same intracellular replication rate as the wild type indicating that the lack of Aas does not confer a disadvantage during infection. An initial experiment in the amoebal model furthermore showed that *aas*/ *plaB* double knockout mutants are also not attenuated in virulence. In the macrophage model, the *aas* mutants again showed the same replication rate as the wild type (Fig. 4.75, upper picture). Additionally, infections were performed with A549 epithelial cells which are known to produce and secrete surfactant lipids (Fig. 4.75). As *L. pneumophila aas* mutants are more susceptible to MPLPC than the wild type, it was of interest to determine whether the presence of lipids and the formation of lysophospholipids during the infection process would affect the mutants more strongly than the wild type. As seen in Fig. 4.75, the growth of the *aas* mutants in A549 cells was comparable to 130b wild type and the CFU of all clones increased by one logarithmic unit during 72 h.

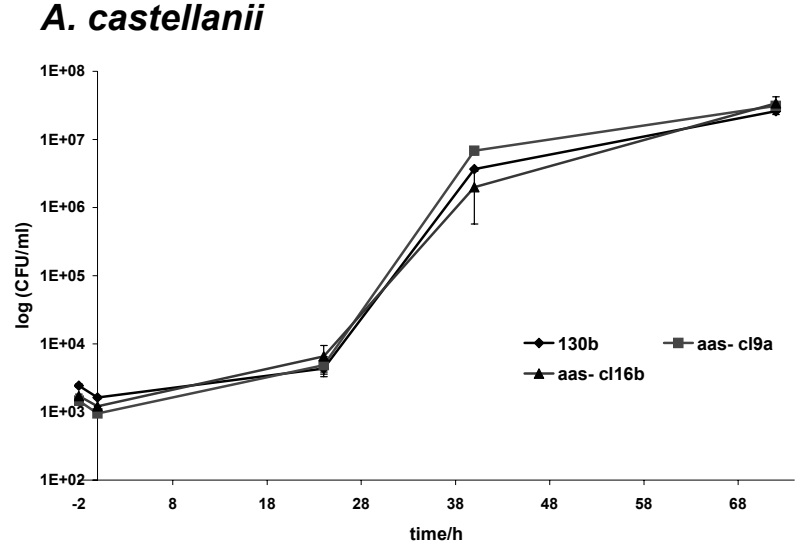

FIG.4.74. Intracellular infection of *A. castellanii* amoebae by wild type 130b and *aas* mutant *L. pneumophila*. *Acanthamoeba castellanii* amoebae were inoculated with *L. pneumophila aas* knockout mutants as well as *L. pneumophila* wild type (MOI of 0.01). At various time points post inoculation, the number of bacteria was quantified by plating aliquots on BCYE agar. Results represent the means and standard deviations of triplicate samples and are representative of three independent experiments.

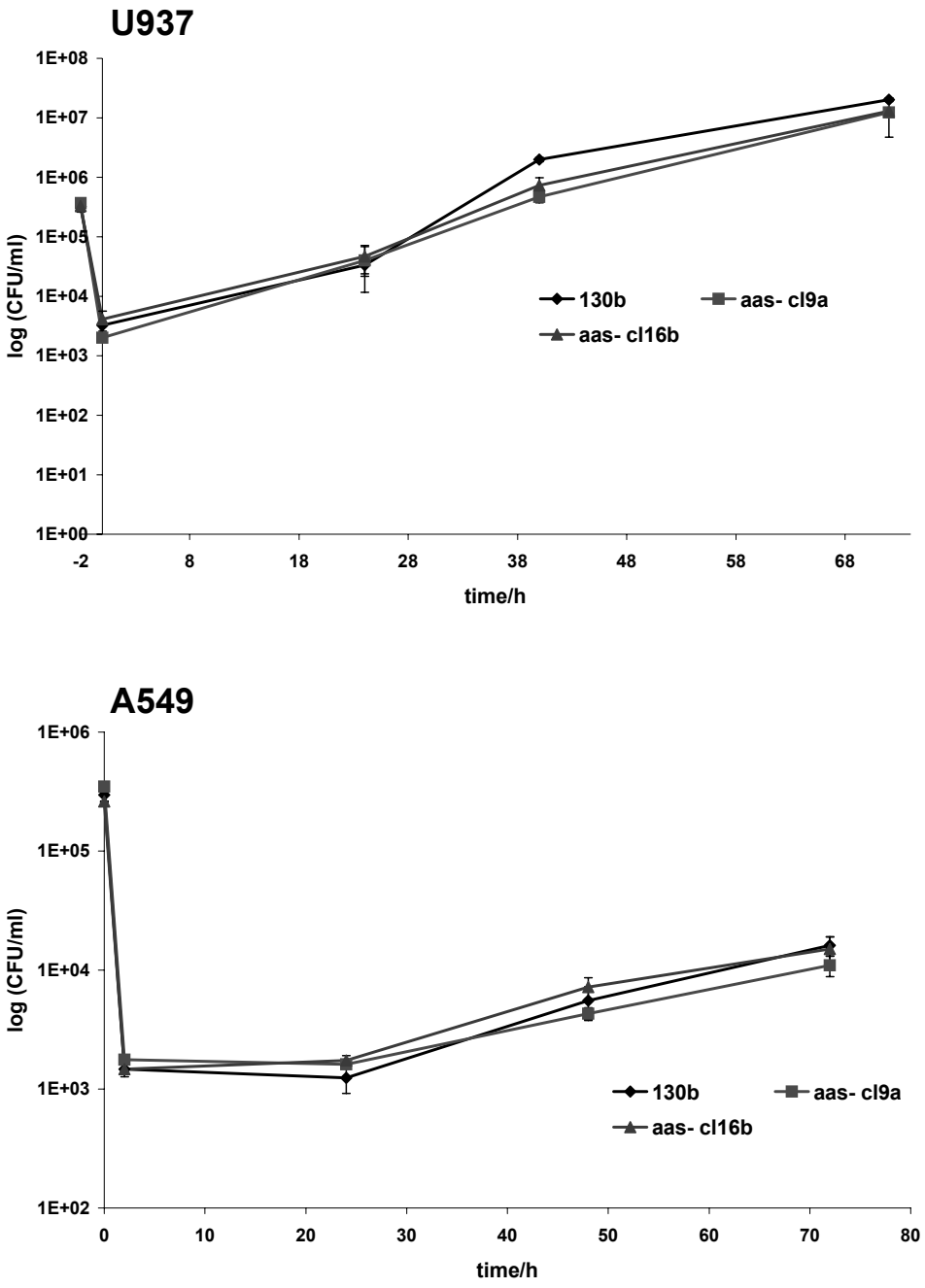

FIG.4.75. Intracellular infection of host cells by wild type and 130b *aas* mutant *L. pneumophila*. U937 macrophages and A549 epithelial cells (upper and lower figures, respectively) were inoculated with *L. pneumophila aas* knockout mutants as well as *L. pneumophila* wild type (MOI of At various time points post inoculation, the number of bacteria was quantified by plating aliquots on BCYE agar. Results represent the means and standard deviations of triplicate samples and are representative of three independent experiments.

In summary, the biochemical purification of PLA activity from *L. pneumophila* 130b culture supernatant resulted in the identification of seven proteins which were present in anion exchange chromatographic fractions showing PLA activity. Three proteins were chosen for further characterization, either based on their homology to lipolytic enzymes, as in the case of Unk1 and Aas, or because it represented the major protein in the corresponding fraction as was the case for LvrE. It was found that Unk1 does not possess distinct lipolytic properties but an *L. pneumophila* 130b *unk1* mutant showed a modest growth defect in the amoebal and macrophage infection models which, however, could not be *trans* complemented so far. Moreover, it was concluded from this study that LvrE is not a lipolytic enzyme but that it indirectly influences the secreted PLA and LPLA activities of *L. pneumophila* strains 130b and Philadelphia-1. LvrE does not seem to be essential for *L. penumophila* infection of host cells. However, LvrE appears to facilitate bacterial susceptibility to amoebal consumption on agar plates. Finally, the third enzyme, designated Aas, was shown to contribute to the cell-associated PLA/LPLA activities of *L. pneumophila* and influences the bacterial membrane lipid composition in a so far unidentified way. Aas is dispensable for the *L. pneumophila* infection of different host cells in the cell culture model, but similar to PlaA has an important role in protecting *L. pneumophila* from the cytolytic effects of MPLPC.